THE INFRARED AND ULTRAVIOLET SPECTRA OF PROPYNAL.

A Thesis

Presented for the Degree of

Doctor of Philosophy

of the

University of Glasgow

by

James Kay Graham Watson.

Chemistry Department

August 1962

PREFACE.

I wish to express my gratitude to Dr. J.C.D.Brand, who supervised this research and devoted a considerable number of hours to discussions in which the analyses herein described were evolved. I am also deeply indebted to Dr. J.H.Callomon, who photographed all the high-resolution ultraviolet spectra and contributed numerous suggestions to the analysis. In addition, thanks are due to Dr. C.C.Costain for the generous gift of his sample of HCCCDO, and to Mrs. F.Lawrie for assistance in recording the infrared spectra.

Financial support from the Department of Scientific and Industrial Research is gratefully acknowledged.

J.K.G.W.

SUMMARY.

The infrared and near ultraviolet vapour spectra of three isotopic forms HCCCHO, DCCCHO and HCCCDO of propynal (propiolaldehyde) have been examined under medium resolution, and the 3820 Å ultraviolet band system of these three molecules has been examined under high resolution.

On the basis of the infrared and high-resolution ultraviolet measurements, supplemented by liquid-phase infrared spectra, a complete set of fundamental vibrational frequencies of the ground electronic state is proposed, and the isotope effects are shown to be consistent with the Teller-Redlich product rule, using the rotational constants found from the microwave spectrum. The fundamental frequencies associated with the stretching of the various bonds agree with those observed for related molecules, but the frequencies of deformation of the bond angles present some unusual features. Information has also been obtained on the interaction of the vibrational motions with rotation about the axis of least inertia.

Four band systems have been found in the ultraviolet spectrum to long waves of 2000 Å, and these are described and their possible assignments to electronic transitions are discussed.

A detailed vibrational and partial rotational analysis of

the 3820 Å band system is presented, leading to a set of fundamental vibrational frequencies of the excited state, which lacks only one fundamental frequency for each isotope, although some of the proposed values are tentative. The direction of the electronic transition moment and the changes in the frequencies of vibration of the formyl group show that this transition is the analogue of the 3530 Å transition of formaldehyde. However, it is concluded that nothing has been observed here which is inconsistent with the present excited state being planar at equilibrium, in contradistinction to the non-planarity found for excited formaldehyde; but the evidence here presented is probably insufficient to preclude the presence of a potential-energy barrier of at most 100 cm^{-1} at the planar configuration.

In addition to the changes in the formyl frequencies, drastic changes are found to take place, as a consequence of the electronic excitation, in the frequencies of vibrational modes localised in the ethynyl group; the excitation cannot therefore be regarded as localised within the formyl group.

A feature of the 3820 Å system is the presence of bands whose vibronic transition moments lie along each of the three principal axes of inertia. The possible meaning of this in terms of vibronic interaction is discussed.

Perturbations of various types have been observed. Purely vibrational interactions of Fermi type are common in the 3820 Å system; and some regular Coriolis perturbations of the sub-band structure have also been found. Two striking examples of

irregular perturbations - one of them perhaps involving predissociation - in the sub-band structure of bands of HCCCDO are described, and their possible causes are examined.

NOTE ON SYMBOLS.

Letters which denote matrix quantities are underlined; small letters represent vectors or column matrices, and capitals represent square matrices. The symbol $\sim$ placed above the letter signifies the transpose of the matrix.

The notation for the assignment of ultraviolet bands is explained on p. 94.

In the text, the position of ultraviolet bands is described in the form "0+1300", which means that the band lies 1300 cm^{-1} to high frequencies of the band which is assigned as the origin of the band system (the "0 band"); the units (cm^{-1}) are usually omitted in this expression.

CHAPTER I.

INTRODUCTION.

I.1. Electronic Spectra.

Those properties of a substance which are characteristically "chemical" depend upon the distribution of the electrons in its molecules, and the manner in which that distribution may be affected by the proximity of other molecules; so the elucidation of the various electronic configurations available to a molecule and the energies of these configurations should eventually give a deeper insight into its chemical properties. The problem can be formulated in terms of quantum mechanics, since the forces involved are electric and magnetic ones which are sufficiently well understood; however, in order to obtain anything approaching a solution of the resulting equations, it is necessary to have recourse to quite drastic approximations which considerably decrease the reliability of the results. In these circumstances, it is desirable to make full use of the information on this topic which can be obtained experimentally; this information can then serve as a test of past calculations and as a guide to future ones.

The various electronic states of an atom or molecule are

studied most readily by an examination of its ultraviolet and visible absorption and emission spectra, which provide directly the difference in energy between atomic or molecular energy levels, this difference being equal to the energy of one photon of the electromagnetic radiation absorbed or emitted. An analysis of such a spectrum involves the deduction of the individual energy levels between which transitions are observed, and an explanation of the intensities of the various transitions.

In this way a considerable body of empirical data on the energy levels of atoms has been amassed; and the information so derived has been of immense value to chemistry, as it forms the basis of all theories of molecular binding and chemical reactivity.

In the case of molecules, as distinct from atoms, the different energy levels do not all correspond to different electronic states, because each electronic state carries with it a manifold of energy levels corresponding to vibration of the nuclei in the potential field defined by the electrons and to the rotation of the molecule as a whole. Thus in the molecular case a band system in the spectrum, consisting of a large number of individual transitions, corresponds to one electronic transition.

It should be mentioned that an atom or molecule may also possess varying amounts of translational energy which is, for the present purpose, effectively unquantised; but changes in the total linear momentum of atoms or molecules cannot occur

by the absorption or emission of radiation, so that no changes in translational energy take place if the atom or molecule remains intact. If ionisation or dissociation occurs, the fragments may have varying amounts of total translational energy with the same total momentum, so that translational transitions are possible and the spectrum is diffuse or "continuous" because of the absence of quantisation.

The detailed analysis of a large number of band systems due to diatomic molecules have now been accomplished, and the principles involved in such an analysis are well understood. The present position with regard to polyatomic molecules is a less happy one, since comparatively few band systems have been fully analysed. This is due to a complicating factor which is not present in atomic spectra and is not serious in diatomic spectra: namely that a molecule in its different electronic states may adopt different equilibrium configurations. The full realisation of the importance of this fact has come only within the last decade, although the possibility was first mooted by Mulliken in 1935 (45) and the spectroscopic consequences of it for a triatomic molecule were worked out by him in 1941 (46). Major changes in shape as well as in dimensions upon electronic excitation have now been established in a good proportion of the spectra so far analysed.

I.2. Molecular Energy Levels and Transitions.

The various energy levels available to a free molecule

are given in quantum mechanics by the eigenvalues of the Hamiltonian operator for the molecule, considered as a system of electrons and nuclei moving in a potential field due to the Coulombic forces between the particles on account of their charges and the magnetic forces between them on account of their spins. In what follows we shall disregard the effects of spin.

It was shown by Born and Oppenheimer in 1927 (2) that, to a good approximation, the energy levels are separable into parts associated with electronic, vibrational, rotational, and translational motions, i.e.

$$E_{total} = E_{elec} + E_{vib} + E_{rot} + E_{trans} .$$

For the present purpose, the electronic energies E_{elec} are constants which have to be determined empirically. On the other hand, the vibrational energies E_{vib} have been found by experience to be those characteristic of a slightly anharmonic oscillator with 3N-6 (or 3N-5 in the case of a linear molecule) degrees of freedom, where N is the number of atoms in the molecule. Likewise, the rotational energies E_{rot} are those of a slightly non-rigid rotor. The translational energies E_{trans} will not concern us. It should be borne in mind that these conclusions only form a general rule, based on the neglect of a large number of interactions, one or more of which may become important in special circumstances.

When the system is in the state of energy E_{total}, it is described in wave mechanics by the corresponding energy eigen-

function Ψ_{total}, which has the property that $|\Psi_{total}|^2$ for a given set of coordinates of all the particles is the probability distribution function for the occurrence of the configuration described by that set of coordinates when the system is in the given state. To the same approximation as before, this eigenfunction may be factorised into electronic, vibrational, rotational, and translational parts, i.e.

$$\Psi_{total} = \psi_{elec}\psi_{vib}\psi_{rot}\psi_{trans} ,$$

the last of which will be disregarded henceforth.

The property of these eigenfunctions of prime importance to spectroscopy is that, corresponding to two states Ψ'' and Ψ', there is defined an electric dipole <u>transition moment</u>, $\underline{m}'$, which is equal to $\int \Psi''^{*}(\sum_n e_n \underline{r}_n')\Psi' d\tau$, in which e_n and $\underline{r}_n'$ are the electric charge and the position vector (relative to the centre of mass) of the n^{th} particle, the sum is over all particles n, and the integral is over all coordinates; and the transition moment is such that the intensity of emission or absorption of electric dipole radiation in a transition between these states is proportional to $\tilde{\underline{m}}'^{*}\underline{m}'$. In particular, if it can be shown that, for a given transition, $\underline{m}' = \underline{0}$, then that transition will not appear in the spectrum and is said to be <u>forbidden</u>. A statement as to whether $\underline{m}'$ vanishes identically or not is called a <u>selection rule</u>.

Using the partial factorisation $\Psi_{total} = \psi_{ev}\psi_{rot}$, where ψ_{ev} is the vibronic (i.e. combined electronic and vibrational) eigenfunction, the transition moment is

$$\underline{m}' = \iint \psi''^{*}_{ev}\,\psi''^{*}_{rot}\left(\sum_n e_n \underline{r}'_n\right)\psi'_{ev}\,\psi'_{rot}\,d\tau_{ev}\,d\tau_{rot}$$

The position vectors $\underline{r}'_n$ may now be referred to an internal Cartesian system $\underline{r}_n$ directed along the principal axes of inertia by means of the transformation $\underline{r}'_n = \underline{L}\,\underline{r}_n$ where $\underline{L}$ is the matrix of the instantaneous direction-cosines of the inertial axes relative to space-fixed axes. We then have

$$\underline{m}' = \left\{\int \psi''^{*}_{rot}\,\underline{L}\,\psi'_{rot}\,d\tau_{rot}\right\}\left\{\int \psi''^{*}_{ev}\left(\sum_n e_n \underline{r}_n\right)\psi'_{ev}\,d\tau_{ev}\right\}$$

For any component of $\underline{m}'$ to be non-zero we must have at least one component of $\underline{m} = \int \psi''^{*}_{ev}\left(\sum_n e_n \underline{r}_n\right)\psi'_{ev}\,d\tau_{ev}$ non-zero, and a suitable component of $\int \psi''^{*}_{rot}\,\underline{L}\,\psi'_{rot}\,d\tau_{rot}$ also non-zero. The first requirement leads to a vibronic selection rule, the second to an associated rotational one.

The main consideration employed in deriving these selection rules is the utilisation of any symmetry possessed by the system. It is usually true that both the rigorous Hamiltonian operator and the approximate Hamiltonian operators derived from it in the separation of the different types of motion are invariant under a set of symmetry operations, which form a group in the mathematical sense. Under the action of these operations, each eigenfunction behaves as one of the "irreducible representations" or "symmetry species" of the appropriate group. For instance, the complete Hamiltonian is invariant to the inversion of all coordinates through any centre, to rotations of the external axes, and to the interchange of any pair of identical particles; the vibronic Hamiltonian is invariant to all the geometrical

symmetry operations of the equilibrium nuclear configuration; and the rotational Hamiltonian is invariant to rotations of 180° about each of the principal axes of inertia, and possesses higher symmetry if two or all three of the principal moments of inertia are equal. In addition, the various components of the matrices $\underline{r}'_n$, $\underline{L}$ and $\underline{r}_n$ each belong to a symmetry speciew of the appropriate group. The symmetry selections then take the general form that if any component of the above integrals is to be non-vanishing, the corresponding component of the integrand must belong to the totally symmetric species of the appropriate group, i.e. it must be unchanged by any symmetry operation of the group.

For purely rotational transitions of the lowest vibronic state, as are observed in the microwave spectrum, we have $\underline{m}$ equal to the permanent dipole moment of the molecule; thus for a molecule to exhibit a microwave spectrum it must possess a dipole moment.

If we restore the approximate factorisation $\psi_{ev} = \psi_{elec}\psi_{vib}$, we have

$$\underline{m} = \iint \psi''^{*}_{elec}\psi''^{*}_{vib}\left(\sum_n e_n \underline{r}_n\right)\psi'_{elec}\psi_{vib}\, d\tau_{elec}\, d\tau_{vib}$$

$$= \left\{\int \psi''^{*}_{elec}\left(\sum_{elec} e_n \underline{r}_n\right)\psi'_{elec}\, d\tau_{elec}\right\}\left\{\int \psi''^{*}_{vib}\psi'_{vib}\, d\tau_{vib}\right\} + \left\{\int \psi''^{*}_{elec}\psi'_{elec}\, d\tau_{elec}\right\}\left\{\int \psi''^{*}_{vib}\left(\sum_{nucl} e_n \underline{r}_n\right)\psi'_{vib}\, d\tau_{nucl}\right\}$$

For transitions between different vibrational levels of the same electronic state we have as a consequence of the orthonormal property of eigenfunctions that

$$\int \psi''^{*}_{vib}\psi'_{vib}\, d\tau_{nucl} = 0 \quad \text{and} \quad \int \psi''^{*}_{elec}\psi'_{elec}\, d\tau_{elec} = 1 ,$$

so that $\underline{m} = \int \psi''^{*}_{vib}\left(\sum_{nucl} e_n \underline{r}_n\right)\psi'_{vib}\, d\tau_{nucl}$; this equation

governs the intensities and selection rules in the pure vibrational spectrum. On the other hand, for transitions between vibrational levels of different electronic states, we have $\int \psi''^{*}_{elec} \psi'_{elec} d\tau_{elec} = 0$, whereas ψ''_{vib} and ψ'_{vib} are not necessarily orthonormal since they are eigenfunctions of different vibrational operators; thus

$$\underline{m} = \left\{ \int \psi''^{*}_{elec} \left(\sum_{nuc} e_n r_n \right) \psi'_{elec} d\tau_{elec} \right\} \left\{ \int \psi''^{*}_{vib} \psi'_{vib} d\tau_{nucl} \right\}$$

The first factor on the right-hand side is a constant for a given electronic transition, and gives a purely electronic selection rule. The second factor is the Condon integral for the vibrational levels involved, and can be non-zero only if $\psi''^{*}_{vib} \psi'_{vib}$ is totally symmetric, a selection rule originally proposed by Herzberg and Teller (1933,29).

The separated electronic and vibrational eigenfunctions ψ_{elec} and ψ_{vib} are classified according to their behaviour with respect to the geometrical symmetry operations of the equilibrium nuclear configuration, which corresponds to a minimum in the vibrational potential energy. However, the considerations employed in deriving this result are equally valid for a configuration corresponding to a maximum in the potential energy. It sometimes happens that a molecule (e.g. ammonia in its ground state) has a potential energy maximum in a configuration of higher symmetry than the equilibrium one. The vibronic Hamiltonian is then invariant to the symmetry operations of the more symmetrical configuration, and the eigenfunctions can be classified accordingly. This classific-

ation is only convenient when the potential-energy maximum is of low energy, as in the cases of unexcited ammonia or excited formaldehyde (see II.2).

Because of the possibility of changes in shape accompanying electronic excitation, the groups appropriate to the classification of the vibronic eigenfunctions of the two states may be different. In this case we must consider the vibronic Hamiltonian operators for the two electronic states together; the group of symmetry operations which leave both operators invariant is the group consisting of those symmetry operations which are common to both groups, and the symmetry selection rules are determined by the behaviour of the eigenfunctions with respect to this common group (46). In the same way, the rotational selection rules are determined by the common symmetry, as rotors, of the two states.

The relative intensities of the bands which are allowed by the Herzberg-Teller selection rule are governed by the values of the appropriate Condon integrals, which are essentially vibrational overlap integrals, and by a factor depending upon the relative populations of the levels of the initial state, which will be of the normal Boltzmann type for a system at thermal equilibrium. Because of this latter factor the strongest bands originate from the ground vibrational level of the initial state. For bands with the same initial level, those transitions will be most intense which allow the greatest overlap between the vibrational eigenfunctions. In particular

if there is a significant change in molecular geometry, the most intense transitions arising from the ground vibrational of the initial state will be to higher vibrational levels of the final state; and the particular vibrations of the final state excited in this way will be those which distort the nuclear configuration of the final state into a configuration similar to the equilibrium configuration of the initial state. This is the extension to polyatomic molecules of the principle originally enunciated for diatomic molecules by Franck (1925, 21) and Condon (1926 and 1928, 10).

It can happen, however, that electronic transitions which are forbidden by symmetry do give rise to a band system in which the individual bands all contravene the Herzberg-Teller selection rule; all the observed vibronic transitions are however allowed by vibronic symmetry. This occurrence is due to the fact that the factorisation of the vibronic eigenfunction into electronic and vibrational parts is only approximate, and the intensity with which these forbidden systems appear is a measure of the extent to which this approximation breaks down. The vibronic bands which appear are of the correct symmetry to acquire their intensity by electronic-vibrational interaction with allowed electronic levels, and their occurrence in the spectrum is usually associated with a nearby allowed electronic transition.

We may suppose that an improved approximation to ψ'_{ev} is constructed by taking a linear combination of the product

functions, e.g. $\psi'_{ev} = \alpha\psi^{A}_{elec}\psi^{A}_{vib} + \beta\psi^{B}_{elec}\psi^{B}_{vib}$ with $|\alpha| >> |\beta|$, where α and β are coefficients chosen to minimise the energy of ψ'_{ev}. We are presuming that the transition $\psi^{A}_{elec}\psi^{A}_{vib} \leftarrow \psi''_{elec}\psi''_{vib}$ is electronically forbidden or Herzberg-Teller forbidden, and that $\psi^{B}_{elec} \leftarrow \psi''_{elec}$ is allowed. Then

$$\underline{m} = \iint \psi'^{*}_{elec}\psi''^{*}_{vib}\left(\sum_n e_n \underline{r}_n\right)\left\{\alpha\psi^{A}_{elec}\psi^{A}_{vib} + \beta\psi^{B}_{elec}\psi^{B}_{vib}\right\} d\tau_{elec}\, d\tau_{vib}$$

$$= \alpha\iint \psi''^{*}_{elec}\psi''^{*}_{vib}\left(\sum_n e_n \underline{r}_n\right)\psi^{A}_{elec}\psi^{A}_{vib}\, d\tau_{elec}\, d\tau_{nucl} + \beta\iint \psi''^{*}_{elec}\psi''^{*}_{vib}\left(\sum_n e_n \underline{r}_n\right)\psi^{B}_{elec}\psi^{B}_{vib}\, d\tau_{elec}\, d\tau_{nucl}$$

$$= \beta\left\{\int \psi''^{*}_{elec}\left(\sum_{elec} e_n \underline{r}_n\right)\psi^{B}_{elec}\, d\tau_{elec}\right\}\left\{\int \psi''^{*}_{vib}\psi^{B}_{vib}\, d\tau_{nucl}\right\}$$

Thus the direction of the vector $\underline{m}$ will be that of $\int \psi''^{*}_{elec}\left(\sum_{elec} e_n \underline{r}_n\right)\psi^{B}_{elec}\, d\tau_{elec}$ and so will be that appropriate to the allowed transition $\psi^{B}_{elec} \leftarrow \psi''_{elec}$.

The 2600Å band system of benzene represents such a forbidden electronic transition. The pure electronic transition $^{e}B_{2u} \leftarrow {}^{e}A_{1g}$ is not permitted by the selection rules of the point group D_{6h}, but the observed bands owe their intensity to the interaction of $^{v}E_{2g}$ vibrational levels with the in-plane polarised $^{e}E_{1u} \leftarrow {}^{e}A_{1g}$ transition which is assigned to the strong absorption at 1850Å (59, 22). The corresponding system of naphthalene, observed at 3200Å, is allowed as a long-axis polarised $^{e}B_{2u} \leftarrow {}^{e}A_{g}$ transition because of the reduced molecular symmetry; but it is intrinsically weak and the strongest vibronic transitions are Herzberg-Teller forbidden ones resulting from interaction with the $^{e}B_{1u} \leftarrow {}^{e}A_{g}$ transition which is polarised along the short in-plane axis (15).

CHAPTER II.

PREVIOUS RELATED ANALYSES.

The object of the present study is an analysis of the lowest singlet electronic transition of propynal, HC≡C-CHO, which is the simplest compound containing a carbonyl group conjugated to a carbon-carbon multiple bond and indeed one of the simplest conjugated compounds. It is therefore convenient to survey at this point the published analyses of band systems of compounds related to propynal. We may consider first the progenitors of the two halves of the propynal molecule, namely acetylene and formaldehyde.

II.1. Acetylene.

The lowest band system so far observed for unperturbed acetylene commences weakly near 2500Å and continues with steadily increasing intensity to 2100Å, where it is possibly overlapped by a stronger system. This weak system was analysed by Ingold and King (1953, 22) and, under higher resolution, by Innes (1954, 23), and was one of the first transitions of a polyatomic molecule to be understood in detail. The outstanding feature of this spectrum is a long upper-state progression in an interval of about 1000 $cm.^{-1}$, the successive members of which increase markedly in intensity, so that the

ratio of the intensities of the sixth to the first is about 5000 to 1. The magnitude of this frequency and its isotopic shift to about 800 $cm.^{-1}$ in C_2D_2 show that it is a bending frequency. This upper-state progression is matched by a lower-state progression in about 600 $cm.^{-1}$, dropping to 500 $cm.^{-1}$ in C_2D_2; and this frequency is known from the Raman spectrum and from infra-red difference bands to be the trans-bending fundamental $\nu_4(\pi_g)$. The occurrence of odd members of a progression in a π_g fundamental is prohibited by the Herzberg-Teller selection rules (see I.2) for the $D_{\infty h}$ linear ground state, but can be accommodated by relaxing the symmetry restrictions to those of C_{2h}, with respect to which the π_g vibration is totally symmetric. The observed intensity distribution in both upper and lower progressions is only compatible with the Franck-Condon principle (I.2) if the excited state is seriously trans-bent in its equilibrium configuration.

Confirmation comes from the J-type rotational structure, where P,Q and R branches are observed, but there is a combination defect between the Q and the Pand R branches which is too large to be explained on any other grounds than the K-type splitting of an asymmetric top, which again requires a non-linear excited state. Moreover the missing lines at the band centres show that we are observing broadly-spaced K-type rotational structure, in which the ground-state axial angular momentum is due to vibration, and so the number of sub-bands

is limited by the range of values open to the quantum number of vibrational angular momentum; thus the smallest moment of inertia of the excited state is small but non-zero, again eliminating a linear state. Comparison of the intensity alternation in the J-structure of different sub-bands shows that the bending must be trans- rather than cis-. The value of almost zero found for the inertial defect confirms a planar structure.

From the perpendicular rotational structure and the sign of the combination defect it is possible to show that the bands are of type C and so the band system marks a $^{e}A_u(C_{2h}) \leftarrow {}^{e}\Sigma_g^+(D_{\infty h})$ transition, presumably singlet-singlet. The rotational analysis shows that the geometry of the excited state is approximately

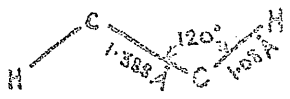

and the electronic wave-function has a nodal surface in the plane of the molecule. The system origin of C_2H_2 is at $\nu_{00} = 42197.7$ cm.$^{-1}$, and the oscillator strength is roughly $f = 10^{-4}$.

The lowest electronic transition expected for acetylene involves the promotion of an electron from the bonding π_u molecular orbital to the anti-bonding π_g orbital:

π_u

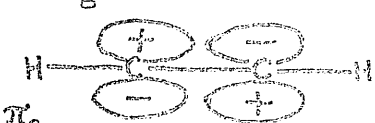

π_g

The lowest singlet state resulting from the $\ldots(\pi_u)^3\pi_g$ configuration was calculated by Ross (1952, 56) for linear acetylene

to be Σ_u^- ; this state becomes A_u in the trans-bent molecule and so it is presumably the one observed here.

The transverse node in the π_g orbital produces a strain which can be relieved by the bending of the molecule, the anti-bonding π_g orbital being converted in the process into a non-bonding n orbital of lower energy. At the same time the bonding π_u orbital is also converted into an n orbital, but one of higher energy ; and changes also occur in the energy of the σ orbitals, corresponding to the altered hybridisation. The geometry adopted by the molecule is the one which achieves the best compromise between these various effects.

In the observed excited state the hybridisation change is apparently complete, so that the in-plane components of the π_u and π_g orbitals are converted completely to non-bonding sp^2 orbitals. The C-C bond is best regarded as a three-electron bond:

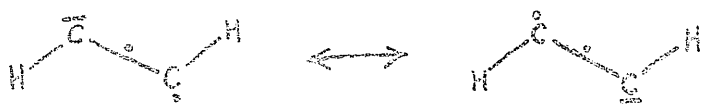

The formal mesomerism confers the necessary symmetry, but little bonding power because of the small overlap. The additional stability conferred on the molecule by bending must be of the order of 5,000 to 10,000 $cm.^{-1}$

II.2. Formaldehyde.

In describing the formaldehyde spectrum we shall use the definition of the C_{2v} symbols employed by Herzberg in his book (28,p. 300) and by some of the later workers, e.g. Brand

(5). This differs from that recommended in the Mulliken report (47).

The lowest singlet electronic transition of formaldehyde is expected theoretically (43) to be that involving promotion of an electron from a non-bonding p orbital (b_1) of the oxygen atom to an anti-bonding π orbital (b_2) of the carbonyl bond. The resulting excited state, if it retains C_{2v} symmetry, will be of species $^1A_2$ and therefore the pure electronic transition will be forbidden.

The absorption system to which this transition is assigned extends from about 3530Å to 2300Å, and is banded to 3000Å, after which it becomes increasingly diffuse. A fluorescence system extending to long wavelengths from near 3530Å is also observed, but there is little apparent similarity between the two spectra and it was sometimes thought that two transitions were involved.

The crucial step in the analysis was the recognition by Walsh (1953, 65) that this excited state may be non-planar, for reasons similar to those advanced for the non-linearity of excited acetylene. A detailed examination of the spectra by Brand (1956, 5) showed this to be the case, and high-resolution measurements by Robinson and DiGiorgio (1958, 55) confirmed Brand's findings.

The non-planarity of the equilibrium configuration may be described as due to the presence of a central maximum in the potential-energy function for the out-of-plane vibration,

and the configuration of maximum potential energy will have C_{2v} symmetry. Thus if the potential-energy barrier is fairly low, it is still convenient to discuss the spectrum in terms of C_{2v} species (see I.2). The same result follows (5) from the C_s symmetry of the equilibrium configuration, if account is taken of the splitting of the usual inversion degeneracy of a non-planar molecule (compare ammonia, 28, p.221).

All the stronger bands of both absorption and fluorescence are of type B_2 so that the upper levels which combine strongly with the lowest level of the ground state are of species B_1. The principal feature of the absorption spectrum is a long progression in a frequency of 1180 $cm.^{-1}$ which must, from its insensitivity to deuteration, be the carbonyl stretching frequency; it follows from the Franck-Condon principle that the length of the C-O bond is changing considerably. In addition to this there is an excited state $^{v}A_1$ interval of 824 cm^{-1} which does not form a progression but is strongly affected by deuteration and so , from its size, must correspond to a bending vibration.

In the fluorescence spectrum however there are, in addition to a progression in the ground-state carbonyl stretching frequency, two progressions α and β in a $^{v}A_1$ interval of 2300 $cm.^{-1}$

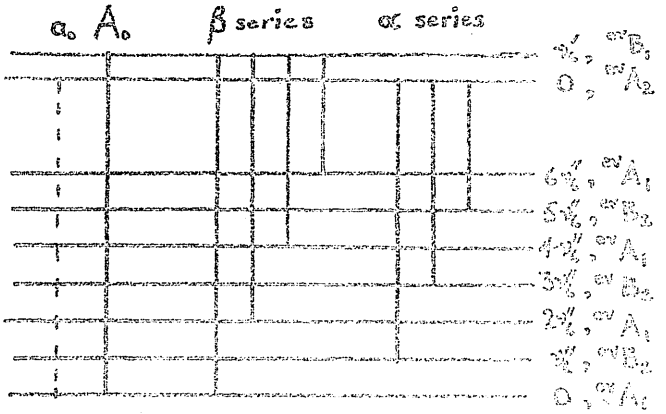

which is strongly sensitive to deuteration. The first member of the β series coincides with the type B apparent origin of the absorption spectrum (A_0), and later members are shown by the intensity alternation in the K-rotational structure to have A_1 or A_2 lower levels, whereas the α series have B_1 or B_2 lower levels. Examination of the rotational structures of these bands shows that all except the lowest A level are affected by a Coriolis rotational perturbation which had previously been observed for the out-of-plane bending fundamental $\nu_6''(b_2)$ in the infra-red, and the interval 2300 $cm.^{-1}$ corresponds closely to $2\nu_6''$. Thus the α and β progressions have lower levels with odd and even numbers of quanta of ν_6'' respectively. The upper level of the α series is then required to be of species ${}^{ev}A_2$ and to lie 124 $cm.^{-1}$ below that of the β series. From the formation of progressions in $2\nu_6''$ if follows from the Franck-Condon principle that the excited state is non-planar.

Returning to the absorption spectrum, we find a weak parallel band $\overset{(a_o)}{\wedge}$ connecting the vibrationless ground state with the upper level of the α series; since this is the band of lowest frequency which is not "hot" we may assign it as the system origin. A similar band lies 540 $cm.^{-1}$ higher. These low levels of the excited state can now be fitted into the anharmonic pattern of a vibration with a central barrier in its potential energy (see III.5):

		v'_6	CH_2O	CD_2O
$^{ev}A_2$	$^{v}A_1$	0	0 cm^{-1}	0 cm^{-1}
$^{ev}B_1$	$^{v}B_2$	1	127	69
$^{ev}A_2$	$^{v}A_1$	2	530	387
$^{ev}B_1$	$^{v}B_2$	3	951	669

The 824 cm^{-1} interval is the separation between the v'_6 and $3v'_6$ levels.

Analysis of the rotational structure of the first member of the α series (55) gives for the excited-state inertial defect $\Delta_0 = I_c^o - I_a^o - I_b^o$ the value of -0.099 amu.$Å^2$; this negative value is further good evidence for a non-planar structure.

Calculations based on the vibrational levels and the rotational constants give the following approximate structure:

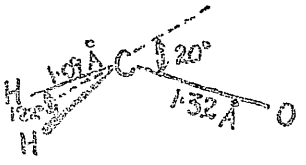

The origin lies at ν_{00} = 28190 cm^{-1} and the oscillator strength is about $f = 2\times10^{-4}$. The extra stability conferred on the excited state by virtue of its bending is near 650 cm^{-1}

The reason why the zero-point level of the excited state, which is shown to be $^{ev}A_2$ by its strong fluorescence bands, should give a weak parallel band in absorption is not fully understood; an $A_2 \leftarrow A_1$ transition is forbidden by the C_{2v} selection rules, and the corresponding $A'' \leftarrow A'$ transition in C_s symmetry would be of type B. Possibilities which have

been suggested are (1) that an electronic-rotational interaction couples this state with an $^{e}A_{1}$ one (52), and (2) that the transition is induced by the magnetic dipole component of electromagnetic radiation (58,42); the first would give an unusual intensity distribution in the K-rotational structure, whereas the second is fully allowed by the selection rules but would be unexpectedly strong. Drs. J.H.Callomon and K.K. Innes have informed us that the intensity distribution is normal, ruling out the first possibility; and independent evidence can be adduced in favour of the magnetic dipole interpretation (42). In any case, all the stronger bands, of B polarisation, must derive their intensity by vibronic interaction (see I.2) with an $^{e}B_{1} \leftarrow {}^{e}A_{1}$ transition, this interaction being induced by the b_2 through-plane vibration.

Unlike the case of acetylene, the hybridisation change from sp^2 to sp^3 in excited formaldehyde is not complete. The carbonyl bond is approximately a three-electron bond:

II.3. Comparison of the Acetylene and Formaldehyde Analyses.

We see that the effects in acetylene and formaldehyde differ so much in degree that they are different in kind. The large bending in acetylene produces a complete breakdown of the $D_{\infty h}$ selection rules, whereas in formaldehyde, as a consequence of the low barrier opposing vibration through the

plane, there is no deviation from the C_{2v} rules.

The formaldehyde spectrum consists of two components, a stronger type B_A one which is of a normal Herzberg-Teller forbidden type, and a weaker type A one which plays the role of a Herzberg-Teller allowed component; the relative intensities of the two components are not directly related to each other because the components appear by different mechanisms. (The fact that the through-plane vibration induces the forbidden component is not a consequence of the bending of the molecule.) Within each component the relative intensities are determined by Franck-Condon effects; the frequency differences between the various bands are totally symmetric intervals, so that the Franck-Condon progressions in the non-totally symmetric vibration $\nu_6(b_2)$ proceed in double quanta. The absence of a long upper-state progression in ν_6' must be due to the fact that in the $3\nu_6'$ level the molecule is already well above the top of the potential-energy barrier, and so for higher levels the excited state behaves in this respect as though it were planar. The vibrational evidence for bending therefore rests on anharmonicities and on Franck-Condon effects rather than on the breakdown of selection rules. This is likely to be general for cases in which the change in shape is accompanied by only a low potential-energy barrier. On the other hand, it would be extremely artificial to attempt to interpret the acetylene spectrum in terms of $D_{\infty h}$ symmetry, because of the high barrier.

The purely rotational evidence for bending in acetylene

is represented by the K-type doubling in the J-structure and the presence of K-structure, whereas for formaldehyde the only decisive test is that using the inertial defect in the vibrationless state. These tests will be general for linear molecules and for out-of-plane bending of planar molecules respectively; the K-type doubling test will also hold for symmetric top molecules. But for non-planar asymmetric tops or for in-plane bending of planar asymmetric tops a fairly complete structure analysis will be required to establish changes in shape from rotational evidence.

II.4. Other Carbonyl Compounds.

A weak absorption with maximum intensity ($\varepsilon \approx 10$ to 50 litre mole^{-1} cm^{-1}) in the 3000Å region is a common feature of carbonyl compounds (58,42) and is usually attributed to a $\pi^* \leftarrow n$ excitation. Unfortunately no other spectrum of this type has been studied in as great detail as the formaldehyde system, so that the conclusions are at present tentative. We shall consider a few of the aldehyde spectra.

II.5. Acetaldehyde.

Observations on the acetaldehyde absorption with $\lambda_{max} = 2900$A were reviewed by Rao and Rao (1954,54), who gave a vibrational analysis. The principal feature of the system is a long progression in an interval of 1125 cm^{-1}, which is presumed to be the excited-state carbonyl frequency, by

analogy with formaldehyde. Measurements by Innes and Giddings (1961,34) of the temperature sensitivities of the band intensities show that the origin lies to considerably longer wavelengths than was suggested by Rao and Rao, and the progressions of 1125 $cm.^{-1}$ can indeed be extended backwards by two or more quanta. In confirmation, the new position proposed for the origin (ca 28700 cm^{-1}) lies close to the onset of the observed fluorescence. Comparison of the new value with the value of 28190 cm^{-1} found for formaldehyde shows that the energy of the transition is little affected by methyl substitution.

From the length of the progressions in the carbonyl frequency, it follows by the Franck-Condon principle that the carbonyl bond lengthens by about the same amount as does that of formaldehyde, namely 0.10 A.

Additional vibrational intervals of the excited state are observed. In particular, one of 480 cm^{-1} is provisionally assigned to the through-plane vibration, assuming a non-planar configuration for the formyl group. However more evidence will be required to establish the details of the excited-state geometry. No rotational analysis of the bands has yet been accomplished.

II.6. Formyl Fluoride.

The effect of replacement of one hydrogen atom of formaldehyde by fluorine is to shift the $\pi^* \leftarrow n$ absorption to much shorter wavelengths, the maximum occurring now at 2100Å ($\varepsilon \approx$

50 litre mole^{-1}cm^{-1}). This system was studied by Giddings and Innes (1961 and 1962,24) using high resolution. They found a very long progression in 1100 cm^{-1} which was insensitive to deuterium substitution and so could be assigned to the excited state carbonyl stretching frequency. It follows from the Franck-Condon principle that the length of the C-O bond, which is unusually short (1.18Å) in the ground state, increases by much more than it does in formaldehyde. The rotational analysis gives 1.35 to 1.38 Å for the excited carbonyl length.

Giddings and Innes claimed from vibrational evidence that the excited state is sufficiently non-planar to exclude the inversion doubling effects found in formaldehyde; but since there appears to be some doubt about the values of the frequencies involved, this assignment must be regarded as tentative.

II.7. Glyoxal.

The conjugated dialdehyde glyoxal is also of interest in relation to propynal. The singlet $\pi^*\leftarrow n$ system is found to extend from 4550 to about 3700 Å, and to consist of two components of nearly equal intensity, the bands being either of type C or hybrids of types A and B (mainly type A). A vibrational analysis by Brand (1954,4) showed that the type C component is the allowed one, representing an $^eA_u \leftarrow {}^eA_g$ transition; while the forbidden hybrid component is induced by the b_g CH-wagging vibration, which is similar to the vibration active in the formaldehyde spectrum. No vibrational evidence

for non-planarity of the excited state was found in either absorption or fluorescence. Examination of the rotational structure of the origin band under high resolution by King (1957, 37) showed that it was consistent with a transition between states of zero inertial defect and therefore presumably planar.

CHAPTER III.

ENERGY LEVELS AND TRANSITIONS OF AN UNSYMMETRICAL PLANAR MOLECULE.

The molecule of propynal is expected from normal valency considerations to be planar in its ground state. We shall attempt to analyse its infra-red and ultraviolet spectra on the basis of this structure, bearing in mind that some excited electronic states may be non-planar, and that the non-planarity will show itself in departures from the anticipated planar behaviour, although not necessarily in departures from planar selection rules.

III.1. Vibronic Symmetries and Selection Rules.

The vibronic Hamiltonian and the separated electronic and vibrational Hamiltonians are invariant under the group of geometrical symmetry operations of the equilibrium configuration of the molecule (I.2); so the corresponding eigenfunctions can be classified in terms of the symmetry species of that group. The plane of the propynal molecule will be its only element of symmetry since all the atoms are chemically, far less symmetrically, non-equivalent. Thus the molecule belongs

to the point group C_s with operations I and σ and symmetry species A′ and A″, as shown in Table 1; the species of the translations (T) along and the rotations (R) about the principal axes of inertia are also shown.

Table 1.

C_s	I	σ^{ab}	T	R
A′	1	1	T_a, T_b	R_c
A″	1	-1	T_c	R_a, R_b

The presence of at least one translation in each symmetry species means that no vibronic transition is forbidden by symmetry. However, vibronic transitions of the types $A' \leftrightarrow A'$ and $A'' \leftrightarrow A''$ have transition moments lying in the molecular plane, whereas $A' \leftrightarrow A''$ transitions have moments perpendicular to the plane. The rotational selection rules differ in the two cases (III.6).

III.2. Modes of Vibration.

Since the molecule has six atoms and is non-linear, there are twelve independent displacement coordinates required to specify the modes of vibration. These coordinates can readily be shown to have the symmetry representation $9A' + 3A''$. Numbering the atoms as shown in Fig. 1, we can conveniently choose these coordinates as follows:

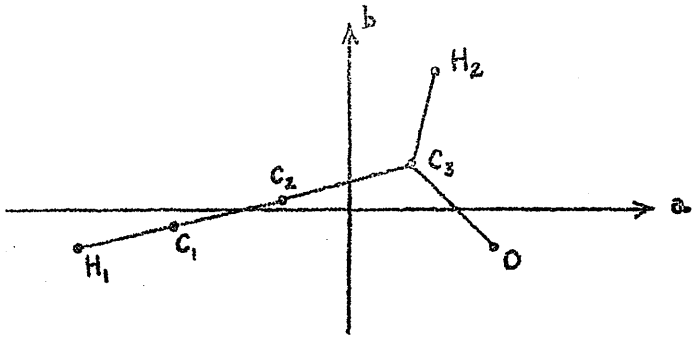

Fig. 1.

A′ coordinates:–

bond-stretching : $\delta r(C_1H_1)$, $\delta r(C_3H_2)$, $\delta r(C_1C_2)$, $\delta r(C_2C_3)$, $\delta r(C_3O)$;

in-plane bending : $\delta\theta(H_1\hat{C}_1C_2)$, $\delta\theta(C_2\hat{C}_3H_2)$, $\delta\theta(C_1\hat{C}_2C_3)$, $\delta\theta(C_2\hat{C}_3O)$.

A″ coordinates:–

out-of-plane bending : $\delta\theta(H_1\hat{C}_1C_2)$, $\delta\theta(C_1\hat{C}_2C_3)$, $\delta\theta(C_2\text{–}\hat{C}_3\begin{smallmatrix}H_2\\O\end{smallmatrix})$

The normal coordinates will be linear combinations of these displacements. It is convenient for descriptive purposes to regard each normal coordinate as being formed largely from one of these basic coordinates, but although this is often true it is not necessarily so.

III.3. Vibrational Term Values.

The vibrational term values of a slightly anharmonic oscillator with twelve degrees of freedom are given to a good approximation (28, p.210) by

$$G(v_1,v_2,\ldots,v_{12}) = E_{vib}/hc = \sum_{i=1}^{12}\omega_i(v_i+\tfrac{1}{2}) + \sum_{i=1}^{12}\sum_{j=i}^{12}x_{ij}(v_i+\tfrac{1}{2})(v_j+\tfrac{1}{2})$$

where ω_i is the zero-order frequence and v_i the vibrational

quantum number for the i^{th} normal mode, and the x_{ij} are small anharmonic coefficients. Each v_i can take the integral values $0,1,2,\ldots$, the lowest level being the zero-point level $v_1 = v_2 = \ldots = v_{12} = 0$ with $G(0,0,\ldots,0) = \frac{1}{2}\sum_i \omega_i + \frac{1}{4}\sum_i \sum_j x_{ij}$. It is more convenient empirically to refer all the vibrational levels to the zero-point level by using

$$G_0(v_1,v_2,\ldots,v_{12}) \equiv G(v_1,v_2,\ldots,v_{12}) - G(0,0,\ldots,0)$$
$$= \sum_i \omega_i^0 v_i + \sum_i \sum_{j \geq i} x_{ij} v_i v_j$$

where $\omega_i^0 = \omega_i + \frac{1}{2}\sum_{j=1}^{12} x_{ij}$.

For a harmonic oscillator in which the instantaneous electric dipole moment is linear in the displacement coordinates, it can be shown that the selection rule $\Delta v = \pm 1$ holds in the pure vibrational spectrum (28, p. 260). Although this rule is strictly valid only in the ideal case, it means that overtone and combination bands will be weak or absent in the infra-red spectrum, so that we are concerned primarily with the fundamental levels $v_i=1$, $v_j=0$ for $j \neq i$, which have

$$\nu_i \equiv G_0(0,0,\ldots,1,\ldots,0) = \omega_i^0 + x_{ii}.$$

III.4. Fermi Resonance.

The vibrational term values given above are obtained by treating the anharmonic terms in the potential energy as a perturbation of the harmonic potential, and adding the largest first- and second-order contributions to the harmonic term values. However, this treatment will not be valid for levels which are nearly degenerate in the harmonic approximation. In

this latter case we must use degenerate perturbation theory in order to evaluate the anharmonic term values. It is found that an unusually large mixing of the harmonic basis functions occurs, so that each level partakes of the character of the other. In this way overtone and combination bands, which are usually weak in the infra-red spectrum, may gain intensity at the expense of a fundamental of nearly the same frequency; they will also be displaced in frequency. This effect is known as Fermi resonance.

Since all the terms of the potential energy expression are totally symmetric, a necessary requirement for Fermi resonance to occur is that the interacting levels have the same vibrational symmetry.

Suppose we are considering a Fermi resonance between n levels whose harmonic basis functions are $\psi_1^\circ, \psi_2^\circ, \psi_3^\circ, \ldots, \psi_n^\circ$. Transitions from some other level ψ_0° (usually the zero-point level) to ψ_i° are assumed to be allowed; transitions to the others are forbidden. Suppose further that H is the complete vibrational Hamiltonian.

Then the matrix $H^\circ_{kl} = \int \psi_k^{\circ *} H \psi_l^\circ d\tau$ has non-zero off-diagonal elements associated with the Fermi resonance. To obtain the true wave-functions we construct linear combinations $\psi_i = \sum_j a_{ij} \psi_j^\circ$ such that:

(1) the matrix of coefficients a_{ij} is unitary, i.e. $\sum_i a_{ik} a_{il}^* = \sum_i a_{ki} a_{li}^* = \delta_{kl}$; and

(2) the Hamiltonian matrix $H_{ij} = \int \psi_i^* H \psi_j d\tau$ is diagonal

i.e. $H_{ij} = \delta_{ij}E_i$, where the E_i will be the observed energies.

Then $\sum_i a^*_{ij}\psi_i = \sum_i \sum_k a^*_{ij}a_{ik}\psi^\circ_k = \sum_k \delta_{kj}\psi^\circ_k = \psi^\circ_j$.

Thus $H^\circ_{kl} = \int \psi^{\circ *}_k H \psi^\circ_l d\tau = \int (\sum_i a_{ik}\psi^*_i) H (\sum_j a^*_{jl}\psi_j) d\tau$

$= \sum_i \sum_j a_{ik}a^*_{jl}H_{ij} = \sum_i \sum_j a_{ik}a^*_{jl}\delta_{ij}E_i = \sum_i a_{ik}a^*_{il}E_i$.

The diagonal elements H°_{kk} are the "unperturbed" energies of the levels. Strictly speaking, they are first-order perturbed, but the effects of the Fermi resonance are not included in them. Then $\sum_k H^\circ_{kk} = \sum_k \sum_i a_{ik}a^*_{ik}E_i = \sum_i E_i$. Thus the sum of the energies is not affected by the Fermi resonance.

The transition moment for $\psi_i \leftarrow \psi_0$ is $\int \psi^*_0 \mu \psi_i d\tau = \sum_j a_{ij} \int \psi^{\circ *}_0 \mu \psi^\circ_j d\tau$ where μ is the instantaneous electric dipole moment. Because of the forbiddenness of $\psi^\circ_j \leftarrow \psi^\circ_0$ unless $j = 1$, the last equation becomes $\int \psi^*_0 \mu \psi_i d\tau = a_{i1}\mu^\circ_{01}$ where $\mu^\circ_{01} = \int \psi^{\circ *}_0 \mu \psi^\circ_1 d\tau$. Thus the intensity of $\psi_i \leftarrow \psi_0$ is proportional to $a_{i1}a^*_{i1}(\vec{\mu}^{\circ *}_{01}\vec{\mu}^\circ_{01})$. The total intensity for the perturbed levels ψ_i is therefore proportional to $\sum_i a_{i1}a^*_{i1}(\vec{\mu}^{\circ *}_{01}\vec{\mu}^\circ_{01}) = (\vec{\mu}^{\circ *}_{01}\vec{\mu}^\circ_{01})$. The total intensity is therefore unaffected by the Fermi resonance.

Finally, from the results that $H^\circ_{11} = \sum_i a_{i1}a^*_{i1}E_i$ and that the intensity for the ψ_i level is proportional to $a_{i1}a^*_{i1}$, it follows that the unperturbed level H°_{11} is given by the weighted mean of the perturbed levels, the weighting factors being the intensities for the individual perturbed levels. It should be noted that the more general proposition, that the intensity-weighted mean energy is unaffected by the Fermi resonance, is not true if more than one of the unperturbed

levels has non-vanishing intensity.

III.5. Double-Minimum Potential.

Larger departures from harmonic behaviour will occur if any of the vibrational modes is seriously anharmonic. This will be particularly true if there are two minima in the potential energy function corresponding to any coordinate, with a fairly low maximum between them. A double-minimum potential well of this type has been found in ammonia and ammonia-like molecules (28, p.221), in formamide (12), in trimethylene oxide (9,16), and in the lowest excited states (singlet and triplet) of formaldehyde (see II.2).

For a slightly anharmonic oscillator the successive quanta are nearly equal and change smoothly with increasing quantum number. On the other hand, the quanta of a double-minimum vibration are alternately small and large, the greatest alternation being observed in the lowest quanta. For a sufficiently high central maximum the small quanta for low quantum numbers are almost zero, and the levels are effectively doubly degenerate with a spacing between successive double levels equal to the harmonic frequency for

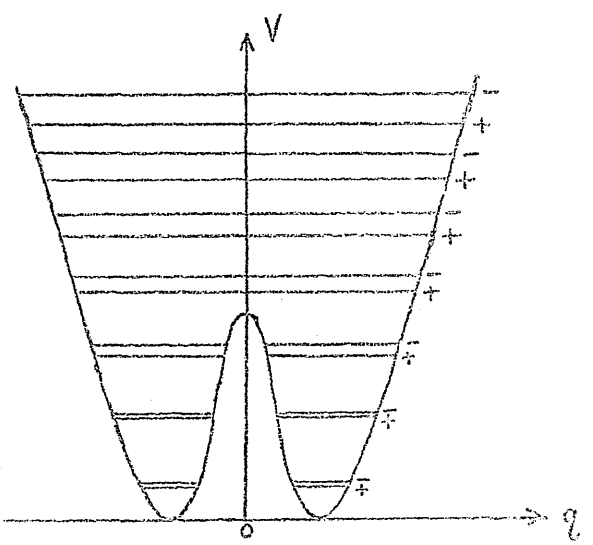

Fig. 2.

one limb of the potential well by itself. As the quantum number increases, the small quanta become larger and the large ones smaller, until their magnitudes converge for energies well above the potential maximum. This behaviour is shown diagrammatically in Fig. 2, where the symbols + and - denote respectively symmetry and antisymmetry of the eigenfunctions about the central maximum, assuming the potential function to be symmetric about its maximum.

The detailed pattern of the energy levels depends on the form assumed for the potential function. A convenient way of introducing the central maximum is to add to the normal harmonic potential a Gaussian function (9,16,61), giving $V = hc\nu(\frac{1}{2}q^2 + \alpha e^{-\beta q^2})$ for the mode involved, where ν is the limiting harmonic wave-number for large v, and α and β are parameters; the variable q is a dimensionless normal coordinate and is equal to $\gamma^{1/2}Q$ in the notation of Wilson, Decius and Cross (68,p.37). The potential has a central maximum only if $2\alpha\beta > 1$; α and β determine respectively the height and breadth of the central hump. The matrix elements of the Hamiltonian corresponding to V, to a basis of harmonic oscillator eigenfunctions, can readily be evaluated. The non-zero elements for $v \leq 4$ are :

$$\langle 0|H|0\rangle = hc\nu\left\{\tfrac{1}{2} + \frac{\alpha}{(\beta+1)^{1/2}}\right\} \qquad \langle 1|H|1\rangle = hc\nu\left\{\tfrac{3}{2} + \frac{\alpha}{(\beta+1)^{3/2}}\right\}$$

$$\langle 2|H|2\rangle = hc\nu\left\{\tfrac{5}{2} + \frac{\alpha(\beta^2+2)}{2(\beta+1)^{5/2}}\right\} \qquad \langle 3|H|3\rangle = hc\nu\left\{\tfrac{7}{2} + \frac{\alpha(3\beta^2+2)}{2(\beta+1)^{5/2}}\right\}$$

$$\langle 4|H|4\rangle = hc\nu\left\{\tfrac{9}{2} + \frac{\alpha(3\beta^4+2\cdot4\beta^2+8)}{8(\beta+1)^{9/2}}\right\}$$

$$\langle 0|H|2\rangle = -hc\nu\frac{\alpha\beta}{2^{1/2}(\beta+1)^{3/2}} \qquad \langle 1|H|3\rangle = -hc\nu\frac{3^{1/2}\alpha\beta}{2^{1/2}(\beta+1)^{5/2}}$$

$\langle 0|H|4\rangle = h\nu \frac{3^{1/2}\alpha\beta^2}{2^{3/2}(\beta+1)^2}$ $\qquad$ $\langle 2|H|4\rangle = -h\nu \frac{3^{1/2}\beta(\beta^2+4)}{4(\beta+1)^{7/2}}$

For low values of α, the diagonal elements will give good approximations to the energy levels.

III.6. Rotational Symmetries and Selection Rules.

The principal axes of inertia of a molecume are conventionally labelled a, b, c in such a way that the moments of inertia about these axes fall in the order $I_a \leqslant I_b \leqslant I_c$.

For a planar molecule one principal axis must for reasons of symmetry be perpendicular to the molecular plane; and this is the c-axis, on account of the relation $I_c^e = I_a^e + I_b^e$ which neglects only the contribution from the electrons. Furthermore in propynal the heavy nuclei (carbon, oxygen) lie roughly in a straight line, about which the moment will be small, so that this will be the a-axis. Consequently $I_a \ll I_b \approx I_c$. Thus the molecule will be an asymmetric top ($I_a \neq I_b \neq I_c$), but will approximate to a prolate symmetric top ($I_a \neq I_b = I_c$).

The symmetry of the total Hamiltonian operator with respect to all possible rotations of the external axes leads to a classification in terms of J, the quantum number of the total angular momentum, the magnitude of the latter being $\sqrt{J(J+1)}h/2\pi$; J can take the values 0,1,2,... . The level J is (2J+1)-fold degenerate with respect to orientations of the angular momentum vector relative to the external axes; and the angular momentum vector can also assume (2J+1) orientations relative to the internal axes, which in the case of an asymm-

etric top all correspond to different energies. J is subject to the following selection rule:

$$\Delta J = J' - J'' = 0, \pm 1 \text{ (except } J=0 \not\rightarrow J=0 \text{)}.$$

The rotational Hamiltonians of the two types of symmetric top, prolate ($I_a \neq I_b = I_c$) and oblate ($I_a = I_b \neq I_c$), are invariant under the point group D_∞, whose symmetry operations are : rotation through any angle about the unique or figure axis; and rotation through π about any axis perpendicular to the figure axis. This leads to a symmetry classification in terms of K, the quantum number of the component of angular momentum about the figure axis, the latter having the magnitude $Kh/2\pi$; K can take the values $0,1,2,\ldots,J$, the levels with $K \neq 0$ being doubly degenerate.

As stated in I.2, the rotational selection rules depend on the matrix of direction-cosines $\underline{L}$. It can be shown that the three components of each column of $\underline{L}$ behave similarly with respect to rotations about the inertial axes, whereas the different columns may behave differently; we may therefore indicate the behaviour of the components of $\underline{L}$ by means of the components of $\underline{m}$ which they multiply when the matrix multiplication is performed. The requirement that $\psi''^*_{rot}\underline{L}\psi'_{rot}$ be totally symmetric then leads to the selection rules

$$m_\parallel \neq 0 \quad : \quad \Delta K = 0$$

$$m_\perp \neq 0 \quad : \quad \Delta K = \pm 1$$

where $\Delta K = K' - K''$, and $m_\parallel$ and $m_\perp$ represent respectively the component of $\underline{m}$ parallel to and one of the pair of components

perpendicular to the figure axis.

The asymmetric top has the lower symmetry $\underline{D}_2$, the operations of which comprise rotations of π about the three axes of inertia; the species of $\underline{D}_2$ are A, B_a, B_b, B_c (Mulliken notation; see 28, p.52). The symmetry properties of the components of $\underline{L}$ give the following selection rules :

$$m_a \neq 0 \; : \; A \leftrightarrow B_a, \quad B_b \leftrightarrow B_c$$

$$m_b \neq 0 \; : \; A \leftrightarrow B_b, \quad B_a \leftrightarrow B_c$$

$$m_c \neq 0 \; : \; A \leftrightarrow B_c, \quad B_a \leftrightarrow B_b$$

If we imagine a top continuously transformed from the prolate symmetric limit through asymmetric intermediates to the oblate symmetric limit, it is found that a given asymmetric top level can be uniquely characterised by the values of K, namely K_a and K_c, of the levels with which it correlates in the prolate and oblate limits respectively; however the values of K_a and K_c only have significance as quantum numbers of angular momentum in the limiting cases. The asymmetric top selection rules are then equivalent to:

$$m_a \neq 0 \; : \; \Delta K_a \text{ even and } \Delta K_c \text{ odd}$$

$$m_b \neq 0 \; : \; \Delta K_a \text{ odd and } \Delta K_c \text{ odd}$$

$$m_c \neq 0 \; : \; \Delta K_a \text{ odd and } \Delta K_c \text{ even} .$$

For a slightly asymmetric prolate top like propynal, the strong rotational transitions are those which are simultaneously allowed by the asymmetric top and the prolate symmetric top selection rules.

III.7. Rotational Term Values.

The rotational Hamiltonian of a rigid rotor is

$$H_{rot} = \frac{1}{2}\left\{\frac{\Pi_a^2}{I_a} + \frac{\Pi_b^2}{I_b} + \frac{\Pi_c^2}{I_c}\right\}$$

where Π_a, Π_b, Π_c are the components of the total angular momentum about the principal axes of inertia and I_a, I_b, I_c are the principal moments of inertia. The slight non-rigidity of molecules may be allowed for by using effective moments of inertia for the various vibrational levels and by introducing small quartic terms in the angular momenta, these terms being associated with centrifugal distortion.

The rotational term values $F_V(J,K) = E_{rot}/hc$ for the vibrational level V of a vibrating prolate symmetric top are then given, to a good approximation, by the equation

$$F_V(J,K) = B_V J(J+1) + (A_V - B_V)K^2 - D_J J^2(J+1)^2 - D_{JK} J(J+1)K^2 - D_K K^4$$

where A_V and B_V are effective rotational constants and D_J, D_{JK} and D_K are small centrifugal coefficients. The dependence of the rotational constants upon the vibrational quantum numbers is well represented by $A_V = A_e - \sum_i \alpha_i^A (v_i + \frac{1}{2})$ and $B_V = B_e - \sum_i \alpha_i^B (v_i + \frac{1}{2})$ in which the α-s are small vibration-rotation interaction constants. The constants A_e and B_e are then related to the moments in the equilibrium configuration by $A_e = h/8\pi^2 c I_a^e$ and $B_e = h/8\pi^2 c I_b^e$. The equations $A_V = A_0 - \sum_i \alpha_i^A v_i$ and $B_V = B_0 - \sum_i \alpha_i^B v_i$ are more convenient empirically.

The rotational term values $F_V(J_{K_a K_c}) = E_{rot}/hc$ of an

asymmetric top cannot be stated explicitly, but for given J they are, to the same approximation as above, the eigenvalues of the matrix F_J with non-zero elements

$$\langle K|F_J|K\rangle = \bar{B}_V J(J+1) + (A_V-\bar{B}_V)K^2 - D_J J^2(J+1)^2 - D_{JK}J(J+1)K^2 - D_K K^4$$

$$\langle K|F_J|K\pm2\rangle = \left\{\tfrac{1}{2}(B_V-C_V) - \delta_J J(J+1) + R_5\left[K^2+(K\pm2)^2\right]\right\} f(J,K\pm1)$$

$$\langle K|F_J|K\pm4\rangle = R_6 f(J,K\pm1)f(J,K\pm3)$$

where $f(J,n) = \left\{\left[J(J+1)-(n-1)n\right]\left[J(J+1)-n(n+1)\right]\right\}^{\frac{1}{2}}$, and K can take the values $-J,-J+1,\ldots,J-1,J$. The significance of C_V is similar to that of A_V and B_V, and $\bar{B}_V=\frac{1}{2}(B_V+C_V)$; δ_J, R_5 and R_6 are additional centrifugal coefficients.

Neglecting the centrifugal corrections, the term values may be represented by Wang's equation

$$F_V(J_{K_aK_c}) = \bar{B}_V J(J+1) + (A_V-\bar{B}_V)W(J_{K_aK_c};b),$$

where $W(J_{K_aK_c};b)$ depends on the asymmetry parameter $b = \dfrac{C_V-B_V}{2(A_V-\bar{B}_V)}$ and is obtainable from tables for the various levels (64). An alternative treatment uses Ray's asymmetry parameter $\kappa = \dfrac{2B_V-A_V-C_V}{A_V-C_V} = \dfrac{3b+1}{b-1}$ (40, 64).

For a near-symmetric prolate top the off-diagonal elements of the matrix F_J are small and its eigenvalues are approximately the symmetric top term values with B_V replaced by $\bar{B}_V$. This approximation is best when J is small and K_a is large, i.e. when the angular momentum vector lies nearly along the a-axis.

III.8. Coriolis Coupling.

Serious departures from the equations of the previous section occur when the molecule possesses internal angular

momentum, as a consequence of the Coriolis coupling of the angular momenta. We consider here the case of vibrational angular momentum.

A vibration-rotation Hamiltonian which allows for the Coriolis interaction but neglects all other vibration-rotation interactions is

$$H_{vib\text{-}rot} = \tfrac{1}{2}\left\{\frac{(\Pi_a-\pi_a)^2}{I_a} + \frac{(\Pi_b-\pi_b)^2}{I_b} + \frac{(\Pi_c-\pi_c)^2}{I_c}\right\} + \tfrac{1}{2}\sum_i (P_i^2 + 4\pi^2 c^2 \nu_i^2 Q_i^2)$$

where Π_a, Π_b, Π_c are the components of total angular momentum; π_a, π_b, π_c are the components of vibrational angular momentum; I_a, I_b, I_c are the principal moments of inertia (assumed constant for all vibrational levels); and Q_i is the i^{th} normal coordinate with conjugate momentum P_i and harmonic wave-number ν_i.

The vibrational angular momentum is given by $\pi_a = \sum_k \sum_l \zeta^a_{kl} Q_k P_l$, etc. The Coriolis coupling coefficient ζ^a_{kl} depends on the transformation from Cartesian displacements to real normal coordinates, and is given by

$$\zeta^a_{kl} = \sum_r \frac{1}{m_r} \frac{\partial(Q_k, Q_l)}{\partial(b_r, c_r)}$$

where b_r, c_r are the Cartesian displacements from equilibrium, in the inertial-axis system, of the r^{th} atom, of mass m_r. This definition of ζ^a_{kl} agrees with that of Nielsen (49) and of Boyd and Longuet-Higgins (3), but is opposite in sign to that of Wilson, Decius and Cross (68, p. 368); the use of Jacobians is due to Boyd and Longuet-Higgins.

The Coriolis coefficients are real, with $|\zeta^a_{kl}| \leqslant 1$ and $\zeta^a_{kl} = -\zeta^a_{lk}$; according to the selection rule of Jahn (36), ζ^a_{kl} can only be non-zero if the product of the symmetry species

of Q_k and Q_l contains the species of a rotation about the a-axis.

The vibration-rotation Hamiltonian consists of the Hamiltonians of a rigid rotor and a harmonic oscillator with the addition of terms of the type $-\frac{\Pi_a \pi_a}{I_a} + \frac{\pi_a^2}{2I_a}$. The second of these is purely vibrational, and contributes to the vibrational energies small terms of the order of magnitude of the rotational constants; we shall regard these as already incorporated in the vibrational energies. The first type of term produces a coupling of vibration and rotation which we shall consider in more detail. We only deal with coupling about the a-axis, which affects the K-rotational structure of a prolate symmetric or near-symmetric top.

It can be shown (for example, using the tables of 68, p.368) that the only non-zero matrix elements of $-\frac{\Pi_a \pi_a}{I_a}$ to a basis of rigid-symmetric-top harmonic-oscillator wave-functions are of the types

$$\left\langle v_1,\dots,v_k+1,\dots,v_l,\dots,v_n;J,K\left|-\frac{\Pi_a\pi_a}{I_a}\right|v_1,\dots,v_k,\dots,v_l+1,\dots,v_n;J,K\right\rangle$$
$$=-\left\langle v_1,\dots,v_k,\dots,v_l+1,\dots,v_n;J,K\left|-\frac{\Pi_a\pi_a}{I_a}\right|v_1,\dots,v_k+1,\dots,v_l,\dots,v_n;J,K\right\rangle$$
$$=ihc\zeta^a_{kl}(v_k+1)^{\frac{1}{2}}(v_l+1)^{\frac{1}{2}}\left\{\left(\frac{\nu_k}{\nu_l}\right)^{1/2}+\left(\frac{\nu_l}{\nu_k}\right)^{1/2}\right\}AK$$

and

$$\left\langle v_1,\dots,v_k+1,\dots,v_l+1,\dots,v_n;J,K\left|-\frac{\Pi_a\pi_a}{I_a}\right|v_1,\dots,v_k,\dots,v_l,\dots v_n;J,K\right\rangle$$
$$=-\left\langle v_1,\dots,v_k,\dots,v_l,\dots,v_n;J,K\left|-\frac{\Pi_a\pi_a}{I_a}\right|v_1,\dots,v_k+1,\dots,v_l+1,\dots,v_n;J,K\right\rangle$$
$$=ihc\zeta^a_{kl}(v_k+1)^{\frac{1}{2}}(v_l+1)^{\frac{1}{2}}\left\{\left(\frac{\nu_k}{\nu_l}\right)^{1/2}-\left(\frac{\nu_l}{\nu_k}\right)^{1/2}\right\}AK.$$

The difference in energy between the diagonal elements connected by these matrix elements is in the first case $hc(\nu_k-\nu_l)$

and in the second case $hc(\nu_k+\nu_l)$.

If the effects of the Coriolis interaction are treatwd by second-order perturbation theory, these matrix elements provide energy corrections proportional to K^2 and so they contribute to the effective rotational consatant A_v. However the second-order corrections contain the above energy differences in the denominator; so when $\nu_k \approx \nu_l$ the corrections due to the first type of matrix element will be large and the second-order treatment will not be valid. The corrections due to the second type of matrix element will only be large when the vibration frequencies themselves are very low; for the sake of simplicity we ignore them in the present case, although they could be allowed for by using effective rotational constants.

When $\nu_k \approx \nu_l$ we are forced to employ degenerate perturbation theory. We shall assume that the off-diagonal elements due to asymmetry of the rotor (see III.7) are negligible.

Fundamental Levels.

There will be matrix elements of the first type connecting the fundamental levels ν_k and ν_l, assuming of course that $\zeta^a_{kl} \neq 0$. For given J and K, the vibration-rotation term values, referred to the zero-point level as origin, are the eigenvalues of

$$\begin{bmatrix} \nu_k + F(J,K) & iZK \\ -iZK & \nu_l + F(J,K) \end{bmatrix}$$

where $Z = \zeta^a_{kl} \left\{ \left(\frac{\nu_k}{\nu_l}\right)^{1/2} + \left(\frac{\nu_l}{\nu_k}\right)^{1/2} \right\} A.$

If $|\nu_K - \nu_1| \gg |ZK|$, second-order perturbation theory gives these eigenvalues as $\nu_K + F(J,K) + \frac{Z^2}{\delta_o}K^2$ and $\nu_1 + F(J,K) - \frac{Z^2}{\delta_o}K^2$, where $\delta_o = \nu_K - \nu_1$.

However, when $\nu_K \approx \nu_1$, we must use the correct eigenvalues, namely

$$\nu_\alpha = \tfrac{1}{2}(\nu_K + \nu_1) + F(J,K) + \tfrac{1}{2}\Delta_K$$

and

$$\nu_\beta = \tfrac{1}{2}(\nu_K + \nu_1) + F(J,K) - \tfrac{1}{2}\Delta_K$$

where $\Delta_K^2 = \delta_o^2 + 4Z^2K^2$ and Δ_K is taken to be positive; thus $\Delta_o = |\delta_o|$ and $\nu_\alpha > \nu_\beta$. Note that the energy levels do not depend upon the sign of ζ^a_{kl}.

Suppose now that ψ_K and ψ_1 are the harmonic oscillator wavefunctions for the levels ν_K and ν_1, so that the unperturbed vibration-rotation wavefunctions are $\psi_K\psi_{rot}(J,K)$ and $\psi_1\psi_{rot}(J,K)$. Then the vibration-rotation wavefunctions for the levels ν_α and ν_β are $(a_K\psi_K - i\sigma b_K\psi_1)\psi_{rot}(J,K)$ and $(-i\sigma b_K\psi_K + a_K\psi_1)\psi_{rot}(J,K)$ respectively, in which $a_K = \left(\frac{\Delta_K + \delta_o}{2\Delta_K}\right)^{1/2}$ and $b_K = \left(\frac{\Delta_K - \delta_o}{2\Delta_K}\right)^{1/2}$ (the positive square roots being taken) and σ is $+1$ or -1 according as ζ^a_{kl} is >0 or <0. Thus we can define effective vibrational wavefunctions $\psi_\alpha = a_K\psi_K - i\sigma b_K\psi_1$ and $\psi_\beta = -i\sigma b_K\psi_K + a_K\psi_1$ for the levels ν_α and ν_β, the vibration-rotation coupling being shown by the dependence of the coefficients upon K.

In calculating the intensities of the various rotational transitions, the rotational functions $\psi_{rot}(J,K)$ will give the normal Hönl-London factors in the intensity expression (28, pp. 422 and 426). However the K-dependence of

the effective vibrational wavefunctions ψ_α and ψ_β will lead to an additional K-dependence of the intensity. We will suppose that $\langle 0|\mu|\psi_K\rangle = \mu_K$, with components $\mu_{aK}, \mu_{bK}, \mu_{cK}$, where 0 refers to the zero-point level and μ is the instantaneous electric dipole moment; and similarly $\langle 0|\mu|\psi_1\rangle = \mu_1$.

Then for parallel transitions (K ← K) from the zero-point level, the intensity factors due to the effective vibrational wavefunctions are:

$|\langle 0|\mu_a|\psi_\alpha\rangle|^2 = a_K^2\mu_{aK}^2 + b_K^2\mu_{a1}^2$ and $|\langle 0|\mu_a|\psi_\beta\rangle|^2 = b_K^2\mu_{aK}^2 + a_K^2\mu_{a1}^2$.

Thus, since $a_K^2 + b_K^2 = 1$, the total intensity is unaltered by the coupling, but its distribution between the levels depends upon K and becomes even as $K\to\infty$ (since $a_K\to(\frac{1}{2})^{\frac{1}{2}}$ and $b_K\to(\frac{1}{2})^{\frac{1}{2}}$).

Assuming the a,b,c axes to be right-handed, the vibrational intensity factors for perpendicular transitions from the zero-point K-1 level are (see 3 or 51):

$|\langle 0|\mu_b - i\mu_c|\psi_\alpha\rangle|^2 = a_K^2(\mu_{bK}^2+\mu_{cK}^2) + b_K^2(\mu_{b1}^2+\mu_{c1}^2) - 2a_Kb_KS$ and

$|\langle 0|\mu_b - i\mu_c|\psi_\beta\rangle|^2 = b_K^2(\mu_{bK}^2+\mu_{cK}^2) + a_K^2(\mu_{b1}^2+\mu_{c1}^2) + 2a_Kb_KS$.

Similarly, for perpendicular transitions from the zero-point K+1 level,

$|\langle 0|\mu_b + i\mu_c|\psi_\alpha\rangle|^2 = a_K^2(\mu_{bK}^2+\mu_{cK}^2) + b_K^2(\mu_{b1}^2+\mu_{c1}^2) + 2a_Kb_KS$,

$|\langle 0|\mu_b + i\mu_c|\psi_\beta\rangle|^2 = b_K^2(\mu_{bK}^2+\mu_{cK}^2) + a_K^2(\mu_{b1}^2+\mu_{c1}^2) - 2a_Kb_KS$.

In all these equations S denotes the quantity $\sigma(\mu_{bK}\mu_{c1} - \mu_{cK}\mu_{b1})$. Since $a_K^2 + b_K^2 = 1$, the total intensity is again unaltered and is the same for $\Delta K = \pm 1$ transitions. However for the levels separately the intensity is distributed unsymmetrically between the $\Delta K=+1$ and $\Delta K=-1$ sub-bands, and since a_K and

b_K are both positive the mode of distribution depends only upon the sign of S. If $S>0$, the level ν_α has stronger P-type sub-bands ($K \leftarrow K+1$) and weaker R-type sub-bands; while the level ν_β has stronger R-type sub-bands and weaker P-type sub-bands. If $S<0$, the opposite intensity relationships hold. Thus it will be possible to determine the sign of S from observations of the relative intensities.

Degenerate Vibrations.

We shall suppose that on account of symmetry ν_k and ν_l are both equal to ν_m, say. The distinction between b and c as inertial axes will no longer hold, but it is sufficient that a,b,c remain a right-handed set. We then choose Q_k and Q_l to be the b- and c-components of the doubly degenerate normal coordinate Q_m, so that ζ^a_{kl} becomes ζ^a_m. Then $S=0$, $\Delta_K = 4|\zeta^a_m|AK$ and $a_K = b_K = (\frac{1}{2})^{\frac{1}{2}}$. Thus

$\nu_\alpha = \nu_m + F(J,K) + 2|\zeta^a_m|AK$, $\psi_\alpha = (\frac{1}{2})^{\frac{1}{2}}(\psi_k - i\sigma\psi_l)$ and

$\nu_\beta = \nu_m + F(J,K) - 2|\zeta^a_m|AK$, $\psi_\beta = (\frac{1}{2})^{\frac{1}{2}}(\psi_k + i\sigma\psi_l)(-i\sigma)$.

Because of the choice of normal coordinates, $\mu_{ck} = \mu_{bl} = 0$ and because of symmetry $|\mu_{bk}| = |\mu_{cl}| = \mu_m$. Thus the intensities of the R- and P-sub-bands to the level ν_α are proportional to $\mu_m^2 - S$ and $\mu_m^2 + S$ respectively; in the same way, the intensities of the R- and P-sub-bands to the level ν_β are proportional to $\mu_m^2 + S$ and $\mu_m^2 - S$ respectively. S now has the value $\sigma\mu_{bk}\mu_{cl}$, so that $|S| = \mu_m^2$. Therefore, depending upon the sign of S, one or other of the two sets of transitions is forbidden; this selection rule is due to

Teller and Tisza (63, 62).

It is now necessary to set up a sign convention. Since the signs chosen for the normal coordinates are arbritary, the sign of ζ^a_{kl} or in other words σ is only determined by this arbitrary choice. For the degenerate case, Boyd and Longuet-Higgins (3) fixed the relative signs of Q_k and Q_l (in our notation) by requiring that (Q_k, Q_l) transforms like (μ_b, μ_c), with particular regard to sign; this immediately implies that μ_{bk} and μ_{cl} have the same sign, so that $\mu_{bk} = \mu_{cl}$. Thus $S = \sigma\mu^2_m$. When the normal coordinates are chosen to satisfy this convention we will denote the value of ζ^a_m so obtained by $[\zeta^a_m]$.

Putting $\sigma = +1$ or -1, we see that the level $\nu_m + F(J,K) - 2[\zeta^a_m]AK$, which may be ν_α or ν_β depending upon σ, forms only R-type sub-bands; and the level $\nu_m + F(J,K) + 2[\zeta^a_m]AK$ forms only P-type sub-bands. The R sub-band origins are given by

$$\nu_0^{sub}(R) = \nu_m + \left\{A(1-2[\zeta^a_m]) - B\right\} + 2\left\{A(1-[\zeta^a_m]) - B\right\} K''$$

where $K'' = 0, 1, 2, \ldots$; and the P sub-band origins by

$$\nu_0^{sub}(P) = \nu_m + \left\{A(1-2[\zeta^a_m]) - B\right\} - 2\left\{A(1-[\zeta^a_m]) - B\right\} K''$$

where $K'' = 1, 2, 3, \ldots$. Thus the two sets of sub-bands form a continuous series with constant spacing $2\left\{A(1-[\zeta^a_m]) - B\right\}$.

General Sign Convention.

As an extension which includes Boyd and Longuet-Higgins's convention as a particular case we shall fix the relative signs of Q_k and Q_l in the general case in such a way that

$\mu_{bk}\mu_{cl} - \mu_{ck}\mu_{bl} > 0$. The sign of S therefore becomes that of Δ, i.e. of $[\zeta^a_{kl}]$, which can therefore be determined experimentally.

On the other hand, if we wish to specify the sign of $[\zeta^a_{lk}]$ according to the convention, the requirement becomes $\mu_{bl}\mu_{ck} - \mu_{cl}\mu_{bk} > 0$. Thus between specifying the signs of $[\zeta^a_{kl}]$ and $[\zeta^a_{lk}]$ we have to change the relative signs of Q_k and Q_l. It follows that the antisymmetry relation $\zeta^a_{kl} = -\zeta^a_{lk}$, which holds for a fixed choice of normal coordinates, becomes $[\zeta^a_{kl}] = [\zeta^a_{lk}]$; this is our reason for distinguishing the ζ-s satisfying the convention. If it had been true that the antisymmetry relation persisted for $[\zeta^a_{kl}]$, we would have been left with the problem of determining whether an observed sign corresponded to $[\zeta^a_{kl}]$ or $[\zeta^a_{lk}]$.

Non-Degenerate Vibrations of Equal Intensity.

We shall have occasion to consider (see VI.3) a case in which $\nu_k \neq \nu_l$, but on account of symmetry $\mu_{ck} = \mu_{bl} = 0$; and it will be a good approximation to take $|\mu_{bk}| = |\mu_{cl}|$, so that as a consequence of our sign convention we have $\mu_{bk} = \mu_{cl} = \mu$ (say).

Then, for K→K-1 transitions, $|\langle 0|\mu_b - i\mu_c|\psi_\alpha\rangle|^2 = \mu^2(1-2\sigma a_K b_K)$ and $|\langle 0|\mu_b - i\mu_c|\psi_\beta\rangle|^2 = \mu^2(1+2\sigma a_K b_K)$; and, for K→K+1 transitions, $|\langle 0|\mu_b + i\mu_c|\psi_\alpha\rangle|^2 = \mu^2(1+2\sigma a_K b_K)$ ans $|\langle 0|\mu_b + i\mu_c|\psi_\beta\rangle|^2 = \mu^2(1-2\sigma a_K b_K)$. Now $a_K b_K = \frac{|Z|K}{\Delta_K}$. Thus, since the Hönl-London factors are nearly equal, the ratio of the intensities of the strong and weak sub-bands of given K′ are

$$\frac{\text{strong}}{\text{weak}} = \frac{1 + 2a_K b_K}{1 - 2a_K b_K} = \frac{\Delta_K + 2|Z|K}{\Delta_K - 2|Z|K} = \left(\frac{\Delta_K + 2|Z|K}{\Delta_K}\right)^2,$$ where K means K′.

Overtone and Combination Levels.

There are also matrix elements of Coriolis type connecting the levels $2\nu_k$, $\nu_k+\nu_l$, and $2\nu_l$. For given J and K, the vibration-rotation term values are given approximately by the eigenvalues of

$$\begin{bmatrix} 2\nu_k+F(J,K) & i2^{\frac{1}{2}}ZK & 0 \\ -i2^{\frac{1}{2}}ZK & \nu_k+\nu_l+F(J,K) & i2^{\frac{1}{2}}ZK \\ 0 & -i2^{\frac{1}{2}}ZK & 2\nu_l+F(J,K) \end{bmatrix}$$

These eigenvalues are found to be

$\nu_{vib-rot} = \nu_k + \nu_l + F(J,K) - \frac{1}{2}\lambda\Delta_K$, where λ can take the values 0, ± 2.

More generally, it appears that, for the set of levels which have $\nu_k + \nu_l = V$, the vibration-rotation term values are $\nu_{vib-rot} = \frac{1}{2}V(\nu_k+\nu_l) + F(J,K) - \frac{1}{2}\lambda\Delta_K$ where λ can take the values $V, V-2, V-4, \ldots, -V+2, -V$. This has been established for V=1,2,3 , but has not been proved in general. In the case of exact degeneracy, λ becomes the quantum number of vibrational angular momentum.

CHAPTER IV.

MICROWAVE SPECTRUM OF PROPYNAL.

The microwave spectrum of propynal was first observed by Howe and Goldstein (1955,30) and later studied exhaustively by Costain and Morton (1959,13); the latter workers obtained spectra of fifteen isotopic forms, including isotopic replacement of each atom in turn. Planar propynal can only have pure rotational transitions of types A and B, since the permanent dipole moment must lie in the molecular plane (see I.2); and only these types were observed. In addition, the inertial defect of the zero-point level was found to be positive for all the isotopes and to increase upon deuterium substitution of each hydrogen atom. It was therefore concluded that the molecule was planar in its electronic ground state.

The rotational constants found by Costain and Morton for the zero-point levels of the various hydrogen and deuterium isotopes containing ^{12}C and ^{16}O are given in cm^{-1} in Table 2 (using $c = 2.997929 \times 10^{10}$ cm sec^{-1}). In addition the asymmetry parameter κ (see III.7) and the inertial defect Δ (see II.2) are given.

The structural parameters presented in Table 3 were obtained by Costain and Morton using the method of substitution

coordinates; the estimated uncertainty in the lengths is ±0.001 Å and in the angles ±10′.

Table 2.

	HCCCHO	DCCCHO	HCCCDO	DCCCDO
A_0	2.26912	2.22715	1.72667	1.70367
B_0	0.160985	0.148895	0.159825	0.147739
C_0	0.150091	0.139359	0.146060	0.135747
$\bar{B}_0$	0.155538	0.144127	0.152942	0.141743
$A_0-\bar{B}_0$	2.11358	2.08303	1.57373	1.56193
κ	−0.9897	−0.9909	−0.9826	−0.9847
Δ_0(amu Å^2)	0.1718	0.1785	0.1775	0.1848

Table 3.

$r(C_1H_1)$	1.055 Å	$C_2\hat{C}_1H_1$	180°
$r(C_1C_2)$	1.209	$C_3\hat{C}_2C_1$	178° 24′
$r(C_2C_3)$	1.445	$C_2\hat{C}_3O$	123° 47′
$r(C_3H_2)$	1.106	$C_2\hat{C}_3H_2$	113° 54′
$r(C_3O)$	1.215	$O\hat{C}_3H_2$	122° 19′

Numbering of atoms and inertial axes of light isotope : see Fig. 1, p. 34.

The $C_3C_2C_1$ angle is bent away from the oxygen atom.

Calculation of asymmetric top rotational energies (see III.7) from these constants shows that the molecule exhibits little departure from symmetric top behaviour for $K_a \geqslant 3$: the effects of asymmetry are only serious for $K_a = 0$ or 1.

CHAPTER V.

EXPERIMENTAL.

V.1. Materials.

Propynal was prepared according to the method of Organic Syntheses (1956,41), which is essentially that originally used by Wille and Saffer (1950,66). To propargyl alcohol (56 g.) dissolved in a mixture of concentrated sulphuric acid (68 ml.) and water (220 ml.) was added dropwise a solution of chromium trioxide (105 g.) in concentrated sulphuric acid (68 ml.) and water (200 ml.), the reaction being carried out with stirring and cooling in an ice-salt mixture. A stream of nitrogen introduced into the mixture through a capillary and drawn through by means of a water pump (ca 20 mm.Hg) swept the propynal as it was formed into two traps in series; the first trap was a large one cooled in a solid carbon dioxide / methanol bath and the second a smaller one cooled in liquid air. Salt was added to the condensate of the first trap after warming to room temperature, and the lower aqueous layer was removed. The organic layer from the first trap was added to the condensate of the second trap and the mixture was dried over anhydrous magnesium sulphate and distilled at atmospheric pressure through a 5-inch column of glass beads. The fraction

of b.pt. 54-56°C (13.7 g. ≡ 25% yield) was collected.

Propynal is a mobile colourless liquid which is rather unstable at room temperature, particularly when wet or when exposed to light, and it readily forms a dark-brown solid (presumably polymer) which dissolves easily in acetone. However it can be stored indefinitely at -80°C.

Since the product from the distillation at atmospheric pressure was slightly discoloured, it was purified by several bulb-to-bulb distillations in vacuo, and volatile impurities (probably acetylene and carbon dioxide) were removed by prolonged pumping from a sample held at -80°C.

Ethynyl-deuterated propynal, DCCCHO, was prepared by using in the above method (reduced in scale) a sample of $DCCCH_2OD$ prepared by exchanging normal propargyl alcohol (2 g.) twice with successive samples of 99.8% D_2O (5 g. each time) containing a trace of anhydrous sodium carbonate (3 mg.). The propargyl alcohol was extracted from the first exchange by continuous ether extraction, with the careful exclusion of normal water; and the ether was removed by pumping. The mixture from the second exchange was put straight through the oxidation procedure. The resulting propynal was estimated from its infra-red spectrum to be over 95% DCCCHO.

Since the propargyl-alcohol oxidation is the only method reported as giving a reasonable yield of propynal, and since the preparation of methylene-deuterated propargyl alcohol would involve a fairly roundabout route, methods of preparing propynal

in a manner suitable for a more direct introduction of formyl deuterium were tried. However, Stephen reduction of cyanoacetylene, controlled $LiAlH_4$ reduction of propiolic acid, and pyrolysis of mixed calcium propiolate and calcium formate all proved unsuccessful. Finally, Dr. C.C.Costain generously gave us his sample of HCCCDO (13) which had been prepared from HCDO (1) by condensing with acetylene to form HCCCHDOH and oxidising the latter by the above method. The methylene H was selectively oxidised and the resulting propynal was found to be HCCCDO of high isotopic purity (over 98%).

V.2. Infra-red Spectra.

Infra-red spectra were recorded on a Unicam SP100 spectrophotometer operated as a NaCl prism-grating double monochromator over the range 3600 to 650 cm^{-1} and as a KBr prism monochromator from 700 to 400 cm^{-1} Slit-widths from 1 to 5 cm^{-1} were employed, the narrower slits being used when good resolution of the K-structure was desired. The spectra were calibrated against spectra of standard vapours (18,35).

Propynal vapour pressures from 5 to 150 mm. Hg in a 10-cm cell were sufficient to develop all the important bands of the spectrum. In addition, spectra of liquid propynal and its solutions in carbon disulphide, diethyl ether, and n-hexane were recorded. The carbon disulphide and hexane solution spectra closely resembled that of the vapour, whereas changes due to hydrogen bonding were observed for the pure liquid and

its ether solution (7).

V.3. Ultraviolet Spectra.

Measurements of the ultraviolet absorption of propynal in the vapour state and in iso-octane solution, under low resolution, have been reported by Howe and Goldstein (1958,31). Our measurements refer exclusively to the vapour phase, under better resolution.

(i) Preliminary spectra were recorded with a Hilger medium glass spectrograph above 3600 Å (dispersion 9 Å / mm. at 3800 Å, resolving about 1 cm^{-1}) and a Hilger medium quartz spectrograph (dispersion 25 Å / mm. at 3500 Å, resolving about 5 cm^{-1}), normally using a slit-width of 20μ. The background for the glass spectrograph was provided by a tungsten filament lamp and for the quartz by a hydrogen discharge lamp. The spectra were calibrated with iron-arc spectra, and wavelengths were determined with a Pye comparator used in conjunction with a Hilger microdensitometer.

Path-lengths of up to 5 m. of vapour saturated at 20°C (pressure ca. 150 mm. Hg) were used, and were necessary for good development of bands in the 4100 Å region; however, 10 cm. of vapour at about 20 mm. Hg pressure sufficed for the strong bands in the 3800 Å system.

The effects of temperatures of up to 250°C on the intensities of bands to long wavelengths of 3800 Å was examined, using an absorption cell wound with an electrical heating coil.

Above 200°C decomposition or polymerisation of the vapour became serious, and the cell walls and windows were gradually coated with a brown tarry substance which could be readily washed off with chloroform. For this reason, only temperatures up to 200°C were normally used; these plates were calibrated for optical density by means of a rotating sector.

(ii) High-resolution spectra of the 3800 Å band system were taken by Dr. J.H.Callomon in the second order of the 6-metre Ebert grating spectrograph at University College, London (38), resolving 0.1 cm^{-1} (dispersion 0.2 Å / mm. at 3800 Å). Theoretical slit-widths (usually about 50 μ) were used throughout, and the background continuum was provided by a Xenon discharge. Iron arc calibration wavelengths were taken from the M.I.T. tables (26) and corrected to vacuum by means of Edlen's tables (19). The wavelengths of spectral features were normally determined from enlarged prints, but when the rotational structure was well-developed they were measured from the plates using the Pye comparator.

Path lengths up to 3 m. were used, with vapour pressures up to 100 mm. Hg.

CHAPTER VI.

INFRA-RED SPECTRUM OF PROPYNAL.

Tables 4,5 and 6 contain lists of the features observed in the infra-red spectra of the molecules HCCCHO, DCCCHO and HCCCDO respectively. In preparing these tables, peaks due to rotational sub-band structure of the bands have been disregarded.

VI.1. Band Envelopes.

For a molecule with the inertial constants of propynal (see IV), the rotational structures of the vibrational bands are those of a symmetric top, perturbed near the band origin by the asymmetry. The only rotational structure resolvable with our infra-red spectrometer is the perpendicular-type sub-band structure ($\Delta K = \pm 1$), which has a spacing of approximately $2(A-\bar{B}) \approx 4$ cm.$^{-1}$ However the envelope of the unresolved structure can be used to determine the direction of the vibrational transition moment $\underline{m}$ (I.2). Type A bands ($\underline{m} \parallel a$) lack the perpendicular sub-band structure, but have a fairly sharp central intensity maximum corresponding to unresolved Q branches of the parallel structure ($\Delta K=0, \Delta J=0$); on either side of this sharp maximum are broad wings of similar intensity due to the

P and R branches of the parallel sub-bands ($\Delta K=0, \Delta J=\pm 1$). Bands of type B ($\underline{m} \parallel b$) and type C ($\underline{m} \parallel c$) lack the parallel structure, so that it is possible to observe the effects of asymmetry at the band centre. In type B bands the transitions near the centre are thrown outwards leaving a central minimum, whereas in type C bands they are drawn towards the centre, producing a sharp central maximum. In summary, type A bands have a sharp central maximum flanked by equally strong or stronger broad maxima, and no sub-band structure on the wings; type B bands have a central minimum lying between the broad maxima of the P and R branches, and have sub-band structure on the wings; and type C bands have a strong central maximum with shoulders due to the P and R branches, and have sub-band structure on the wings.

The only distinction which results from symmetry in propynal is between type C bands ($A' \leftrightarrow A''$) and bands which are hybrids of types A and B ($A' \leftrightarrow A'$, $A'' \leftrightarrow A''$). Most of the bands arise from the zero-point level which has symmetry species A'.

The separation between the P and R branches of the hybrid bands can be calculated for a symmetric top according to the formula of Gerhard and Dennison (23). This gives, for the normal isotope, $\nu_R - \nu_P = 16.9$ cm^{-1}; the mean of the observed separations for twelve well-resolved bands was 18 ± 1 cm.$^{-1}$

When the perpendicular sub-band structure was well resolved, it was analyzed by using combination sums and differences (see VIII.3 or 28, p. 434). The sub-bands were

numbered so that the origin would be close to the band centre as determined from the band envelope. The origin and the best value of $(A' - \bar{B}') - (A'' - \bar{B}'')$ were then obtained from the combination sums; less accurate values of $(A' - \bar{B}')$ and $(A'' - \bar{B}'')$ separately were obtained from the combination differences, where it was found necessary to include the centrifugal term in D_K.

Vibrational Analysis.

The fundamentals of the normal isotope are numbered according to the usual convention (28, p.271); the fundamentals of the other isotopes are numbered to correspond with the numbering of the normal isotope. Except where explicitly stated otherwise, the following discussion refers to the normal isotope HCCCHO.

VI.2. Region 0 to 400 cm^{-1}

Frequencies below 400 cm^{-1} are beyond the range of our infra-red spectrometer and have to be obtained from other sources.

Howe and Goldstein (1955, 30) observed satellites to their rotational lines which they attributed to vibrationally excited molecules, and from the temperature dependence of the intensities they derived approximate frequencies of 150±15 and 230±10 cm^{-1} for the two lowest fundamentals.

The low-frequency part of the infra-red spectrum was

examined for us by Professor W.C.Price and his colleagues at King's College, London. Unfortunately, owing to experimental difficulties on account of the instability of propynal, he was only able to observe broads bands centred at 200±10 and 280±10 $cm.^{-1}$

Frequencies of 226 and 261 cm^{-1} were observed in the Raman spectrum by King and Moule (1961, 39) and on the basis of qualitative measurements of Raman depolarisation these were assigned to a″ and a′ modes respectively.

The analysis of the high-resolution ultraviolet spectrum (see VIII.6 and 7) shows that these fundamentals are active in forming hot bands. Howevef, the observed band structures establish that the lower frequency, 205 cm^{-1}, must be an a′ mode and the higher frequency, 261 cm^{-1}, an a″ mode, i.e. the assignments are opposite to those of King and Moule. From the analysis of the K-type rotational structure in the ultraviolet spectrum, it is found that these fundamentals are coupled quite strongly by Coriolis interaction (see III.8 and VIII.7) with rotation about the a-axis, the coupling coefficient being $|\zeta^{a}_{9,12}| = 0.64$. A possible explanation of the positions of the maxima observed by Price could be that the intensity asymmetry produced by the coupling is such that 261 cm^{-1} forms strong R sub-bands and 205 cm^{-1} forms strong P sub-bands; this would imply that $[\zeta^{a}_{9,12}]$ is negative.

These two low-frequency fundamentals were also observed for the two deuterium isotopes, and show only small isotopic

Table 4. Vapour Infra-red Spectrum of HCCCHO.

Peaks with an apparent ε_{max} of >100, 10-100, 1-10 and <1 litre mole^{-1} cm^{-1} are labelled vs, s, m and w respectively.

b = broad band , sh = shoulder

c = central minimum of type B band , C = central maximum of type C band

	cm^{-1}		Assignment
	606	P m	
	615	c	$\nu_8(a')$
sh	628	R	
sh	650	c	$\nu_7(a')$
	661	R vs	
	677	P s	
	695	C s	$\nu_{11}(a'')$
	809	P m	
	818	c	$\nu_8+\nu_9(A')=819$
	826	R m	
	935	P vs	
	945	c	$\nu_6(a')$
	952	R vs	
sh	980		$\nu_{10}(a'')$
	990	R m	
	1143	P w	
	1153	c	$\nu_6+\nu_9(A')=1149$
	1160	R w	
	1169	w	?
	1210	C w	$\nu_6+\nu_{12}(A'')=1204$
	1288	P m	
	1298	c	$2\nu_7(A')=1300$
	1306	R m	
	1322	P m	
	1330	C m	$\nu_7+\nu_{11}(A'')=1343$
	1342	R m	
	1382	P m	
	1389	Q m	$\nu_5(a')$
	1401	R m	
	1687	P vs	
	1697	c	$\nu_4(a')$
	1704	R vs	
	1871	P	
	1877	c	$2\nu_6(A')=1887$
	1889	R m	
	1911	w	?

Table 4 (continued).

	cm^{-1}		Assignment		cm^{-1}		Assignment
	1948	P w			3060	Q w	$\nu_2+\nu_9(A')=3064$
	1959	c	$2\nu_{10}(A')=1962$	sh	3076	P	
	1967	R w			3084	c	$\nu_4+\nu_5(A')=3086$
	1991	P w			3093	R w	
	2000	c	$\nu_5+\nu_8(A')=2003$		3317	P s	
	2013	R w			3326	Q s	$\nu_1(a')$
b	2106	s	$\nu_3(a')$		3335	R s	
	2669	C w	$\nu_4+\nu_{10}(A'')=2678$		3364	P m	
	2733	P m			3374	c	$2\nu_4(A')=3394$
	2742	Q m	$2\nu_5(A')=2778$		3381	R m	
	2753	R m					
	2849	P s					
	2859	Q s	$\nu_2(a')$				
	2870	R s					

Table 5. Vapour Infra-red Spectrum of DCCCHO.

Symbols as in Table 4.

	cm^{-1}		Assignment	cm^{-1}		Assignment
sh	508	c	$\nu_7(a')$	621	R m	
	521	R vs		797	P m	
	531	P s		807	c	$\nu_8+\nu_9(A')=806$
	549	C m	$\nu_{11}(a'')$	814	R m	
	605	P m		927	P vs	
	611	c	$\nu_8(a')$	935	c	$\nu_6(a')$

Table 5 (continued).

	cm^{-1}		Assignment
	943	R vs	
	976	C m	$\nu_{10}(a'')$
	998	P m	
	1015	c	$2\nu_7(A') = 1016$
	1022	R m	
	1042	P m	
	1048	C m	$\nu_7+\nu_{11}(A'') = 1057$
	1059	R m	
	1090	P m	
	1096	c	$2\nu_{11}(A') = 1097$
	1107	R m	
	1133	c	$\nu_6+\nu_9(A') = 1129$
	1139	R w	
	1187	C vw	$\nu_6+\nu_{12}(A'') = 1182$
	1236	w	?
	1378	P ms	
	1386	Q m	$\nu_5(a')$
	1397	R ms	
	1687	P vs	
	1698	c	$\nu_4(a')$
	1705	R vs	
	1853	P w	
	1861	c	$2\nu_6(A') = 1867$
sh	1871	R w	
	1875	P mw	
	1887	Q mw	$\nu_4+\nu_9(A') = 1893$
	1900	R mw	
	1972	P s	
	1977	c	$\nu_3(a')$
	1984	R s	
	2596	P m	
	2605	Q m	$\nu_1(a')$
	2614	R m	
	2671	C w	$\nu_4+\nu_{10}(A'') = 2678$
	2733	P m	
	2742	Q m	$2\nu_5(A') = 2772$
	2753	R m	
	2848	P s	
	2858	Q s	$\nu_2(a')$
	2869	R s	
	3045	P w	
	3053	Q w	$\nu_2+\nu_9(A') = 3054$
	3074	P mw	
	3084	c	$\nu_4+\nu_5(A') = 3085$
	3093	R mw	
	3110	Q mw	?
	3363	P m	
	3373	c	$2\nu_4(A') = 3394$
	3380	R m	

Table 6. Vapour Infra-red Spectrum of HCCCDO.

Symbols as in Table 4.

	cm^{-1}		Assignment		cm^{-1}		Assignment
	602	P m			1344	m	
	610	Q m	$\nu_8(a')$		1378	P m	
sh	620	R m			1385	c	$2\nu_{11}(A')=1383$
sh	650	c	$\nu_7(a')$		1394	R m	
	662	R vs			1661	P vs	
	677	P s			1666	Q vs	$\nu_4(a')$
	692	C s	$\nu_{11}(a'')$		1678	PR vs	
	805	P mw			1690	Q vs	$2\nu_{10}(A')=1682$
	812	Q mw	$\nu_8+\nu_9(A')=813$		1696	R vs	
	841	C s	$\nu_{10}(a'')$	sh	1720		?
	870	P s			1741	P m	
sh	879	Q s	$\nu_6(a')$		1751	c	$2\nu_6(A')=1753$
	888	R s			1760	R m	
	1071	P s			1862	P w	
	1080	c	$\nu_5(a')$		1869	c	$\nu_4+\nu_9(A')=1868$
	1091	R s			1883	P w	
	1108	vw	$\nu_8+2\nu_{12}(A'')=1112$		1891	c	$2\nu_{10}+\nu_9(A')=1892$
	1287	P m			1899	R w	
	1296	c	$2\nu_7(A')=1299$	sh	2101	c s	$\nu_3(a')$
	1303	R m			2108	PR s	
	1328	C m	$\nu_7+\nu_{11}(A'')=1341$		2118	Q s	$\nu_2(a')$
	1336	m			2124	R s	

Table 6 (continued).

cm^{-1}		Assignment	cm^{-1}		Assignment
sh 2150	m	$2\nu_5(A')=2160$	3326 Q	s	$\nu_1(a')$
3317 P	s		3336 R	s	

---

shifts for each substitution; they thus correspond to skeletal modes and so represent the a′ and a″ deformations of the C≡Ĉ-C chain, $\nu_9(a')$ and $\nu_{12}(a'')$ respectively.

Bands arising from the summation levels built from ν_9 and ν_{12} were also observed in the ultraviolet spectra of all three isotopes (see VII.6,7,8); no absorption due to any of these levels was detected in the infra-red spectrum.

VI.3. Region 600 to 750 $cm.^{-1}$

Three overlapping bands are observed between 600 and 750 $cm.^{-1}$ The lowest in frequency, which is also the weakest, has a central minimum at 615 cm^{-1} flanked by P and R branches, and so represents an a′ mode. The upper two bands, roughly equal to each other in intensity, show good K-structure on the wings and so must be essentially perpendicular in type; the central region between 650 and 700 cm^{-1} is complex.

The bands behave differently in the liquid or in ether solution, the 615 absorption remaining sharp and virtually unshifted whereas the upper pair coalesce into a very broad band centred around 705. The 615 band is little affected by

either deuteration; but the upper pair, unaffected by formyl deuteration, undergo a shift of 145 cm^{-1} to low frequency, with little change in appearance, upon ethynyl deuteration.

These observations enable us to characterise the 615 band as the remainigg skeletal fundamental, $\delta(C\hat{C}O)$, $\nu_8(a')$; while the upper pair represent the a′ and a″ deformations $\delta(H-\hat{C}\equiv C)$, ν_7 and ν_{11}, which are seriously affected by hydrogen bonding in the liquid state.

The K-structure on either side of the ν_7,ν_{11} pair has an almost constant spacing of about 7.2 cm^{-1} (see Table 7). This behaviour is quite incompatible with the normal equations for symmetric top energies, which would give either a constant separation of 4.2 cm^{-1} or a degradation of the structure; however it resembles the behaviour of degenerate, Coriolis-coupled, frequencies which show a constant separation of $2\{A(1-[\zeta]) - B\}$ (see III.8). Substitution of the known rotational constants (see IV) gives $[\zeta] = -0.65$ for all three isotopes.

To use the theory of non-degenerate Coriolis coupling (III.8), we must first number the K-structure correctly, which is equivalent to choosing approximate values for the band origins. It was originally assumed (Brand and Watson, 1960, 8) that the upper band was of type B centred at the minimum of intensity at 688 cm^{-1} and the lower band was of type C centred at the strong maximum at 661 cm^{-1}; this then gave $|\zeta^a_{7,11}| = 0.71$. However strong evidence has now been

obtained from the ultraviolet spectrum for the value of ν_{11} in HCCCHO (VIII.10) and slightly weaker evidence for ν_7 in DCCCHO (VIII.11). These observations show that ν_{11} is the higher fundamental whose type C centre is assigned to the peak at 695 cm^{-1}; and the type B centre of ν_7 is to be identified with the onset (at 650 cm^{-1}) of a shoulder on the low frequency side. The numbering of the K-structure can now be revised to take account of these changes.

The frequencies of the sub-bands are given by (III.8):

$$^{R}Q_{K-1}(\nu_{11}) = \tfrac{1}{2}(\nu_{11}+\nu_7) + (\overline{A-B})K^2 + \tfrac{1}{2}\left\{(\nu_{11}-\nu_7)^2+4Z^2K^2\right\}^{\frac{1}{2}} - F_0(0,K-1)$$

$$^{P}Q_{K+1}(\nu_7) = \tfrac{1}{2}(\nu_{11}+\nu_7) + (\overline{A-B})K^2 - \tfrac{1}{2}\left\{(\nu_{11}-\nu_7)^2+4Z^2K^2\right\}^{\frac{1}{2}} - F_0(0,K+1).$$

Thus

$$^{R}Q_{K-1}(\nu_{11}) + {}^{P}Q_{K+1}(\nu_7) = \nu_{11} + \nu_7 - 2(A_0-\bar{B}_0) + 2\left\{(\overline{A-B})-(A_0-\bar{B}_0)\right\}K^2$$

and

$$\left\{{}^{R}Q_{K-1}(\nu_{11}) - {}^{P}Q_{K+1}(\nu_7) - \Delta_2^K F_0(0,K)\right\}^2 = (\nu_{11}-\nu_7)^2 + 4Z^2K^2.$$

The barred rotational constant $(\overline{A-B})$ is a mean value for the ν_{11} and ν_7 levels. Observed values of the ground state combination difference $\Delta_2^K F_0(0,K) = F_0(0,K+1) - F_0(0,K-1)$ from other bands (the best values are from the ultraviolet spectrum) can be used. By plotting the left-hand sides of these equations against K^2, the band origins can be obtained from the intercepts and the rotational constants from the gradients. We then calculate $\left|\zeta^a_{7,11}\right| = \frac{Z(\nu_{11}\nu_7)^{1/2}}{A(\nu_{11}+\nu_7)}$. The results are presented in Table 8. We see that the increased separation of the band origins requires a concomitant increase in $\left|\zeta^a_{7,11}\right|$ to explain the observed structure. The values of

Table 7. Sub-Band Structure of ν_{11} and ν_7 of HCCCHO

K	$^{R}Q_K(\nu_{11})$ observed	$^{P}Q_K(\nu_{11})$ calculated[1]	$^{R}Q_K(\nu_7)$ calculated[2]	$^{P}Q_K(\nu_7)$ observed
2	706.6		657.0	
3	713.0		658.7	638.8
4	720.5	681,3	659.9	631.7
5	728.0	679.3	660.9	625.0
6	735.5	678.5	662.2	617.9
7	742.7	677.8	664.6	610.7
8	750.2	677.1	664.0	603.8
9	758.0	676.3	665.5	597.2
10	765.5	675.8		589.6
11		675.8		583.3
12		675.6		

[1] from $^{P}Q_K = {}^{R}Q_{K-2} - \frac{K}{2}F(0,K-1)$

[2] from $^{R}Q_K = {}^{P}Q_{K+2} + \frac{K}{2}F(0,K+1)$

Table 8. Rotational Analysis of ν_{11} and ν_7.

	HCCCHO	DCCCHO	HCCCDO	
ν_{11}	692.2	548.6	691.9	cm^{-1}
ν_7	649.5	507.9	649.7	cm^{-1}
$(\overline{A-B}) - (A_0-\bar{B}_0)$	+0.019	-0.012	+0.013	cm^{-1}
$[\zeta^{a}_{7,11}]$	$+0.92_2$	$+0.89_2$	$+0.91_5$	

$|\zeta^{a}_{7,11}|$ are now near the value 1 which it must have for the degenerate vibrations of a linear molecule.

By using the known ground state combination differences it is possible to calculate the positions of the sub-bands $^{P}Q_{K}(\nu_{11})$ and $^{R}Q_{K}(\nu_{7})$; these are found to converge strongly with increasing K (see Table 7) and up to at least K=20 they will lie in the region between the origins. No resolved sub-band structure is observed in this region, but the total intensity is considerably greater between the origins than outside them (see Fig. 3). These sub-bands must therefore be the strong set expected from III.8, i.e. the upper level forms strong P sub-bands and the lower level forms strong R sub-bands. Thus $[\zeta^{a}_{7,11}]$ is positive. The reason for the negative sign previously obtained from the sub-band spacing is that we were using there the weak set of sub-bands, which are forbidden in the degenerate case.

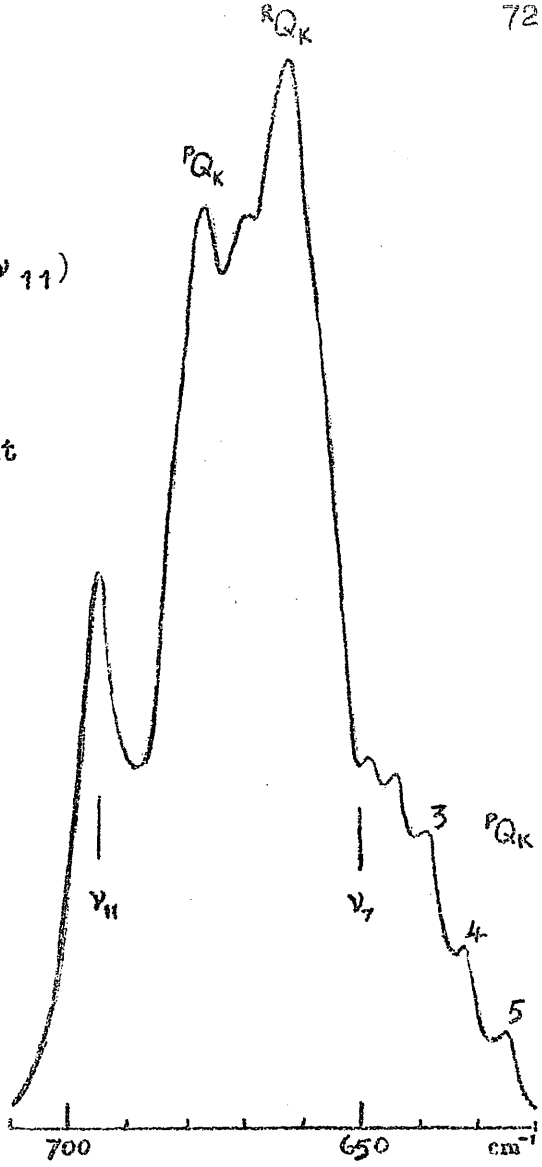

Fig. 3. The 620 to 710 cm^{-1} region of HCCCHO.

On the assumption - which is realised approximately -

that the two bands have equal intensities, we have sufficient information to use the theory of III.8 to calculate the ratio of the intensities of the strong to weak sub-bands of the same K′; the calculated values are given in Table 9, where it can be seen that the ratio rapidly becomes quite large.

Table 9. Ratios of Sub-band intensities (calc.).

K′	strong / weak
1	1.5
2	2.2
3	3.1
4	4.2
5	5.8
6	7.6
7	9.6
8	11.7
9	14.3
10	17.1

An additional point in favour of the new positions of the band origins is that the large anharmonicities previously required to explain the overtones $2\nu_7$ and $2\nu_{11}$ are reduced almost to zero. There is still quite a large anharmonicity involved in the $\nu_7+\nu_{11}$ level.

VI.4. Region 750 to 1000 cm^{-1}.

A hybrid band of medium intensity at 818 cm^{-1}, virtually unshifted by either deuteration, is readily interpreted as the A′ combination $\nu_8+\nu_9$, showing very slight anharmonicity; this provides confirmation of the symmetry of the 205 frequ-

ency. This band has about the same intensity as the fundamental ν_8, which would lead one to expect in addition the unobserved difference band $\nu_8-\nu_9 = 408\ cm^{-1}$; however the combination may derive some of its intensity by Fermi resonance with the nearby C-C stretching fundamental.

This latter fundamental, ν_6, is assigned to the intense hybrid band at 945 cm^{-1} which is 10 cm^{-1} lower in DCCCHO, and in HCCCDO shows a fairly large drop of 66 cm^{-1}, which is however not large enough to be characteristic of a hydrogen vibration. The ν_6 band of HCCCHO and DCCCHO is essentially of type B so that there is well-developed K-structure on the sides of the band; analysis shows that this structure is appreciably degraded to low frequencies, the value of $(A_6-\bar{B}_6) - (A_0-\bar{B}_0)$ being $-0.032\ cm^{-1}$ for HCCCHO.

Immediately to high frequencies of ν_6 is a medium-intense band at 980 cm^{-1} whose envelope is obscured by the sub-bands of ν_6; this band is unshifted and still obscured in DCCCHO. In HCCCDO however there is a well-resolved type C band of similar intensity at 841 cm^{-1} which must be interpreted as a new fundamental and so must correspond to the remaining a″ mode, the out-of-plane wagging of the formyl D atom, ν_{10}. The product rule then shows that the corresponding frequency of the other isotopes is near 980 cm^{-1} and so it is identified with the above band. This assignment is confirmed by the observation of an A″ ground-state interval of 981 cm^{-1} active in the ultraviolet spectra of HCCCHO and DCCCHO; the 841 cm^{-1}

frequency of HCCCDO is also present in its ultraviolet spectrum (see VIII.9). From the K-rotational structure in the ultraviolet bands it is possible to obtain $(A_{10}-\bar{B}_{10}) - (A_0-\bar{B}_0)$ for the ground state of all three isotopes. The values for the ν_6 and ν_{10} levels are collected in Table 10; unfortunately no rotational data is available for ν_6 of HCCCDO yet.

Table 10.

	HCCCHO	DCCCHO	HCCCDO
ν_6	943.7	933.6	879
$(A_6-\bar{B}_6) - (A_0-\bar{B}_0)$	-0.032	-0.029	(+0.042 assumed)
ν_{10}	981.2	980.9	841.0
$(A_{10}-\bar{B}_{10}) - (A_0-\bar{B}_0)$	+0.040	+0.027	-0.042
$\nu_{10} - \nu_6$	37.5	47.3	-38
$\lvert\zeta^a_{6,10}\rvert$	0.25_6	0.25_8	(0.36_6)

The common feature of these observations is that the higher vibrational level has an unusually high value of $(A-\bar{B})$ and the lower has an unusually low value; and these values lie almost symmetrically about the normal value. This effect may be attributed to Coriolis coupling of the fundamentals. Second-order perturbation theory (see III.8) shows that the effective $(A-\bar{B})$ values are $(\overline{A-B})_{6,10} \pm \frac{(\nu_6+\nu_{10})^2 A^2 \lvert\zeta^a_{6,10}\rvert^2}{\nu_6\nu_{10}\lvert\nu_{10}-\nu_6\rvert}$; the values of $\lvert\zeta^a_{6,10}\rvert$ obtained from this equation are included in Table 10. It is seen that the results for the two -CHO isotopes are consistent , but quite different from that

obtained for HCCCDO on the assumption that it conforms to the same pattern; ζ is of course not expected to be isotopically invariant.

VI.5. Region 1000 to 1500 $cm.^{-1}$

Weak bands at 1150 (hybrid) and 1210 (type C), with analogues in DCCCHO but obscured in HCCCDO, can be attributed to $\nu_6+\nu_9$ and $\nu_6+\nu_{12}$ respectively, providing further confirmation of the symmetries of the 205 and 261 vibrations.

Three overlapping bands of medium intensity are found at 1298 (hybrid), 1330 (type C) and 1389 (hybrid), in positions appropriate to the summation tones $2\nu_7$, $\nu_7+\nu_{11}$ and $2\nu_{11}$; and, in agreement, three similar bands occur in almost identical positions for HCCCDO. However, in DCCCHO although the bands $2\nu_7$, $\nu_7+\nu_{11}$ and $2\nu_{11}$ are found suitably shifted to 1015, 1048 and 1096, a medium-intense band at 1386 is still present. This difficulty is removed by an examination of the liquid-phase spectra, where the ν_7 and ν_{11} summations form a very broad absorption ($\Delta\nu_{\frac{1}{2}}$ = 170 cm^{-1}) centred at 1400 cm^{-1}; and on this there is superimposed a sharp band at 1392 cm^{-1}. The 1389 band is therefore assigned as a fundamental (ν_5) largely unchanged in DCCCHO. The band at 1385 in HCCCDO has diminished intensity and is assigned to $2\nu_{11}$, because there is a hitherto unexplained strong band at 1080 cm^{-1}, which is assigned to ν_5. The large isotope shift (309 cm^{-1}) characterises ν_5 as the

formyl in-plane C-H rocking mode. The ν_5 band of HCCCHO is single - no Fermi resonance with $2\nu_{11}$ seems to occur.

The relative intensities of ν_5 and ν_6 change drastically on formyl deuteration. For the two -CHO isotopes ν_6 is five to ten times as strong as ν_5, whereas for the -CDO isotope the intensities are about equal; there appears to be some mixing of the characters of the two modes.

VI.6. Region 1500 to 2000 cm^{-1}.

A strong hybrid band at 1697 cm^{-1}, unchanged in DCCCHO, marks the carbonyl stretching frequency ν_4. In HCCCDO, this band is double, with components of very nearly equal intensity at 1666 and 1690. We attribute this to a Fermi resonance between ν_4 and $2\nu_{10}$ (harmonic value 1682); from the equality of the intensities, it follows that there is an almost exact coincidence of the unperturbed frequencies, which places them both at 1678. This resonance is also observed in the ultraviolet spectrum, where ν_4 is active as a ground-state interval.

Several weak bands in this region can readily be assigned on the basis of the fundamentals so far identified.

VI.7. Region 2000 to 3000 cm^{-1}.

The strong band at 2106 cm^{-1}, which drops to 1977 cm^{-1} in DCCCHO, is assigned to the C≡C stretching fundamental ν_3, while the strong band at 2858 cm^{-1}, which is unaffected

by ethynyl deuteration, is assigned to the formyl C-H stretch (ν_2).

The large drop in ν_2 which occurs on formyl deuteration causes ν_2 to be nearly coincident with the undisplaced ν_3. On account of poor resolution in this region it was not originally realised (Brand and Watson, 8) that the broad band centred at 2108 cm^{-1} in the HCCCDO spectrum is actually double; however, improved resolution has enabled us to separate it into two components of nearly equal intensities, with centres at 2101 and 2118 cm^{-1}. We therefore assign these to ν_3 and ν_2 respectively. The high-frequency shoulder previously identified with ν_2 can be readily reinterpreted as $2\nu_5$.

The presence of a medium-intense band attributable to $2\nu_5$ close to the strong band ν_2 is a common feature of all three spectra; the overtone presumably derives its intensity from Fermi resonance with the fundamental, since a large coupling may be expected on account of the fact that both motions are largely localised in the formyl hydrogen atom.

A weak type C band at 2669 cm^{-1} is readily accounted for by the combination $\nu_4+\nu_{10}$, confirming the value of ν_{10}.

VI.8. Region 3000 to 3600 cm^{-1}.

The only remaining strong band is the hybrid at 3326 in HCCCHO and HCCCDO, which drops to 2605 in DCCCHO; the large isotope effect shows this to be the ethynyl C-H

stretching fundamental ν_1.

The carbonyl overtone $2\nu_4$ at 3374 might be thought to owe its medium intensity to Fermi resonance with ν_1; however this resonance must be discounted since the overtone occurs with comparable intensity in DCCCHO although the fundamental is shifted 721 cm^{-1}.

VI.9. Summary.

The "best" values of all the ground-state fundamental frequencies of the three isotopes are collected in Table 11. Where values are available from several sources the order of preference is :

(a) rotational analysis of ultraviolet bands

(b) rotational analysis of infra-red bands

(c) differences between ultraviolet band centres

(d) infra-red band centres.

The sources are indicated in Table 11. The reasons for this choice are the improved resolution and better calibration used in the ultraviolet, together with the fact that the ultraviolet band centres are better-defined features. The discrepancies between the different values were usually less than 1 cm^{-1}.

A final test of the consistency of the assignments is made by applying the Teller-Redlich product rule (28, p. 231) to the frequencies of each symmetry species. Satisfactory agreement between the observed frequency product ratios

Table 11. Fundamental Frequencies of Propynal (Ground State).

The frequencies are quoted in cm^{-1}.

Species	Mode	HCCCHO	DCCCHO	HCCCDO
	ν_1 C-H_1 stretch	3326 d	2605 d	3326 d
	ν_2 C-H_2 stretch	2858.2 b	2858.6 b	2118 d
	ν_3 C≡C stretch	2106 d	1977 d	2101 d
	ν_4 C=O stretch	1696.9 c	1697.0 c	1679 [1] c
a′	ν_5 C-H_2 rock	1389 d	1387.6 b	1080.0 c
	ν_6 C-C stretch	943.7 b	933.6 b	876.5 c
	ν_7 C-H_1 rock	650.0 b	507.9 b	649.7 b
	ν_8 C-C=O bend	613.7 c	609.9 c	611.9 c
	ν_9 C-C≡C bend	205.3 a	195.6 a	201.5 a
	ν_{10} C-H_2 wag	981.2 a	980.9 a	841.0 a
a″	ν_{11} C-H_1 wag	692.7 a	548.6 b	691.5 b
	ν_{12} C-C≡C bend	260.6 a	248.5 a	249.9 a

[1] corrected for Fermi resonance.

Table 12. Frequency Product Ratios.

The harmonic values are in parentheses.

Species	$\frac{\text{HCCCHO}}{\text{DCCCHO}}$	$\frac{\text{HCCCHO}}{\text{HCCCDO}}$
a′	1.861 (1.892)	1.936 (1.937)
a″	1.324 (1.336)	1.219 (1.218)

and the harmonic values calculated from the microwave rotational constants (13) is obtained (see Table 12).

The zero-point energies of HCCCHO, DCCCHO and HCCCDO are calculated to be 7862, 7275 and 7213 cm^{-1} respectively.

The present measurements show frequency differences of up to more than 20 cm^{-1} from those obtained, apparently under lower resolution, by King and Moule (39). Apart from these, the principal differences in the assignments are :
(i) the interchange of symmetry assignment within each pair of bending modes of the ethynyl group; our choice of these is dictated mainly by the observations in the ultraviolet spectrum to be discussed in Chapter VIII;
(ii) the ν_{10} fundamental of HCCCDO was taken by King and Moule as being near 650 cm^{-1} and so lying under the strong ν_7, ν_{11} absorption; however, our spectrum shows a prominent type C band at 841 cm^{-1}, and this value for ν_{10} is fully confirmed from the ultraviolet spectrum.

VI.10. Related Molecules.

Since it has been possible to assign the fundamentals of propynal largely from the internal evidence of the spectra, it is interesting to compare the frequencies obtained with those of other molecules.

The most closely related molecules for which the effects of the relevant deuterations have been studied are acet-

aldehyde (20a) and propyne (25a). Our observations on the effects of deuterium substitution agree well with those found for these molecules. There is also fairly good agreement in the actual values of the various stretching frequencies, but significant differences occur for some of the bending modes. The formyl C-H wag is considerably higher for propynal (981) than for acetaldehyde (767); however, values of 1030 for formamide (20), 1032 for methyl formate (67), and 1014 (obtained by applying the product rule to DCOF) for formyl fluoride (60) have been found. The C-C=O bend of propynal (614) is also much higher than that for acetaldehyde (512).

The ν_{11} frequency of propynal is higher than the normal range of 630 to 650 in which most ethynyl C≡C-H bends occur (50,57), and the splitting of the a′ and a″ components of this motion is unusually large. Our assignment of ν_7 and ν_{11} contradicts the arguments advanced by Nyquist and Potts (50) concerning the order of these frequencies in conjugated acetylenes. On the other hand, the C-C≡C bending frequencies (205,261) lie well below the range 330 to 350 which is normal for substituted acetylenes (50,57); again the separation of the a′ and a″ components is unusually large.

In view of these unusual features it would be interesting to have a normal coordinate analysis of the propynal frequencies; Prof. G.W.King has informed us that he is engaged on such a calculation.

VI.11. Fermi Resonances.

On account of the low molecular symmetry, the number of theoretically possible Fermi resonances is large. However, Fermi resonance has only to be invoked on comparatively few occasions. Examples are the (ν_2,$2\nu_5$) resonance observed for all three isotopes, and the (ν_4,$2\nu_{10}$) resonance observed for HCCCDO. On the other hand no Fermi resonance seems to occur between ν_1 and $2\nu_4$ of the -C≡C-H isotopes or between the closely degenerate levels ν_5 and $2\nu_{11}$ of the normal isotope. It would seem that, for appreciable anharmonic coupling to occur, the motions involved must be localised in the same region of the molecule, and that the opposite ends of the propynal molecule are well enough separated to avoid this.

The (ν_2,$2\nu_5$) type of resonance appears to be a common feature of aldehydes, since the formyl C-H stretching band is frequently doubled (1a).

VI.12. Coriolis Coupling.

We have seen that each of the a″ modes of propynal is coupled quite strongly to an a′ mode by the Coriolis forces produced by rotation about the a-axis. However the possibility of observing this coupling depends on a more-or-less accidental degeneracy of the fundamentals involved, because the effects produced by the coupling of two fundamentals which are well separated in frequency are small.

Meal and Polo (44) have given sum rules for ζ in asymmetric top molecules; for propynal their rules give $\sum_{k=1}^{9}\sum_{l=10}^{12}(\zeta^{a}_{kl})^{2} = 3$. The sum of our observed $(\zeta^{a})^{2}$ is only 1.32, so we may conclude that there are large ζ^{a}'s connecting the a'' fundamentals to the other a' fundamentals.

VI.13. Centrifugal Distortion.

In the rotational analysis of infra-red bands by combination differences, the rotational constant $(A_0-\bar{B}_0)$ was found to agree within the probable limits of error with the much more accurate values from the microwave spectrum (13). However in each case it was found necessary to include the centrifugal correction term in D_K in order to represent accurately the dependence of the observed combination differences on K. The coefficient D_K could not be determined from the transitions observed in the microwave study, where its effects are included in A.

The values of D_K obtained from the infra-red spectrum (8) are confirmed by the more accurate results of the ultraviolet analysis, which are presented in Table 13.

According to the treatment of Dowling (17), only four of the six asymmetric top distortion constants (see III.7) are independent for a planar molecule. Thus it should be possible to calculate D_K for propynal from the values of D_J, D_{JK}, R_6 and δ_J obtained by Costain and Morton (13).

The value of D_K obtained in this way is included in

Table 13. Observed and Calculated Values of D_K.

		HCCCHO	DCCCHO	HCCCDO
10^4 D_K (in cm^{-1})	observed	2.93	3.15	1.03
	calculated	0.64	0.71	0.40

Table 13. It is seen that the observed D_K's are considerably higher than the calculated ones. In the calculation the ratio of D_K to D_J is found to depend almost entirely upon the principal rotational constants, so that although Costain and Morton's distortion constants are subject to quite large uncertainties it would seem that the calculated values should be accurate to ± 50 %. The discrepancy between observed and calculated is therefore significant. It may be a result of Coriolis effects, which were not allowed for in the theoretical treatment.

CHAPTER VII.

ULTRAVIOLET SPECTRUM OF PROPYNAL.

The absorption spectrum of HCCCHO vapour between 1900 A and 3900 Å under low resolution is shown in Figs. 4 and 5. Four band systems of propynal have been observed to long waves of 2000 Å, the first strong bands of these occurring at 4140, 3820, 2570 and 2140 Å. Brief descriptions and tentative assignments follow.

VII.1. 4140 Å System.

The longest wavelength system is extremely weak, requiring a path length of about 5m. of saturated vapour (ca. 150 mm. Hg) for good development of even the strongest bands; the oscillator strength can be very crudely estimated by comparison with the 3820 Å system to be about 10^{-6}. To short wavelengths of 3920 Å this system is obscured by the bands of the much stronger 3820 Å system.

The 4140 Å system has been examined only under medium resolution, where it shows good vibrational and K-rotational structure. The sub-bands however appear much less sharp than those of the 3820 Å system, probably because of a different degradation of the J-structure. The strong bands of the

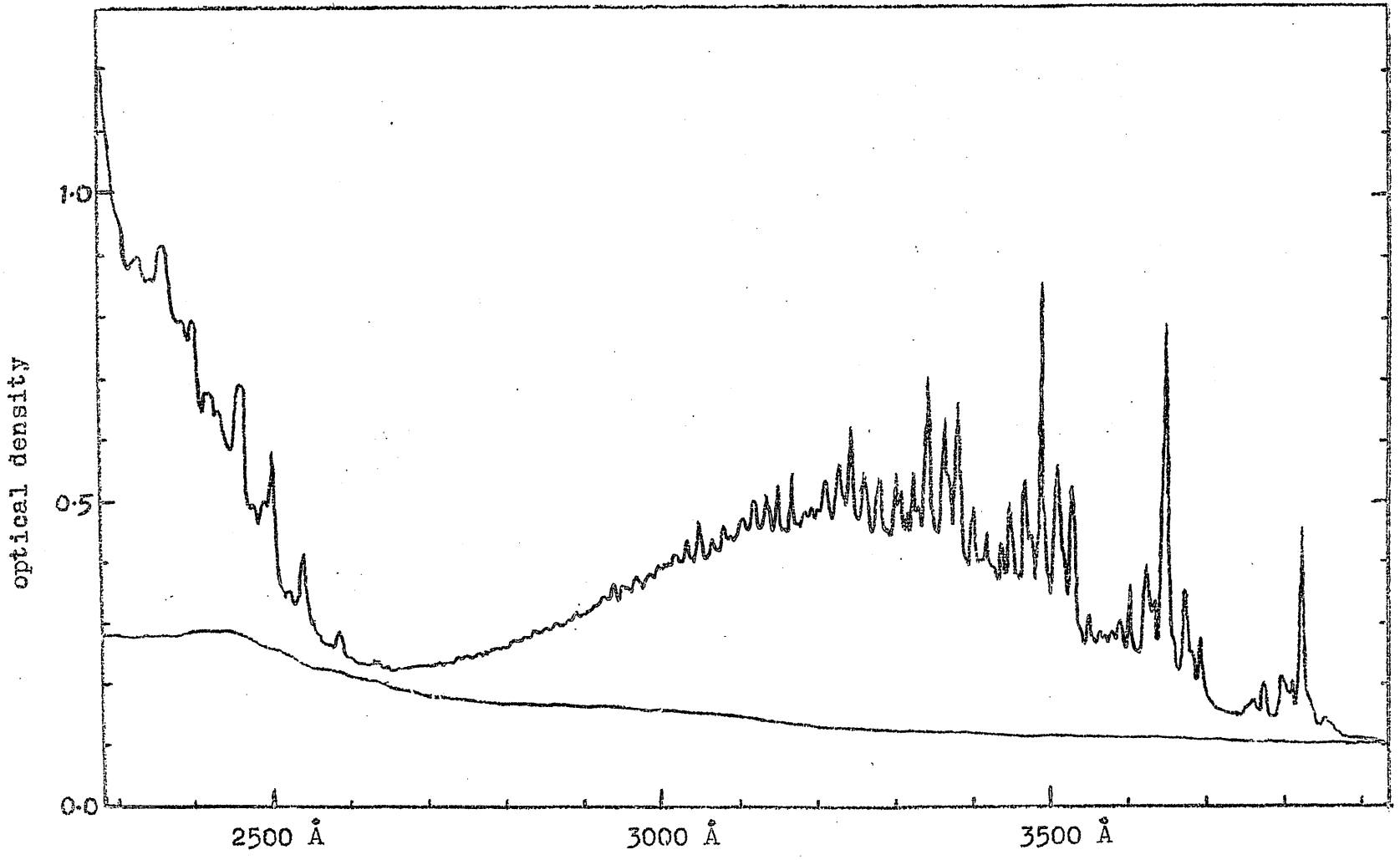

Fig. 4. The low-resolution ultraviolet spectrum of propynal vapour (2300 to 3900 Å). Pressure 50 mm. Hg. Path length 10.4 cm. Lower curve = empty cell.

4140 Å system are of perpendicular type, the K-structure being strongly degraded to low frequencies, with $\Delta(A-\bar{B}) \approx -0.41$ cm^{-1}, so that a head of sub-bands is formed close to the band origin on the high-frequency side.

The origin band of the system is tentatively assigned as the 4140 Å band, whose strongest feature is the R-type sub-band head at 24128.0 cm^{-1}; the origin of this band is near 24118.5 cm^{-1}. The pattern of bands around 4140 Å is repeated with greater intensity in the region of 3930 Å, so we may take the difference, namely 1322 cm^{-1}, as the principal progression-forming interval of this system.

In the strong degradation of the K-structure, the pattern of vibrational structure around the system origin, and the magnitude of the progression-forming vibration, this system closely resembles the 3820 Å system; so we may conclude that the electronic transitions involved are similar.

VII.2. 3820 Å System.

Although still quite weak, the 3820 Å system is several hundred times as strong as the 4140 Å one, so that even the weak bands to the red of the origin submerge the bands of the previous system. An approximate oscillator strength for this transition was estimated from the low-resolution spectra of the vapour; it is 5×10^{-4}. This system was previously examined by Howe and Goldstein (1958, 31); our observations agree with theirs.

Under high resolution the bands of this system show sharp K- and J-rotational structure, and are therefore suitable for detailed study. The strongest bands are of perpendicular type with strongly degraded K-structure ($\Delta(A-\bar{B}) = -0.38$ cm^{-1}) so that a head of sub-bands is formed at high frequencies close to the band origin. The J-structure is, on the other hand, only very weakly degraded to the blue.

We follow Howe and Goldstein in assigning the 3820 Å band (26163.1 cm^{-1}) as the system origin. The vibrational structure is dominated by a progression in 1300 cm^{-1} (see Fig. 4) which passes through an intensity maximum at the third member; all except the first band (the system origin) of this progression are heavily perturbed by Fermi resonance. On either side of the strong bands of this progression is a repeating pattern of weaker bands which closely resembles the pattern around the origin of the 4140 Å system. After the principal progression has died out the complexity of the vibrational structure increases, at the same time becoming more diffuse; the intensity finally falls to nearly zero at 2600 Å.

The 1300 cm^{-1} frequency is unaffected by ethynyl deuteration, but falls to 1268 cm^{-1} on formyl deuteration. It is therefore assigned to the excited state carbonyl stretching frequency, as was suggested by Howe and Goldstein.

The positions, intensities and general structures of the 4140 and 3820 Å systems bear a marked resemblance to those of the two lowest transitions of formaldehyde, and they are

accordingly assigned to similar electronic excitations, namely the promotion of an electron from a non-bonding oxygen p-orbital (a′) to an anti-bonding orbital (a″) of the out-of-plane π-electron shell. The resulting excited electronic configuration (A″) can have singlet and triplet components, and so the weak 4140 Å system is assigned to the spin-forbidden $^3A'' \leftarrow {}^1A'$ transition and the stronger 3820 Å system to the spin-allowed $^1A'' \leftarrow {}^1A'$ transition.

The singlet origin is 2030 cm^{-1} to low frequencies of the corresponding formaldehyde band; the triplet-singlet separation is smaller, being 2045 cm^{-1} in propynal as against 2990 cm^{-1} in formaldehyde (55).

VII.3. 2570 Å System.

The 2570 Å system is largely overlapped by the much stronger 2140 Å one. Discrete vibrational structure is present, but the bands were completely diffuse on our quartz spectrograph plates. These bands show a steep rise in intensity in passing to short waves, so that it is difficult to locate the origin with any certainty; this rise of intensity may be partly due to the background provided by the onset of the intense system.

The vibrational structure of this system is rather irregularly spaced, but the strongest bands and many of the weaker ones show separations in the range 670 ± 50 cm^{-1}. The spectrum is almost unaffected by formyl deuteration, but a

striking closing-up of the structure occurs on ethynyl deuteration, the characteristic spacing in DCCCHO being 510 ± 20 cm^{-1}. The frequency involved can only be one or both of the components of the C≡C-H bending motion. From these rather limited observations we conclude from the Franck-Condon principle that the C≡C-H chain is probably bent in this excited state.

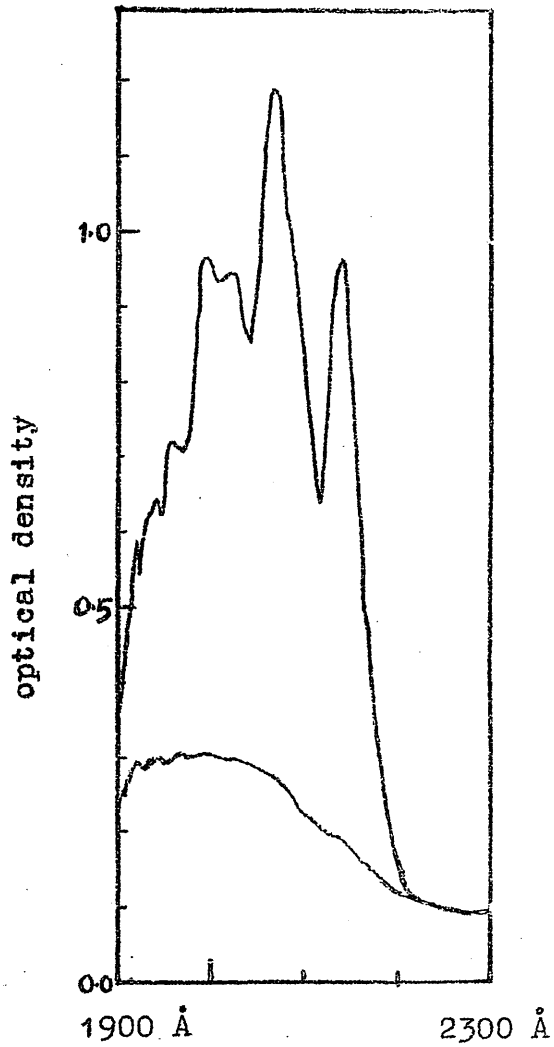

Since this transition resembles the lowest singlet transition of acetylene (origin 2370 Å), it is assigned to an analogous $\pi^* \leftarrow \pi$ transition of the ethynyl group. The transition is regarded as taking place between two mutually perpendicular lobes of the orbitals involved, giving A″ as the electronic symmetry of the excited state. However the individual electron jump

Fig. 5. Low-resolution spectrum of propynal vapour (1900 to 2300 Å). Pressure ca. 0.3 mm Hg. Path length 10.4 cm. Lower curve = empty cell.

is not unique, since it may be $a'' \leftarrow a'$ or $a' \leftarrow a''$, so there may be more than one transition in this region.

VII.4. 2140 Å System.

The 2140 Å absorption is 300 to 500 times as intense as the 3820 Å system. The bands are completely diffuse, but some vibrational structure is evident, involving principally one or two progressions with separations of about 1600 to 1700 cm^{-1}. The probable origin is at 2140 Å (46800 cm^{-1}). The system has maximum absorption at 2080 Å, to short waves of which the intensity falls gradually until 1600 Å where a further region of strong absorption commences. This system was examined in solution by Howe and Goldstein (31) and is being studied in the vapour by Prof. W.C.Price.

A strong transition in this region is a common feature of conjugated carbonyl compounds and is usually assigned to a $\pi^* \leftarrow \pi$ transition within the out-of-plane a'' π-orbitals. The excited state will therefore have $^eA'$ symmetry.

CHAPTER VIII.

ANALYSIS OF THE 3820 Å BAND SYSTEM OF PROPYNAL.

VIII.1. Introduction.

We have previously pointed out (I.1) that the possibility always arises that an electronic transition of a molecule may be accompanied by a change in the equilibrium configuration of the nuclei. In particular, in the light of the formaldehyde analysis (II.2), we must bear in mind that the upper state of the 3820 Å system of propynal may be non-planar, so that all symmetry is lost. However, the formaldehyde results also suggest that, as long as the out-of-plane bending is not too large, the vibronic selection rules will still be those appropriate to the higher symmetry of the ground state. On the other hand, any bending may lead to unusual anharmonicities in the corresponding vibrational modes, and it will be difficult to establish the assignments of bands involving these strongly anharmonic vibrations. The hypothesis of a planar excited state is therefore one which suggests more definite expectations regarding the stricture of the spectrum, and so is one which is more readily tested. Accordingly, our approach to the analysis will be based on a provisional assumption of the planarity of the excited state. Only if inconsistencies arise in

this treatment can the excited state be proved to be non-planar; and in such a case the form of the inconsistencies may tell us something about the bending.

We find it convenient to use the following notation to designate the vibrational assignments of bands in electronic band systems.. If the quantum number v_N of the N-th vibrational mode has the values m and n in the lower and upper levels of a given band, this situation is denoted by the symbol N_m^n ; and the full vibrational assignment is denoted by writing consecutively such symbols for each mode which does not have m = n = 0. Thus $4_0^2 9_1^2 12_1^1$ - which is our assignment of the band at 28961.2 cm^{-1} in HCCCDO - in this shorthand represents (000200002001) - (000000001001) in the conventional notation. It is sometimes more meaningful to separate the symbol into progression and sequence parts, in which case the above transition would be written $4_0^2 9_0^1 . 9_1^1 12_1^1$. Since there is no symbol to represent the origin band, we shall refer to it as the 0 band.

In this context it should be noted that we number the excited state modes to correspond with the most closely analogous mode of the ground state, instead of numbering them within themselves according to the usual rules (28, p. 271). Although rather difficult to define in principle, since the molecular symmetry and normal coordinates may alter drastically on excitation, this procedure has certain practical advantages because the excited state symmetry may be in doubt, the excited state fundamentals are rarely all known, and strict

adherence to the rule can be slightly confusing (e.g. the mode which is essentially trans-bending in acetylene is strictly speaking ν_4 in the ground state but ν_3 in the lowest excited state). In any case, excited state modes are most readily characterised by the formation of sequence bands with the corresponding ground state modes. This will be one of our guides in making the assignments.

Lists of the bands of the 3820 Å system observed for HCCCHO, DCCCHO and HCCCDO will be found in Tables 14, 15 and 16 respectively. These tables are as far as possible comprehensive for the regions covered, although of course some weak bands will have escaped notice. It seemed unwise to attempt to extend the DCCCHO table beyond the band 4_0^1 on account of the numerous Fermi resonances present.

For type C bands the frequencies refer to the sharp line-like feature observed near the band origin; for other bands they are merely estimates of the band origins and do not correspond to observed spectral features. The intensities were estimated from the pressures and path-lengths required for similar development of the various bands, but they have only qualitative significance; they are on an arbitrary scale on which the 0 band of each isotope is taken as 10. The 0 bands of the different isotopes had about the same absolute intensity. The calculated positions of the bands were obtained harmonically from the fundamental frequencies listed in Tables 11 (p.80) and 23(p.156), except that the anharmonic coefficients for ν_4'

given in VIII.5 were used. Negatively running sequences in about 16 cm^{-1} which occur throughout the spectra are disregarded in the columns of separations from the origin band and of intensities; successive members of this sequence usually had a ratio of about 3:1 in intensity, although the ratio was often less when ν_9 was also active in progression. Bands which are thought to involve a Fermi resonance in either state are bracketed together.

VIII.2. Rotational Structures of Bands.

Under high resolution, the K- and J-rotational structures of the bands are readily identified, and are found to correspond to typical prolate symmetric top behaviour when $K > 2$, with minor deviations when $K=2$. Thus the excited state resembles the ground state in being very nearly a symmetric rotor.

The J-structure is only very slightly degraded to high frequencies, so that each sub-band consists of a P and an R branch composed of almost equally-spaced lines and an unresolved Q branch possessing a fairly sharp head on the low-frequency side. In accordance with the normal expectation (28, p.426), the ^{P}P branches are stronger than the ^{P}R ones, and the ^{R}R stronger than the ^{R}P.

In contrast to the J-structure, the K-structure is strongly degraded to low frequencies, and in consequence the R-type sub-bands of perpendicular bands form a head on the high

(cont. on p.117)

Table 14. Band Frequencies and Assignments in the 3820 Å Band System of HCCCHO.

For explanation see p.95. The frequencies are in $cm.^{-1}$

(i) Frequency	(ii) Separation from 0 band	(iii) Band type	(iv) Intensity	(v) Assignment	(vi) Calculated separation
24465.4	-1696.9	C	.004	4_1^0	-1697
549.3	-1613.0	C	.001	$4_1^0 12_1^1$	-1612
657	-1505	C	.001	$4_1^0 9_0^1$	-1508
25180	- 982	B	.02	10_1^0	- 981
219.7	- 942.6	C	.04	6_1^0	- 944
609.2		C		$10_1^1 9_2^2$	
626.2		C		$10_1^1 9_1^1$	
642.6	- 519.7	C	.2	10_1^1	- 519
692	- 470	A	.03	$9_1^0 12_1^0$	- 466
714.2		C		9_4^2	
733.1		C		9_3^1	
750.6	- 411.7	C	.06	9_2^0	- 411
814.9	- 347.4	C	.1	$11_1^0 12_2^1$	- 347
858.7	- 303.6	C	.3	11_1^1	- 303
902.0	- 260.3	A	.7	12_1^0	- 261
904.1		C		9_4^3	
922.8		C		9_3^2	
940.4		C		9_2^1	
956.0	- 206.3	C	1.7	9_1^0	- 205

Table 14 (continued).

(i)	(ii)	(iii)	(iv)	(v)	(vi)
26038.4	- 123.9	C	.04	$9_1^0 12_1^1$	- 120
055.6	- 106.7	C	.2	8_1^1	- 107
130.2	- 32.1	C		9_2^2	- 32
146.7	- 15.6	C		9_1^1	- 16
162.3	0.0	C	10.0	0	0
229.3		C		$12_1^1 9_1^1$	
247.3	85.0	C	2.0	12_1^1	85
272.1		C		$11_0^1 12_1^0 9_1^1$	
291.2	128.9	C		$11_0^1 12_1^0$	129
301.9		C		9_3^4	
319.8		C		9_2^3	
332.2	169.9	C	.2	12_2^2	171
337.0		C		9_1^2	
353.3	191.0	C	3.0	9_0^1	189
390.7	228.4	C	0.1	-	
420.4		C		$9_1^2 12_1^1$	
438.5	276.2	C	0.3	$9_0^1 12_1^1$	275
508.7	346.4	A	3.0	12_0^1	346
526.0		C		9_1^3	
542.5	380.2	C	0.4	9_0^2	379
560.1	397.8	C	0.08	-	
565.7	403.4	C	0.08	8_1^2	400
594.0	431.7	A	0.5	12_1^2	431
625.0	462.7	B	1.5	10_0^1	462

Table 14 (continued).

(i)	(ii)	(iii)	(iv)	(v)	(vi)
26655.2		C		$8_0^1 9_1^1$	
669.3	507.0	C	0.8	8_0^1	507
712	550	B	0.3	$10_0^1 12_1^1$	547
755.2	592.9	C	0.2	$8_0^1 12_1^1$	592
814	652	B	0.3	$9_0^1 10_0^1$	652
839.4		C		$12_0^2 9_1^1$	
855.2	692.9	C	0.3	12_0^2	692
884.4		C		$10_0^2 9_2^1$	
900.4	738.1	C	0.4	$10_0^2 9_1^0$	719
911.4	749.1	C	0.4	$6_0^1 9_1^0$	746
936.2	772.9	C	0.2	$4_0^1 10_1^1$	785
955.0	792.7	C	0.2	$5_0^1 9_0^1 10_1^1$	790
980.2		C		$10_0^2 8_1^1 9_1^1$	
996.0	832.7	C	0.3	$10_0^2 8_1^1$	817
27008.9	846.6	C	0.3	$6_0^1 8_1^1$	845
090.7		C		$10_0^2 9_1^1$	
104.7		C		$6_0^1 9_1^1$	
106.2	943.9	C	2.0	10_0^2	924
119.0	956.7	C	3.0	6_0^1	952
179.2	1016.9	C	0.5	8_0^2	1014
208.5	1046.2	C	0.7	$6_0^1 12_1^1$	1037
236.8		C		$4_0^1 9_2^1$	
27256.6	1094.3	C	3.0	$4_0^1 9_1^0$	1099
270.5	1108.2	C	3.0	$5_0^1 9_1^1$	1104

Table 14 (continued).

(i)	(ii)	(iii)	(iv)	(v)	(vi)
27282.3	1120.0	C	4.0	5_0^1	1120
339.2	1166.9	C	0.3	$4_0^1 9_1^0 12_1^1$	1184
352.7	1190.4	C	0.3	$5_0^1 9_1^1 12_1^1$	1189
356.1	1193.8	C	0.4	$4_0^1 8_1^1$	1197
368.4	1206.1	C	0.8	$5_0^1 9_0^1 8_1^1$	1202
443.3		C		$4_0^1 9_1^1$	
459.9		C		$5_0^1 9_1^2$	
462.3	1300.0	C	15.0	4_0^1	1304
474.3	1312.0	C	7.5	$5_0^1 9_0^1$	1309
526.9		C		$4_0^1 12_1^1 9_1^1$	
548.0	1385.7	C	3.0	$4_0^1 12_1^1$	1389
563.2	1400.9	C	1.0	$5_0^1 9_0^1 12_1^1$	1394
592.6	1430.3	C	0.4	$4_0^1 11_0^1 12_1^0$	1433
606.3	1444.0	C	0.4	$5_0^1 9_0^1 11_0^1 12_1^0$	1438
630.4		C		$4_0^1 9_1^2$	
649.7	1487.4	C	5.0	$4_0^1 9_0^1$	1493
665.8	1503.5	C	2.0	$5_0^1 9_0^2$	1498
736.4	1574.1	C	0.3	$4_0^1 9_0^1 12_1^1$	1579
754.8	1592.5	C	0.1	$5_0^1 9_0^2 12_1^1$	1584
788.6	1626.3	C	1.0	$5_0^1 8_0^1$	1626
809	1647	A	5.0	$4_0^1 12_0^1$	1650
822	1660	A	2.0	$5_0^1 9_0^1 12_0^1$	1655
835.8	1673.5	C	0.3	-	
839.7	1677.4	C	0.2	$4_0^1 9_0^2$	1683
855.8	1693.5	C	0.1	$5_0^1 9_0^3$	1688

Table 14 (continued).

(i)	(ii)	(iii)	(iv)	(v)	(vi)
27918	1756	B	2.5	$4_0^1 10_0^1$	1766
936	1774	B	0.4	$5_0^1 9_0^1 10_0^1$	1771
966.5	1804.2	C	0.4	$4_0^1 8_0^1$	1811
977.6	1815.3	C	0.4	$5_0^1 9_0^1 8_0^1$	1816
28049.3	1887.0	C	0.5	$6_0^1 10_0^2$	1876
056.1	1893.8	C	0.5	6_0^2	1903
088.2		C		$3_0^1 9_1^1$	
107.8	1945.5	C	1.8	3_0^1	1946
208.8	2046.5	C		$5_0^1 9_1^1 10_0^2$	2028
214.8	2052.5	C		$4_0^1 6_0^1 9_1^0$	2050
226.8	2064.5	C	2.0	$5_0^1 10_0^2$	2044
238.8	2076.5	C	0.8	$5_0^1 6_0^1$	2071
294.0	2131.3	C	0.2	$3_0^1 9_0^1$	2135
363.4	2201.1	C	0.8	$4_0^1 5_0^1 9_1^0$	2218
395.8	2233.5	C	4.0	5_0^2	2239
405.5	2243.2	C	1.0	$4_0^1 10_0^2$	2226
411.5	2249.2	C	2.0	$5_0^1 9_0^1 10_0^2$	2233
417.8	2255.5	C	3.0	$4_0^1 6_0^1$	2256
429.9	2267.6	C	2.0	$5_0^1 9_0^1 6_0^1$	2261
504.5	2342.2	C	0.5	$4_0^1 6_0^1 12_1^1$	2341
516.3	2354.0	C	0.2	$5_0^1 6_0^1 9_0^1 12_1^1$	2346
538.5	2376.2	C	2.5	$4_0^2 9_1^0$	2388
551.5	2389.2	C	1.5	$4_0^1 5_0^1 9_1^1$	2408
569.7	2407.4	C	5.0	$4_0^1 5_0^1$	2424
589.1	2426.8	C	3.0	$5_0^2 9_0^1$	2428

Table 14 (continued).

(i)	(ii)	(iii)	(iv)	(v)	(vi)
28656.7	2494.4	C	0.6	$4_0^1 5_0^1 12_1^1$	2509
677.7	2515.4	C	0.4	$5_0^2 9_0^1 12_1^1$	2514
745.2	2582.9	C	12.0	4_0^2	2593
758.9	2596.6	C	12.0	$4_0^1 5_0^1 9_0^1$	2613
780.8	2618.5	C	3.0	$5_0^2 9_0^2$	2618
830.9	2668.6	C	1.0	$4_0^2 12_1^1$	2678
847.4	2685.1	C	1.2	$4_0^1 5_0^1 9_0^1 12_1^1$	2698
871.5	2709.2	C	1.0	$5_0^2 9_0^2 12_1^1$	2703
891.7	2729.4	C	0.3	$4_0^1 5_0^1 9_0^1 11_0^1 12_1^0$	2742
911.1	2748.8	C	1.0	$5_0^2 9_0^2 11_0^1 12_1^0$	2747
907.0		C		$4_0^2 9_1^2$	
928.6	2766.3	C	5.0	$4_0^2 9_0^1$	2782
947.9	2785.6	C	3.5	$4_0^1 5_0^1 9_0^2$	2802
972.2	2809.9	C	0.3	$5_0^2 9_0^3$	2807
29098.6		C		$2_0^1 9_1^1$	
114.8	2952.5	C	2.5	2_0^1	2953
166.7	3004.4	C	0.3	-	
191	3029	B	1.5	$4_0^2 10_0^1$	3055
215	3053	B	0.5	$4_0^1 5_0^1 9_0^1 10_0^1$	3075
261.3	3099.0	C	0.8	$4_0^2 8_0^1$	3100
342.1	3179.8	C	1.5	$5_0^2 10_0^2$	3163
362.4	3200.1	C	0.5	$5_0^2 6_0^1$	3191
395.4	3233.1	C	0.8	$3_0^1 4_0^1$	3250
410.7	3248.4	C	0.8	$3_0^1 5_0^1 9_0^1$	3255

Table 14 (continued).

(i)	(ii)	(iii)	(iv)	(v)	(vi)
29505	3343	C	1.0	$4_0^1 5_0^1 10_0^2$	3348
519	3357	C	0.6	$4_0^1 5_0^1 6_0^1$	3375
533	3371	C	0.6	$5_0^2 6_0^1 9_0^1$	3380
634.1	3471.8	C	1.0	$4_0^2 5_0^1 9_1^0$	3507
653.1	3490.8	C	1.0	$4_0^2 10_0^2$	3517
665.0	3502.7	C	1.5	$4_0^2 6_0^1$	3544
670.9	3508.6	C	3.5	$4_0^1 5_0^2$	3543
689.3	3527.0	C	3.5	$4_0^1 5_0^1 9_0^1 10_0^2$	3537
694.3	3532.0	C	3.5	$4_0^1 5_0^1 9_0^1 6_0^1$	3575
708.9	3546.6	C	3.5	$5_0^2 9_0^2 6_0^1$	3569
717.2	3554.9	C	1.0	$5_0^3 9_0^1$	3548
748.3	3586.0	C	0.5	-	
802.2	3639.9	C	2.5	$4_0^3 9_1^0$	3661
820.5	3658.2	C	2.5	$4_0^2 5_0^1 9_1^1$	3697
846.0	3683.7	C	3.5	$4_0^1 5_0^2 9_1^2$	3717
838.5	3676.2	C	5.0	$4_0^2 5_0^1$	3712
861.8	3699.5	C	5.0	$4_0^1 5_0^2 9_0^1$	3732
889.6	3727.3	C	1.5	$5_0^3 9_0^2$	3737
926.8	3764.5	C	1.0	$4_0^2 5_0^1 12_1^1$	3798
950.7	3788.4	C	1.0	$4_0^1 5_0^2 9_0^1 12_1^1$	3818
30007.6	3845.3	C	5.0	4_0^3	3866
025.6	3863.3	C	5.0	$4_0^2 5_0^1 9_0^1$	3902
050.9	3888.6	C	3.5	$4_0^1 5_0^2 9_0^2$	3922
080.1	3917.8	C	0.8	$5_0^3 9_0^3$	3927

Table 15. Band Frequencies and Assignments in the 3820 A Band System of DCCCHO.

(i)	(ii)	(iii)	(iv)	(v)	(vi)
24494.8	-1697.0	C	0.004	4_1^0	-1697
25211.0	- 980.8	B	0.02	10_1^0	- 981
259.2	- 932.6	C	0.04	6_1^0	- 934
581.7	- 610.1	C	0.02	8_1^0	- 610
656.5		C		$10_1^1 9_1^1$	
670.2	- 521.6	C	0.15	10_1^1	- 522
683.6	- 508.2	C	0.04	-	
694.8	- 497.0	C	0.02	12_2^0	- 497
710.2		C		$11_1^1 9_3^2$	
724.2		C		$11_1^1 9_2^1$	
738.4	- 453.4	C	0.08	$11_1^1 9_1^0$	- 453
769.6		C		9_4^2	
784.6		C		9_3^1	
800.4	- 391.4	C	0.08	9_2^0	- 391
895.7		C		$11_1^1 9_3^3$	
908.1		C		$11_1^1 9_2^2$	
920.9		C		$11_1^1 9_1^1$	
934.0	- 257.8	C	0.5	11_1^1	- 258
943.4	- 248.4	A	0.5	12_1^0	- 249
951.8		C		9_4^3	
966.8		C		9_3^2	
981.3		C		9_2^1	
995.7	- 196.1	C	1.0	9_1^0	- 196

Table 15 (continued).

(i)	(ii)	(iii)	(iv)	(v)	(vi)
26016.7	- 175.1	C	0.08	$9_1^0 7_1^1$	- 174
055.7		C		$8_1^1 9_1^1$	
068.3	- 123.5	C	0.4	8_1^1	- 123
111.2	- 80.6	C	0.4	$7_0^1 8_1^0$	- 81
149.1	- 41.7	C		9_3^3	- 36
164.2	- 27.6	C		9_2^2	- 24
178.3	- 13.5	C		9_1^1	- 12
191.8	0.0	C	10.0	0	0
213.1	21.3	C	0.6	7_1^1	21
233.1	41.3	C	0.2	$11_0^1 12_1^0$	43
258.6		C		$12_1^1 9_2^2$	
274.4		C		$12_1^1 9_1^1$	
290.1	98.3	C	2.0	12_1^1	98
330.8		C		9_3^4	
346.7		C		9_2^3	
360.7		C		9_1^2	
375.4	183.6	C	2.5	9_0^1	184
387.6	195.8	C	0.6	12_2^2	197
441.9		C		$12_1^1 9_2^3$	
458.4		C		$12_1^1 9_1^2$	
473.9	282.1	C	0.5	$12_1^1 9_0^1$	282
527.5		C		9_2^4	
538.9	347.1	A	2.5	12_0^1	347
542.7		C		9_1^3	

Table 15 (continued).

(i)	(ii)	(iii)	(iv)	(v)	(vi)
26556.7	364.9	C	0.2	9_0^2	367
635.8	444.0	A	0.8	12_1^2	445
650.9	459.1	B	1.5	10_0^1	459
678.2	486.4	C	0.5	8_0^1	487
720.8	529.0	C	0.5	7_0^1	529
748	556	B	0.3	$10_0^1 12_1^1$	557
780.0	588.2	C	0.5	11_0^2	582
838.2	646.4	C	0.5	$11_0^1 12_0^1$	638
860.8	669.0	C	0.2	$8_0^1 9_0^1$	670
876.4	684.6	C	0.2	-	
885.0	693.2	C	0.2	12_0^2	694
904.6	712.8	C	0.1	$7_0^1 9_0^1$	713
927.8	736.0	C	0.3	$6_0^1 9_1^0$	741
942.9	751.1	C	0.3	$10_0^2 9_1^0$	722
997.5	805.7	C	0.2	$10_0^1 12_0^1$	806
27051.0	859.2	C	0.3	-	
072.5	880.7	C	0.5	-	
115.8		C		$6_0^1 9_1^1$	
124.0	932.2	C	2.0	6_0^1	937
127.0		C		$10_0^2 9_1^1$	
139.3	947.5	C	0.8	10_0^2	918
167.8	976.0	C	0.5	8_0^2	973
183.2	991.4	C	0.5	$5_0^1 8_1^1$	992
203.8	1012.0	C	0.3	$7_0^1 8_0^1$	1016

Table 15 (continued).

(i)	(ii)	(iii)	(iv)	(v)	(vi)
27226.8	1035.0	C	0.7	$5_0^1 7_0^1 8_1^0$	1034
238.5	1046.7	C	1.5	$4_0^1 11_1^1$	1041
252.3		C		$5_0^1 9_3^3$	
270.1		C		$5_0^1 9_2^2$	
276.8		C		$4_0^1 9_2^1$	
285.0		C		$6_0^1 9_2^3$	
287.5	1095.7	C	3.5	$5_0^1 9_1^2$	1103
294.0	1102.2	C	1.0	$4_0^1 9_1^0$	1103
301.6	1109.8	C	1.0	$6_0^1 9_1^2$	1108
304.6	1112.8	C	3.5	5_0^1	1115
311.6	1119.8	C	2.5	$6_0^1 9_0^1$	1120
346.6	1154.8	C	0.3	-	
370.1	1178.3	C	0.5	$4_0^1 8_1^1$	1175
384.6	1192.8	C	1.0	$5_0^1 9_1^1 12_1^1$	1201
406.6	1214.8	C	1.0	$5_0^1 12_1^1$	1213
483.7	1291.9	C	8.0	$5_0^1 9_0^1$	1299
490.1	1298.3	C	8.0	4_0^1	1299
497.5	1305.7	C	8.0	$6_0^1 9_0^2$	1304

Table 16. Band Frequencies and Assignments in the 3820 A Band System of HCCCDO.

(i)	(ii)	(iii)	(iv)	(v)	(vi)
24514	-1692	C	0.002	10_2^0	-1682
537	-1669	C	0.002	4_1^0	-1679
25126	-1080	C	0.01	5_1^0	-1080
317.2		C		$6_1^0 9_1^1$	
329.5	- 876.5	C	0.04	6_1^0	- 877
365	- 841	B	0.02	10_1^0	- 841
686.3	- 519.7	C	0.01	$10_1^0 12_0^1$	- 519
740.6	- 465.4	C	0.04	-	
761.0		C		$10_1^1 9_1^1$	
775.3	- 430.7	C	0.2	10_1^1	- 430
801.7	- 404.3	C	0.04	9_2^0	- 403
875.9		C		$11_1^1 9_1^1$	
889.3	- 316.7	C	0.3	11_1^1	- 317
956.6	- 249.4	A	0.5	12_1^0	- 250
958.4		C		9_4^3	
973.9		C		9_3^2	
989.2		C		9_2^1	
26004.3	- 201.7	C	1.0	9_1^0	- 202
057.1		C		$12_1^1 9_2^1$	
073.0	- 133.0	C	0.3	$12_1^1 9_1^0$	- 130
094.2	- 111.8	C	0.8	8_1^1	- 112
161.2	- 44.8	C		9_3^3	- 42
176.4	- 29.6	C		9_2^2	- 28

Table 16 (continued).

(i)	(ii)	(iii)	(iv)	(v)	(vi)
26191.8	- 14.2	C		9_1^1	- 14
206.0	0.0	C	10.0	0	0
261.6		C		$12_1^1 9_1^1$	
277.6	71.6	C	1.6	12_1^1	72
347.6		C		9_3^4	
349.8	143.8	C	0.4	12_2^2	144
363.8		C		9_2^3	
379.3		C		9_1^2	
393.9	187.9	C	2.5	9_0^1	187
422.3	216.3	C	0.1	12_3^3	216
433.2		C		$12_1^1 9_2^3$	
450.3		C		$12_1^1 9_1^2$	
466.0	260.0	C	0.6	$12_1^1 9_0^1$	259
528.3	322.3	A	2.0	12_0^1	322
550.4		C		9_2^4	
566.5		C		9_1^3	
581.2	375.2	C	0.4	9_0^2	375
599.0	393.0	A	0.8	12_1^2	394
617.7	411.7	AB	1.2	10_0^1	411
666.2	460.2	C	0.3	-	
675.3		C		$8_0^1 9_2^2$	
691.1		C		$8_0^1 9_1^1$	
697.5	491.5	A	0.3	$10_0^1 12_1^1$	483
706.1	500.1	C	1.0	8_0^1	500

Table 16 (continued).

(i)	(ii)	(iii)	(iv)	(v)	(vi)
26777.3	571.3	C	0.1	$8_0^1 12_1^1$	572
796.1	590.1	C	0.05	-	
849.1	643.1	C	0.1	12_0^2	644
862.0		C		$8_0^1 9_2^3$	
878.3		C		$8_0^1 9_1^2$	
893.3	687.3	C	0.3	$8_0^1 9_0^1$	687
903.6		C		$6_0^1 9_4^3$	
918.0		C		$6_0^1 9_3^2$	
932.6		C		$6_0^1 9_2^1$	
945.9	739.9	C	0.3	$6_0^1 9_1^0$	741
952.7		C		$10_0^1 11_0^1 9_2^2$	
968.5		C		$10_0^1 11_0^1 9_1^1$	
982.9	776.9	C	0.5	$10_0^1 11_0^1$	786
27003.1	797.1	C	0.1	-	
007.0		C		$4_0^1 10_1^1 9_2^2$	
008.2	802.2	C	0.1	-	
022.6		C		$4_0^1 10_1^1 9_1^1$	
030.1	824.1	C	0.2	5_0^1	824
038.4	832.4	C	0.3	$4_0^1 10_1^1$	838
040.8	834.8	C	0.2	10_0^2	823
053.1	847.1	C	0.1	-	
121.1		C		$6_0^1 9_2^2$	
134.9		C		$6_0^1 9_1^1$	
147.9	941.9	C	4.0	6_0^1	942

Table 16 (continued).

(i)	(ii)	(iii)	(iv)	(v)	(vi)
27193.9		C		$8_0^2 9_1^1$	
209.0	1003.0	C	0.7	8_0^2	1000
223.2		C		$4_0^1 9_4^3$	
224.1	1018.1	A	1.0	$4_0^1 12_1^0$	1018
239.5		C		$4_0^1 9_3^2$	
255.6		C		$4_0^1 9_2^1$	
271.5	1065.5	C	3.0	$4_0^1 9_1^0$	1066
321.2		C		$6_0^1 9_1^2$	
336.7	1130.7	C	1.0	$6_0^1 9_0^1$	1130
358.0	1152.0	C	1.2	$4_0^1 8_1^1$	1156
443.0		C		$4_0^1 9_2^2$	
458.5		C		$4_0^1 9_1^1$	
473.4	1267.4	C	16.0	4_0^1	1268
526.5		C		$4_0^1 12_1^1 9_1^1$	
543.9	1337.9	C	4.0	$4_0^1 12_1^1$	1340
611.5		C		$4_0^1 9_3^4$	
614.0	1408.0	C	0.8	$4_0^1 12_2^2$	1411
628.5		C		$4_0^1 9_2^3$	
644.6		C		$4_0^1 9_1^2$	
660.1	1454.1	C	6.0	$4_0^1 9_0^1$	1455
695.4		C		$4_0^1 12_1^1 9_2^3$	
714.0		C		$4_0^1 12_1^1 9_1^2$	
731.2	1525.2	C	0.8	$4_0^1 12_1^1 9_0^1$	1527
795.1	1589.1	A	3.0	$4_0^1 12_0^1$	1589

Table 16 (continued).

(i)	(ii)	(iii)	(iv)	(v)	(vi)
27797.5		C		$4_0^1 9_3^5$	
814.8		C		$4_0^1 9_2^4$	
831.4		C		$4_0^1 9_1^3$	
847.2	1641.2	C	1.2	$4_0^1 9_0^2$	1642
880.0	1674.0	AB	1.7	$4_0^1 10_0^1$	1679
969.7	1763.7	C	2.0	$4_0^1 8_0^1$	1768
28042	1836	C	0.5	-	
084.5	1878.5	C	1.0	6_0^2	1885
139.9		C		$4_0^1 8_0^1 9_1^2$	
151.8	1945.8	C	1.2	3_0^1	1946
155.7	1949.7	C	1.2	$4_0^1 8_0^1 9_0^1$	1955
194.3	1988.3	C	0.3	$2_0^1 9_1^0$	2003
209.5	2003.5	C	1.5	$4_0^1 10_0^1 12_0^1$	2001
225.1	2019.1	C	0.5	$4_0^1 6_0^1 9_1^0$	2008
254.5	2048.5	C	0.5	$4_0^1 10_0^1 11_0^1$	2054
325.4	2119.4	C	0.2	-	
395.8	2189.8	C	4.0	2_0^1	2204
427.3	2221.3	C	3.5	$4_0^1 6_0^1$	2210
468.6	2262.6	C	1.0	$2_0^1 12_1^1$	2276
489.8		C		$4_0^2 9_3^2$	
496.7	2290.7	C	0.5	$4_0^1 6_0^1 12_1^1$	2282
507.1		C		$4_0^2 9_2^1$	
523.7	2317.7	C	3.0	$4_0^2 9_1^0$	2319
550.7	2344.7	C	0.3	-	

Table 16 (continued).

(i)	(ii)	(iii)	(iv)	(v)	(vi)
28568.3		C		$2_0^1 9_1^2$	
583.1	2377.1	C	2.0	$2_0^1 9_0^1$	2391
605.5	2399.5	C	0.3	$4_0^2 8_1^1$	2408
613.8	2407.8	C	1.5	$4_0^1 6_0^1 9_0^1$	2397
709.4		C		$4_0^2 9_1^1$	
725.4	2519.4	C	25	4_0^2	2520
779.3		C		$4_0^2 12_1^1 9_1^1$	
793.1	2587.1	C	5.0	$4_0^2 12_1^1$	2592
810.4	2604.4	C	0.5	-	
877.7		C		$4_0^2 9_2^3$	
895.1		C		$4_0^2 9_1^2$	
911.3	2705.3	C	5.0	$4_0^2 9_0^1$	2708
961.2		C		$4_0^2 12_1^1 9_1^2$	
979.1	2773.1	C	1.5	$4_0^2 12_1^1 9_0^1$	2780
29044.7	2838.7	A	2.0	$4_0^2 12_0^1$	2842
045.0		C		$4_0^2 9_3^5$	
063.3		C		$4_0^2 9_2^4$	
080.3		C		$4_0^2 9_1^3$	
096.8	2890.8	C	3.0	$4_0^2 9_0^2$	2895
128.7	2922.7	AB	1.5	$4_0^2 10_0^1$	2932
166.1	2960.1	C	0.6	$4_0^2 12_1^1 9_0^2$	2967
216.1	3010.1	C	3.0	$4_0^2 8_0^1$	3020
321.2	3115.2	C	3.0	$2_0^1 6_0^1$	3146
364.7	3158.7	C	2.5	$4_0^1 6_0^2$	3152

Table 16 (continued).

(i)	(ii)	(iii)	(iv)	(v)	(vi)
29418.0	3212.0	C	2.5	$4_0^1 3_0^1$	3213
459.7	3253.7	C	0.8	$4_0^2 10_0^1 12_0^1$	3254
632.6		C		$4_0^1 2_0^1 9_1^1$	
648.9	3442.9	C	10.0	$4_0^1 2_0^1$	3472
694.6	3488.6	C	3.5	$4_0^2 6_0^1$	3463
713.2	3507.2	C	1.5	-	
721.9	3515.9	C	1.5	$4_0^1 2_0^1 12_1^1$	3544
744.4		C		$4_0^3 9_2^1$	
761.0	3555.0	C	4.0	$4_0^3 9_1^0$	3557
778.0	3576.0	C	0.5	-	
818.7		C		$4_0^1 2_0^1 9_1^2$	
834.8	3628.8	C	5.0	$4_0^1 2_0^1 9_0^1$	3659
882.6	3676.6	C	1.0	$4_0^2 6_0^1 9_0^1$	3650
946.4		C		$4_0^3 9_1^1$	
962.8	3756.8	C	15	4_0^3	3759
30036.0	3857.8	C	0.2	-	
038.1	3882.1	C	0.2	-	
114.8		C		$4_0^3 9_2^3$	
131.7		C		$4_0^3 9_1^2$	
148.5	3942.5	C	2.0	$4_0^3 9_0^1$	3946
212.8	4006.8	C	0.3	$4_0^3 9_0^1 12_1^1$	4018
268.8	4062.8	C	0.1	-	
282.1		C		$4_0^3 9_3^5$	
299.8		C		$4_0^3 9_2^4$	

Table 16 (continued).

(i)	(ii)	(iii).	(iv)	(v)	(vi)
30317.3		C		$4_0^3 9_1^3$	
333.8	4127.8	C	1.5	$4_0^3 9_0^2$	4134
366	4160	B	0.8	$4_0^3 10_0^1$	4170
381.3		C		$4_0^3 12_1^1 9_1^3$	
399.4	4193.4	C	0.3	$4_0^3 12_1^1 9_0^2$	4205
434.6		C		$4_0^3 8_0^1 9_1^1$	
451.2	4245.2	C	0.3	$4_0^3 8_0^1$	4259
471.5	4265.5	C	0.5	-	
504.7	4298.7	C	1.0	-	
528.5	4322.5	C	1.0	-	
559.2		C		$4_0^1 2_0^1 6_0^1 9_1^1$	
575.5	4369.5	C	2.5	$4_0^1 2_0^1 6_0^1$	4414
618.6		C		$-.9_1^1$	
633.2	4427.2	C	1.5	-	
645.5	4439.5	C	2.0	-	
663.6	4457.6	C	3.5	$4_0^2 3_0^1$	4466
683.2	4477.2	C	1.5	$4_0^2 2_0^1 9_1^0$	4523
723.4		C		$4_0^3 10_0^1 11_0^1 9_1^1$	
741.4	4535.4	C	0.8	$4_0^3 10_0^1 11_0^1$	4545
760.9	4554.9	C	0.8	$4_0^1 2_0^1 6_0^1 9_0^1$	4601
884.5	4678.5	C	10	$4_0^2 2_0^1$	4724
944.0	4738.0	C	1.5	$4_0^3 6_0^1$	4701
970.5		C		$4_0^4 9_2^1$	
986.1	4780.1	C	1.0	$4_0^4 9_1^0$	4781

Table 16 (continued).

(i)	(ii)	(iii)	(iv)	(v)	(vi)
31054.1		C		$4_0^2 2_0^1 9_1^2$	
070.1	4864.1	C	3.5	$4_0^2 2_0^1 9_0^1$	4912
174.9		C		$4_0^4 9_1^1$	
187.5	4981.5	C	10	4_0^4	4982
239.0		C		$4_0^4 12_1^1 9_1^1$	
255.5	5049.5	C	1.5	$4_0^4 12_1^1$	5054
303.1	5097.1	C	0.5	-	
359.7		C		$4_0^4 9_1^2$	
374.3	5168.3	C	3.0	$4_0^4 9_0^1$	5170

frequency side about 10 cm^{-1} from the origin. This head makes it difficult to follow the R-sub-bands for $K \geqslant 4$ or 5, on account of overlapping.

From a cursory examination of various bands, it is immediately apparent that there are bands of the following three types:

(1)Perpendicular bands with an intense central peak very close to the band origin (see Fig. 6). All the stronger bands and most of the weaker ones are of this type.

(2)Perpendicular bands with a central minimum (see Fig. 7).

(3)Parallel bands, i.e. type A bands (see Fig. 8).

Bands of types (1) and (2) bear a marked resemblance to infra-red bands of types C and B respectively, but this is not an adequate proof of such an identification since, for example, the ultraviolet type C bands of glyoxal superficially resemble infra-red type B bands because of the changes in the rotational constants (4,37). However in the present case the assignment is supported by two independent arguments:

(i)Although most of the bands belong fairly purely to one of the three types, a few are definitely observed to be hybrids of types (2) and (3). On the other hand, of the many type (1) bands recorded, none was found to have a parallel component. The only hybrid bands allowed by the C_s vibronic selection rules are of the type AB.

(ii)From the observed symmetric-top structure and an assumption of nearly zero inertial defect, it is possible to calcul-

ate the asymmetric top structure of the band centres. Features of bands of types (1) and (2) can then only be explained if type C selection rules hold for the former and type B for the latter (see VIII.4).

We therefore conclude that the strong component of this system consists of type C bands, with transition moment perpendicular to the molecular plane; and that there is a weaker component of bands polarised in the molecular plane.

VIII.3. Analysis of K-Structure.

Apart from the origin bands, our rotational analysis is concerned almost entirely with the K-structure. Sub-band measurements refer to the low-frequency heads of the Q branches, which must be near the sub-band origins. The K numbering of the P- and Q-type sub-bands presents no difficulty since the differences ${}^{P}Q_{K}-{}^{P}Q_{K+1}$ and ${}^{Q}Q_{K}-{}^{Q}Q_{K+1}$ should be nearly linear in K, and should extrapolate back to the known $2(A''-\bar{B}'')$ at $K=\frac{1}{2}$ in the first case and to zero at $K=-\frac{1}{2}$ in the second. Because of the overlapping at the head, the R sub-bands are difficult to identify; but their numbering follows readily from that of the P sub-bands.

For perpendicular bands the combination differences $({}^{R}Q_{K-1} - {}^{P}Q_{K+1})/ 4K = (A''-\bar{B}'') - 2D''_K(K^2+1)$ and $({}^{R}Q_{K} - {}^{P}Q_{K})/ 4K = (A'-\bar{B}') - 2D'_K(K^2+1)$ are used to separate the lower and upper states respectively. Using these values of D''_K and D'_K, the combination sum

$$R_{Q_K} + P_{Q_{K+1}} + (D'_K - D''_K)\{K^4 + (K+1)^4\} = 2\nu_0 + \{(A' - \bar{B}') - (A'' - \bar{B}'')\}\{K^2 + (K+1)^2\}$$

gives the band origin ν_0 and an improved value of $\{(A' - \bar{B}') - (A'' - \bar{B}'')\}$.

For parallel bands, the best coefficients in the equation

$$Q_{Q_K} = \nu_0 + \{(A' - \bar{B}') - (A'' - \bar{B}'')\} K^2 - (D'_K - D''_K) K^4$$

were determined.

For pairs of bands with a common lower or upper level, the differences between similar sub-bands give gyro-vibrational differences within the one electronic state. In particular, for perpendicular bands arising from the zero-point level of the ground state the differences

$$P_{Q_{K+1}}(V \leftarrow 0) - P_{Q_{K+1}}(0 \leftarrow 0) = G_0(V) + \{(A'_V - \bar{B}'_V) - (A'_0 - \bar{B}'_0)\} K^2 - \{D'_K(V) - D'_K(0)\} K^4$$

are normally linear in K^2 and give good values of $G_0(V)$ and $(A'_V - \bar{B}'_V) - (A'_0 - \bar{B}'_0)$ without the use of the R sub-bands. Large slopes and curvatures in these plots indicate gyro-vibrational interaction.

In what follows, the term "band centre" will refer to the central peak of a type C band or to the estimated position of the band origin of a type A or type B band. The term "band origin" will refer only to the vibronic frequency difference ν_0 resulting from an analysis of the K-structure.

VIII.4. Origin Bands.

The band which we are assigning as the origin of the band

system is the first member of the principal progression and is centred at 26162.3 , 26191.8 and 26206.0 cm^{-1} in HCCCHO , DCCCHO and HCCCDO respectively; this isotope shift is fairly normal, its direction being consistent with a general fall in the vibrational frequencies during excitation. The band is shown to arise from the zero-point level of the ground state by its roughly threefold drop in intensity on heating to 200°C; the factor of three is in approximate agreement with the ratio of the vibrational partition functions at the two temperatures calculated from our ground state frequencies. The only bands to low frequencies of the 0 band which exhibit this behaviour are attributed to the 4140 Å system. Since this band is therefore the lowest in frequency which is not "hot", and since no pure electronic transition is forbidden by symmetry, the assignment as the 0 band is justified.

In order to obtain details of the structure of the excited state we require a fairly complete rotational analysis of the 0 band. This analysis may be taken in two phases : (i) the sub-band structure with $K > 2$ and the accompanying J-structure can be used to obtain the best symmetric top type constants $A'_o - \bar{B}'_o$ and $\bar{B}'_o$, and (ii) the asymmetry parameter may then be estimated from the structure at the band centre. At present only a preliminary analysis has been achieved, and the asymmetric top structure has been studied only for HCCCHO.

The frequencies of the ^{P}Q and ^{R}Q branches of the origin bands are listed in Table 17 ; it proved possible

Table 17. Sub-band Frequencies of the Origin Bands.

	HCCCHO		DCCCHO		HCCCDO	
K	$^{R}Q_{K}$	$^{P}Q_{K}$	$^{R}Q_{K}$	$^{P}Q_{K}$	$^{R}Q_{K}$	$^{P}Q_{K}$
2	26170.24		26198.86		26212.28	
3	171.65	26151.06	200.21	26180.04	213.71	26197.75
4	172.40	144.86	200.86	173.88	214.79	193.36
5	172.40	138.04	200.66	167.03	215.21	188.68
6	171.65	130.42	199.87	159.55	215.26	183.43
7	169.97	122.13	198.12	151.18	214.88	177.73
8	167.60	113.22	195.84	142.56	214.03	171.54
9		103.56		132.97		165.02
10		093.21		122.70		157.93
11		082.12		111.42		150.43
12		070.62				142.69
13		058.33				134.20
14		045.34				125.34
15		031.77				116.23

to calculate the positions of the ^{R}Q branches by a combination of the readily identified ^{P}Q and ^{Q}Q branches of other bands, once their vibrational assignments were known,(see VIII.8), and the identifications quoted are based on this calculation. The symmetric top rotational constants and origins of the O bands are collected in Table 18; wherever possible the rotational constants quoted are derived from mean combination

Table 18. Rotational Constants and Origins of the Q Bands.
The units are cm^{-1} in each case.

	HCCCHO	DCCCHO	HCCCDO
ν_{oo}	26163.12	26191.88	26206.54
$(A-\bar{B})''_o$	2.114	2.082	1.574
D''_K	2.93×10^{-4}	3.15×10^{-4}	1.03×10^{-4}
$(A-\bar{B})'_o$	1.731	1.696	1.339
D'_K	2.60×10^{-4}	2.70×10^{-4}	1.04×10^{-4}
$\Delta\bar{B}_o$	+0.00101	+0.00104	+0.00105
$\bar{B}'_o$	0.15655	0.14518	0.15398
A'_o	1.888	1.841	1.493

differences for bands which are shown by the vibrational analysis to involve one or other of these levels.

The K-structure analysis is subject to the error involved in using the observed onset of the Q branches instead of the hypothetical sub-band origins; this error should be largely cancelled out in forming the combination differences. However the best symmetric top constants will be obtained by using excited-state combination differences between the individual lines of the ^{R}R and ^{P}P branches; the ^{R}R branches of the various sub-bands overlap, but they may be identified by using ground-state combination differences once a reasonably accurate value of D_K is known. This work is in progress.

A preliminary calculation of the Q branches for low K was made, allowing for the asymmetry, with the following constants :

$A'_o = 1.886$, $B'_o = 0.16254$, $C'_o = 0.15008$ cm^{-1} (corresponding to $\Delta'_o = -0.33$ amu A^2) and Costain and Morton's ground-state constants (see IV). The excited-state constants were not based on the best values of the symmetric top constants now available and were not fitted to the observed spectrum; the calculation merely has qualitative significance at present, but it enables us to identify the band types from the J-structure.

Asymmetric top energies for low K were calculated for both states by means of Golden's method (25), which is asymptotic for high J. The refinements envisaged by Golden were neglected and the simple form

$$F(J_{K_a K_c}) = \bar{B}J(J+1) + (A-\bar{B})\{b_{K_a}(s) - \tfrac{1}{2}s\}$$

was used. In this equation

$$s = \left(\frac{B-C}{A-\bar{B}}\right)\left\{J(J+1) - 1 - \frac{1}{2J(J+1)}\right\},$$

and $b_{K_a}(s)$ is a characteristic value of Mathieu's equation which can be obtained from tables (48); when $(J+K_a+K_c)$ is even we use $be_{K_a}(s)$ for $b_{K_a}(s)$, when it is odd we use $bo_{K_a}(s)$. Comparison with Polo's series expansion (53) for low J showed that the simplified Golden method was good to $\pm .001$ cm^{-1} even in this range.

The wave-numbers of the various Q branch transitions were then calculated using type C and type B selection rules (III.6). The calculated spectra are represented by means of Fortrat

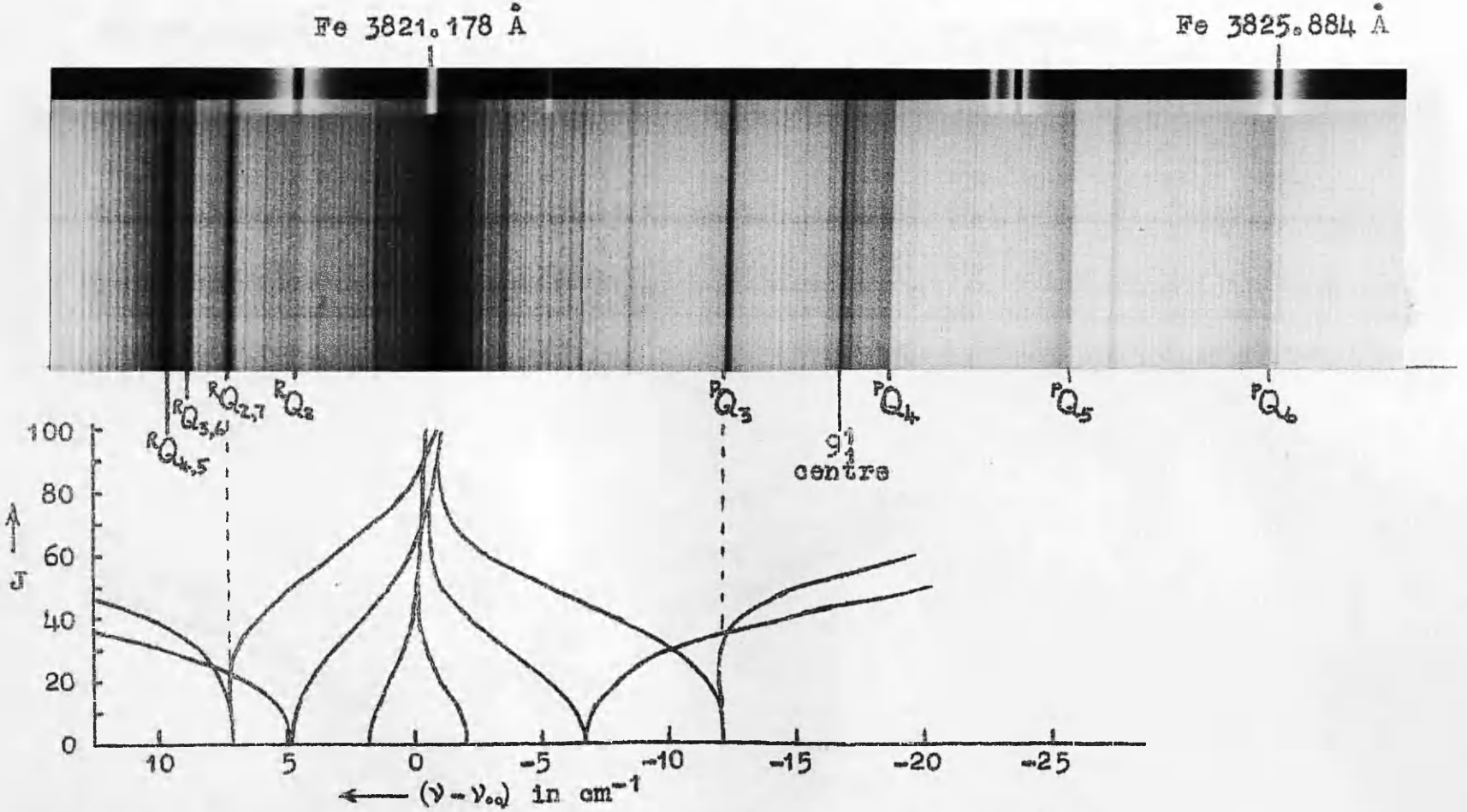

Fig. 6. Above: centre of the origin band of HCCCHO at 26163 cm^{-1}

Below: central Q branches of calculated type C band.

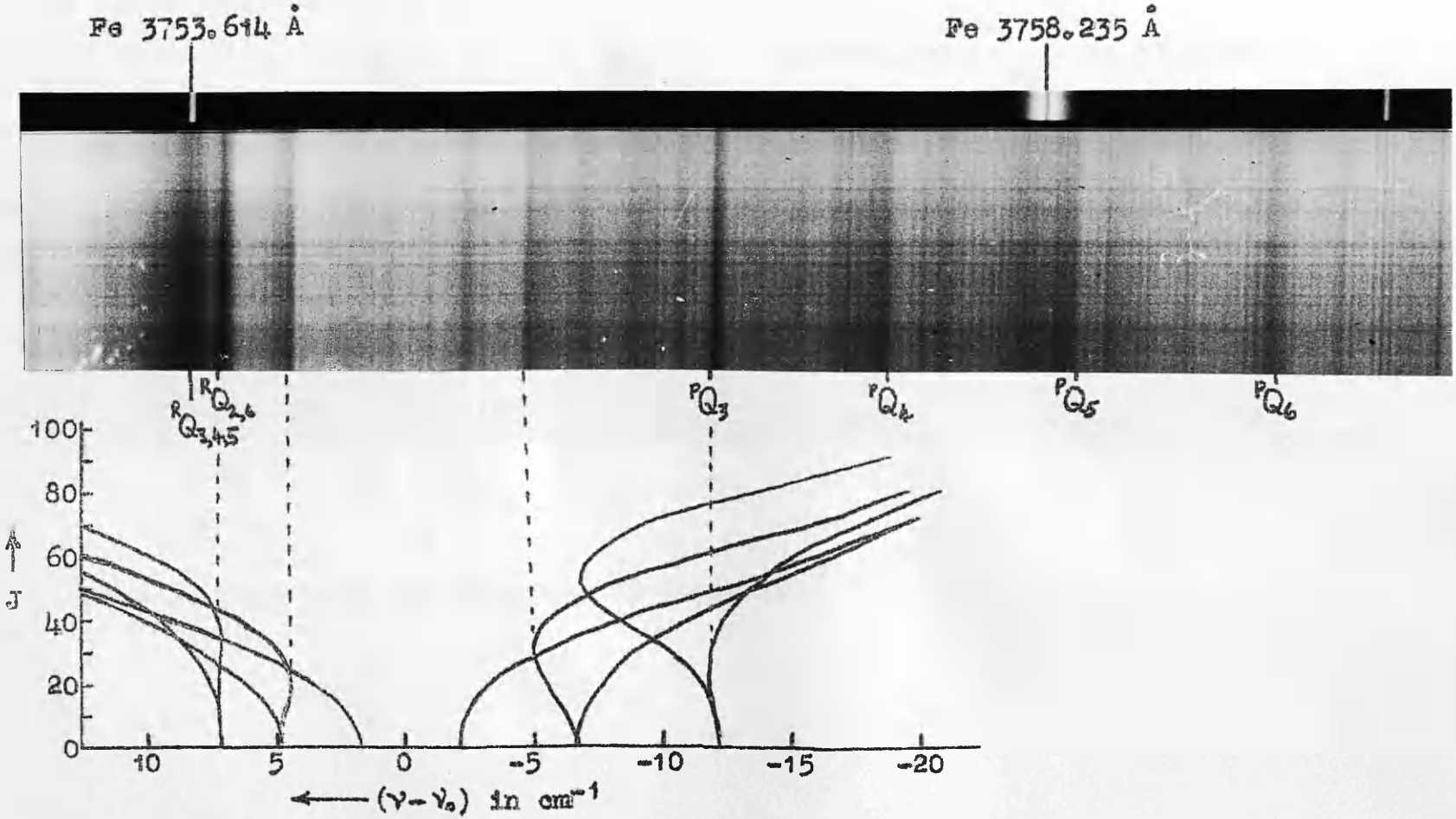

Fig. 7. Above: centre of the band 10_0^1 of HCCCHO at 26625 cm^{-1}
Below: central Q branches of calculated type B band.

Fe 3774.827 Å Fe 3776.459 Å

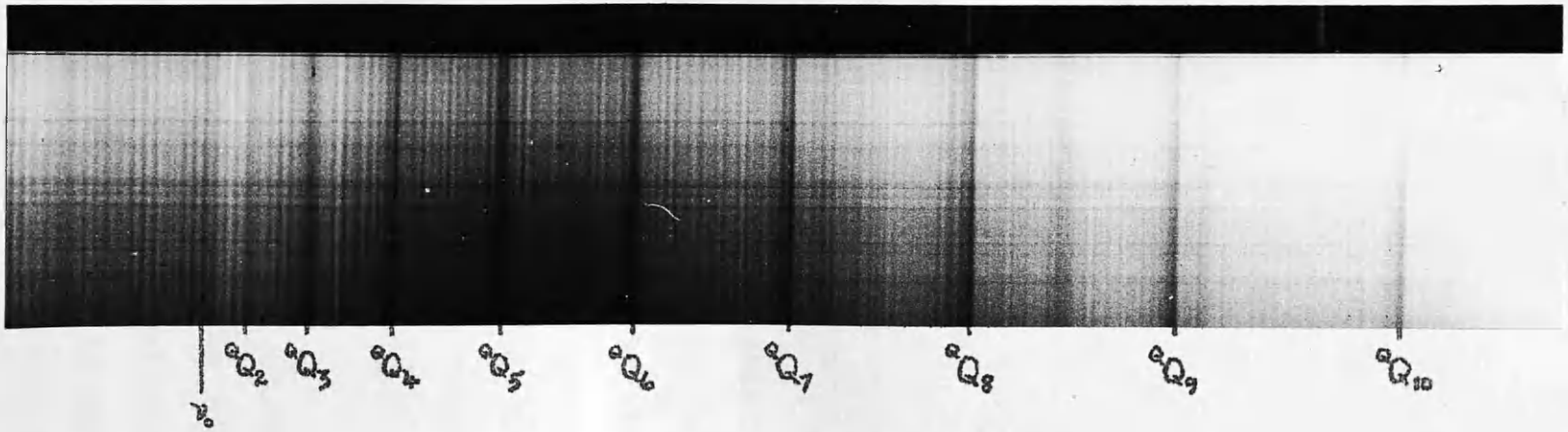

Fig. 8. The band 12_0^1 of HCCCHO at 26509 cm^{-1}.

diagrams (27, p.47) in Figs. 6 and 7, where they are compared with the 0 band and the band at 26625 cm^{-1} respectively. This comparison leaves little doubt that the band-type assignments are correct, since small changes in $B'-C'$ did not have any first-order effect on the calculated band centres.

Vibrational Assignments.

We shall consider in turn the evidence relating to each of the excited-state fundamental frequencies.

VIII.5. ν_4.

As mentioned previously (VII.2) the principal progression-forming frequency (ca 1300 cm^{-1}) is assigned from its isotope effect as the carbonyl stretching fundamental ν'_4. The bands 4^1_0, 4^2_0, 4^3_0 and 4^4_0 of HCCCHO and DCCCHO are seriously perturbed by a close Fermi resonance, as are the bands formed by addition of other vibrations to these bands. On the other hand, 4^1_0, 4^2_0, 4^3_0 and 4^4_0 of HCCCDO are all single. In direct antithesis, 4^0_1 is observed as a weak but strongly temperature-sensitive band among the triplet bands and is single in HCCCHO and DCCCHO, but double in HCCCDO (see VI.6).

For HCCCHO, the centres of the 4^1_0 doublet are at 0+1300.0 and 0+1312.0 with an intensity ratio of former : latter $\approx 3 : 1$. On the assumption that the intensity is due entirely to the fundamental (see III.4) we can place the unperturbed fundamental at $\nu'_4 = 1304.0$ and the perturbing frequency at 1308.0. Similarly

the 4_0^2 triplet has centres at 0+2582.9 (12), 0+2596.6 (12) and 0+2618.5 (3), the approximate intensities being in parentheses; the method of III.4 then gives $2\nu_4' = 2592.9$. Again, 4_0^3 has centres at 0+3845.3 (5), 3863.3 (5), 3878.6 (3.5) and 3917.8 (0.8) which give $3\nu_4' = 3866.2$. From the unperturbed frequencies we derive $\omega_4' = 1311.6$ cm^{-1}, $x_{44}' = -7.6$ cm^{-1}.

For DCCCHO, the 4_0^1 band has three centres at 0+1291.9, 0+1298.3 and 0+1305.7 with roughly equal intensities; thus $\nu_4' = 1298.6$ cm^{-1}. The higher ν_4' bands are complex, and no analysis was attempted.

The assignments of the perturbing frequencies will be discussed later (VIII.13).

The centres of the 4_0^n progression of HCCCDO are all single. However one member, 4_0^2, is affected by a perturbation in the sub-band structure which is most easily seen in the ^PQ sub-bands (see Fig. 9). As K' increases from 6 to 10, the sub-bands acquire a low-frequency satellite which gradually takes over the intensity so that only the low-frequency component persists for $K'>10$. The K-numbering of the two components can be obtained independently, the high-frequency one by using the normal method for low K, and the low-frequency one by using the well-developed J-structure of $^PP_{13}$, $^PP_{14}$ and $^PP_{15}$; it is found that the components with the same K value lie closest together. The effect is best demonstrated by plotting the differences $^PQ_{K+1}(4_0^2) - {}^PQ_{K+1}(0)$ against K^2. For

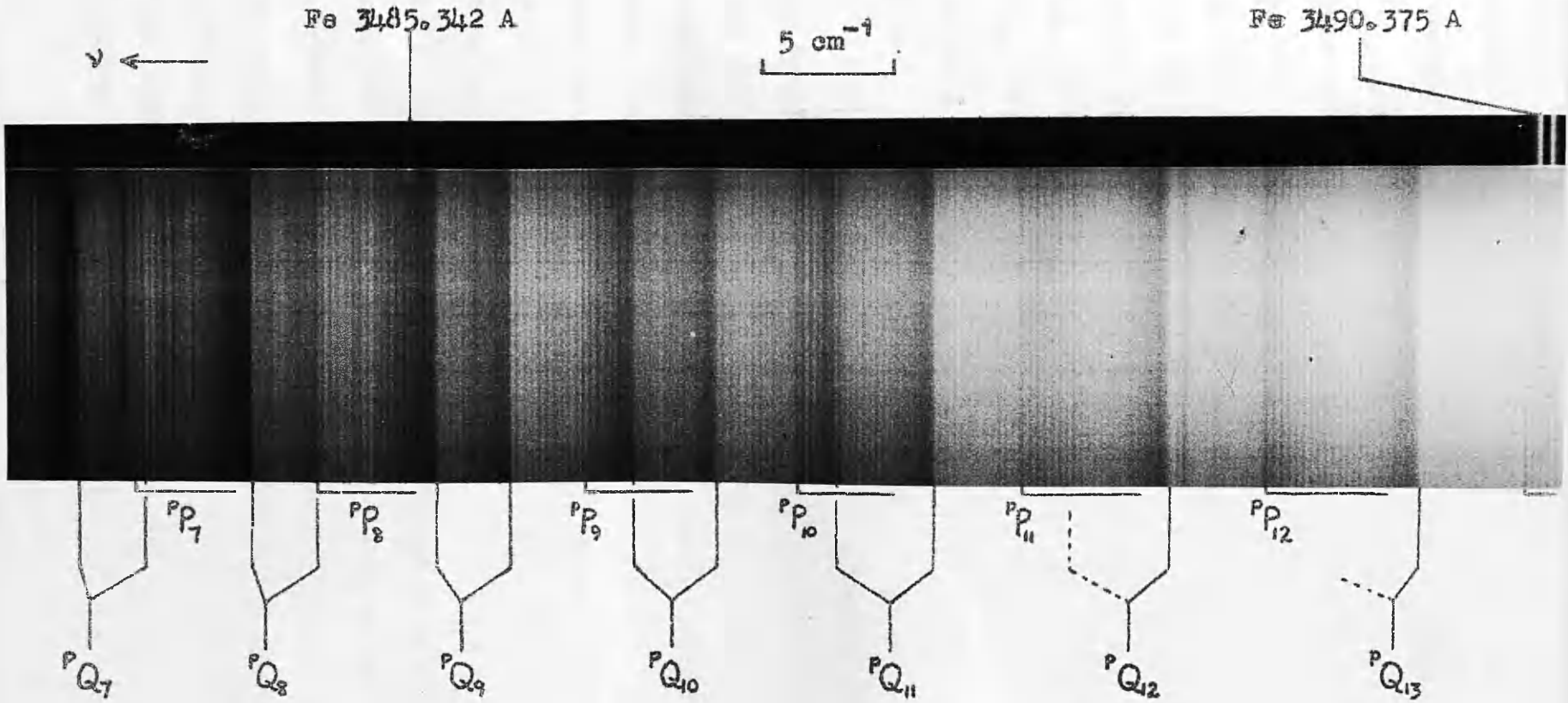

Fig. 9. Irregular perturbation in the sub-band structure of the band 4_0^2 of HCCCDO. The unperturbed ^{P}Q branches are shown below.

comparison with the rest of the progression, the differences $\{{}^{P}Q_{K+1}(4_0^n) - {}^{P}Q_{K+1}(0)\}/n$ are plotted against K^2 in Fig. 10; these graphs should have intercept $\omega_4'+nx_{44}'$ and gradient $-\alpha_4^{(A-\bar{B})'}$ for the unperturbed bands (see III.3 and III.7). The bands 4_0^1, 4_0^3, 4_0^4 give $\omega_4' = 1274.8$, $x_{44}' = -7.3$ and $\alpha_4^{(A-\bar{B})'} = +0.0304$ (all in cm^{-1}). The line obtained for 4_0^2 from these values should represent the unperturbed sub-bands, and it is seen from Fig. 10 that the observed sub-bands lie on either side of this line; the mean positions of the sub-band pairs, each component being weighted with its intensity, fall close to this line.

The effect is obviously to be attributed to an irregular (or "rotational") perturbation (28, p.466) with a crossing point near $K'=9$, the perturbing level lying about 3 cm^{-1} below $2\nu_4'$. Since the sub-bands of high K are still displaced, we may conclude that the perturbation is K-dependent (27, p.288) and so must involve a vibration-rotation interaction, as distinct from a purely vibrational interaction of Fermi type. A perturbation with $\Delta K \neq 0$ would involve coupling by rotation about the b- or c-axis; and since the angular momenta about these axes are small when $J \approx K$ (cf. last paragraph of III.7), such a perturbation should not lead to a serious displacement of the onsets of the Q branches. It seems likely therefore that the present example has $\Delta K = 0$. Possible perturbations of this type involve coupling about the a-axis through either the Coriolis forces or the centrifugal forces; the vibronic

Fig. 10. 4_0^n bands of HCCCDO (see p. 130).

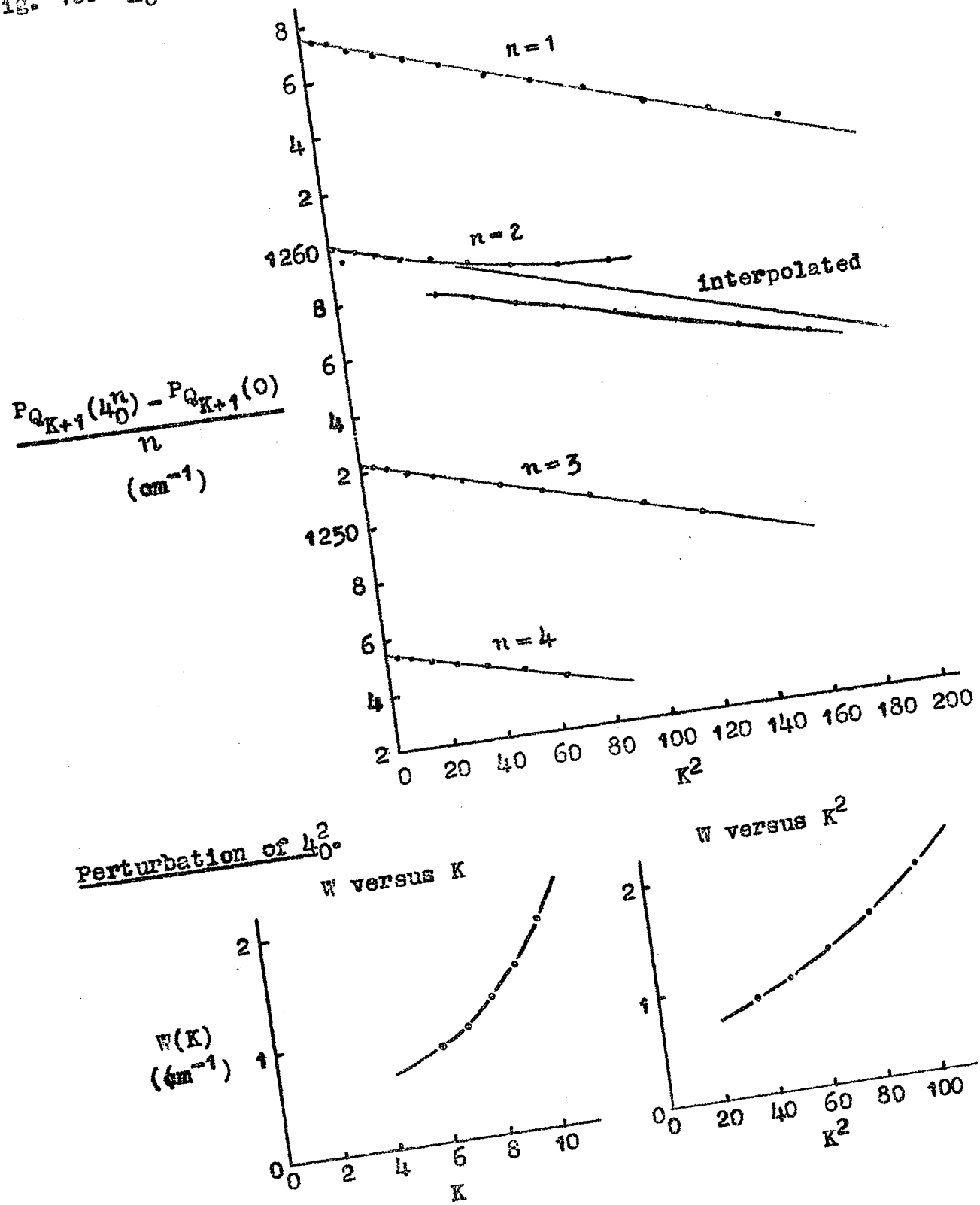

selection rules differ in the two cases, being $A' \leftrightarrow A''$ for Coriolis coupling (cf. III.8) and $A' \leftrightarrow A'$, $A'' \leftrightarrow A''$ for centrifugal coupling. For Coriolis coupling the perturbation matrix element should be proportional to K, for centrifugal coupling proportional to K^2.

The difficulty confronting a more detailed analysis of the present perturbation is that the (unweighted) mean of the observed sub-bands does not give a straight line on the graph; in theory it should correspond to the mean of the unperturbed levels and so should give a straight line. Thus it seems that at least one additional level is involved in the perturbation.

Nevertheless, since we have, for each of the doubled sub-bands, the two perturbed levels and one unperturbed level, we can analyse the perturbation in terms of only two levels (27, p.282) if we do not require the rotational energies of the other unperturbed level to obey the normal equations. The values of $|W(K)|$ obtained in this way are graphed against K and against K^2 in Fig. 10 . The plots are smooth but appreciably curved in both cases, the plot against K^2 being the more nearly linear. This, and the fact that $|W(K)|$ appears to extrapolate to a non-zero value at K=0, suggest that the perturbation is of centrifugal type with a small Fermi contribution (the vibronic selection rules of the two are consistent). However this treatment is not valid if more than two levels are involved.

A decision between the alternatives could be made from the symmetry of the perturbing level if it could be identified. This has not been possible so far.

VIII.6. ν_9.

Most of the type C bands of the system have a weaker satellite about 16 cm^{-1} to low frequencies, whose centre usually lies between $^PQ_3$ and $^PQ_4$ of the parent band. With the centre and head of the parent, this feature gives the bands a triple-headed appearance under low resolution. This satellite is presumably the first member of a sequence, and it is frequently possible to see a second and sometimes later members. On account of the Boltzmann factors involved, the fundamental which forms this sequence must lie below 300 cm^{-1} and so must be either the a' or a'' component of the C≡Ĉ-C bending vibration. Sequences of the same type are presumably also attached to the type A of B bands, but the lack of a sharp centre makes them less easy to observe.

If the vibration forming this sequence is also active in forming progressions we would expect to find the (1-0) and (0-1) bands within about 300 cm^{-1} of the origin on either side and nearly symmetrical about the origin. A pair of fairly strong type C bands centred at 0+191.0 and 0-206.3 obviously fit the requirements. We may therefore assign the sequences mentioned above to the a' bending frequency, which will be ν_9; thus ν'_9=191.0 and ν''_9=206.3 cm^{-1}. These frequencies are only

slightly altered in the deuterium isotopes.

It is possible to find a second member of both the upper- and lower-state progression. Because of the activity of this fundamental in forming both progressions and sequences, it is possible to follow it up to four quanta in both states, and it is closely harmonic in both.

The lower-state combination differences across the band 9^0_1 are found to be much lower than those across the 0 band, and the graph of ${}^PQ_K(0)-{}^PQ_K(9^0_1)$ against K^2 is slightly curved and has the large slope of $(A-\bar{B})''_9 - (A-\bar{B})''_0 \approx -0.14$ cm^{-1}. Thus ν''_9 is involved in a fairly strong vibration-rotation interaction, which will be discussed in VIII.8 . The internal consistency of the present assignments can be demonstrated by means of gyro-vibrational combinations; for instance, the equation ${}^PQ_K(9^1_0) + {}^PQ_K(9^0_1) = {}^PQ_K(9^1_1) + {}^PQ_K(0)$ is well satisfied.

VIII.7. ν_{12}.

A pair of fairly strong type A bands are observed at 0+346.4 and 0-260.3. If these are the first members of progressions in a non-totally-symmetric frequency, one would expect the sequence to occur at 0+86.1 . A type C band is indeed observed at 0+85.0 , and it is shown to be "hot" by the temperature measurements and by its lower-state K-type combination differences, which are quite incompatible with those for the zero-point level. The vibration must be the a''

component of the C≡$\overset{A}{C}$-C bend, which will be ν_{12}; the above bands are therefore assigned to 12^1_0, 12^0_1 and 12^1_1 respectively. Similar bands, with minor changes in the frequencies, are found for the deuterium isotopes. It should be noted that the 85.0 cm^{-1} interval is definitely not an excited-state fundamental, as Howe and Goldstein suggested.

The lower-state K-type combination differences across the 12^1_1 band are much higher than those across the 0 band, showing that $(A-\bar{B})''_{12}$ is considerably greater than $(A-\bar{B})''_0$; this vibration-rotation interaction will be discussed in VIII.8 . The consistency of the ν_{12} assignments is again shown by gyro-vibrational combinations, such as

$$^QQ_{K+1}(12^1_0) + {}^QQ_K(12^0_1) = {}^RQ_K(12^1_1) + {}^PQ_{K+1}(0) \ ;$$

the relation $^RQ_K(0) = {}^QQ_K(12^1_0) + {}^QQ_{K+1}(12^0_1) - {}^PQ_{K+1}(12^1_1)$ then assists us in identifying the R sub-bands of the 0 band.

The following additional bands involving only ν_{12} are observed for all three isotopes : 12^2_0 (type C), 12^2_1 (type A) and 12^2_2 (type C) ; these show that ν_{12} is closely harmonic in both states.

VIII.8. Coriolis Coupling of ν''_9 and ν''_{12}.

The vibration-rotation interaction present in ν''_9 and ν''_{12} is best shown by a comparison of the lower-state combination differences $^RQ_{K-1} - {}^PQ_{K+1} = \Delta^K_2F''(0,K)$ across the perpendicular bands 12^1_1 and 9^0_1 with those across the 0 band. These are shown in Table 19, where it can be seen that the mean of the

Table 19. Coriolis Coupling in ν''_9 and ν''_{12} in HCCCHO.

K	$\Delta^{K}_{2}F''(0,K)$ in cm^{-1}			
	12^1_1	9^0_1	mean of 12^1_1 and 9^0_1	0
3	27.3	23.6	25.45	25.38
4	36.1	31.5	33.8	33.61
5	44.9	39.5	42.2	41.98
6	53.5	47.4	50.45	50.27
7	62.1	55.3	58.7	58.43
8		63.2		66.41
9		71.2		74.39
10		78.9		82.14

Table 20. Analysis of (ν''_9, ν''_{12}) Coupling.

The units are cm^{-1}, except for the dimensionless ζ.

	HCCCHO	DCCCHO	HCCCDO
$\nu_0(9^0_1)$	25957.9	25996.3	26005.0
ν''_9	205.3	195.6	201.5
$\nu_0(12^0_1)$	25902.5	25943.4	25956.6
ν''_{12}	260.6	248.5	249.9
$(\overline{A-B})''_{9,12}$	2.122	2.090	1.570
$\lvert\zeta^{a}_{9,12}''\rvert$	0.639	0.634	0.675

ν''_9 and ν''_{12} values is close to the zero-point value.

This behaviour of ν''_9 and ν''_{12}, in that their K-type rotational energies lie fairly symmetrically below and above the

normal values, is typical of Coriolis coupling by rotation about the a-axis, which is allowed for these vibrations by the Jahn selection rule. This interaction was analysed in more detail for the two fundamental bands 9_1^0 and 12_1^0, which are of types C and A respectively. Upper-state combination differences, ${}^{R}Q_K - {}^{P}Q_K = \Delta_2^K F'_0(0,K)$, across 9_1^0 agree with those of the O band. The value of $(A-\bar{B})'_0$ so obtained was used in the following equations :

$$\tfrac{1}{2}\{{}^{R}Q_K(9_1^0) + {}^{P}Q_K(9_1^0)\} + {}^{Q}Q_K(12_1^0)$$
$$= \{\nu_0(9_1^0) + \nu_0(12_1^0) + (A-\bar{B})'_0\} + 2\{(A-\bar{B})'_0 - (\overline{A-B})''\}K^2$$

and

$$\left[\tfrac{1}{2}\{{}^{R}Q_K(9_1^0) + {}^{P}Q_K(9_1^0)\} - {}^{Q}Q_K(12_1^0) - (A-\bar{B})'_0\right]^2$$
$$= \{\nu_0(9_1^0) - \nu_0(12_1^0)\}^2 + 4\frac{(\nu''_9+\nu''_{12})^2}{\nu''_9\nu''_{12}}(\zeta^{a''}_{9,12})^2 A''_0{}^2 K^2 ,$$

in which $(\overline{A-B})''$ is a mean value for the ν''_9 and ν''_{12} levels. The left-hand sides plotted against K^2 gave good straight lines. From the intercepts the two origins were obtained, and hence ν''_9 and ν''_{12} ; the gradients then gave $(\overline{A-B})''$ and $|\zeta^{a''}_{9,12}|$. The results for the three isotopes are displayed in Table 20.

In addition to the data referring to the fundamentals, we have sub-band structure for some of the overtone and combination levels. Table 21 shows results for HCCCDO, for which these sub-bands are most clearly developed. The $2\nu''_9$ and $2\nu''_{12}$ levels are seen to satisfy approximately the theory of III.8 , namely that their K-type rotational energies should be symmetrical about the zero-point values, and twice as far

Table 21. Coupling in $2\nu''_9$ and $2\nu''_{12}$ of HCCCDO.

K	$\Delta^{K}_{2}F''(0,K)$ in cm^{-1}.				
	9^1_2	9^0_1	0	12^1_1	12^2_2
3	16.21	17.46	18.92	20.24	21.86
4	22.07	23.14	25.03	26.83	29.26
5	27.59	29.39	31.36	33.44	36.25
6	33.40	35.29	37.48	40.08	43.07

from them as those for the ν''_9 and ν''_{12} levels are.

VIII.9. ν_{10}.

A type B band is observed at 0-982, with the position and polarisation expected from the infra-red for 10^0_1. A type B band of medium intensity is also found at 0+462.7, and the assignment of this as 10^1_1 is confirmed by the observation of the sequence 10^1_1 as a prominent type C band at 0-519.7. The fact that 0-519.7 does not represent 12^0_2 is shown by its rotational structure, its extreme temperature sensitivity and its isotope shift.

An improved value of ν''_{10} may be obtained by plotting $^{P}Q_K(10^1_0) - {}^{P}Q_K(10^1_1)$ against K^2 ; theband 10^0_1 has been observed only under medium resolution, but the differences $^{P}Q_K(0) - {}^{P}Q_K(10^0_1)$ agreed within the limits of error with the above. The values of ν''_{10} and $(A-\bar{B})''_{10} - (A-\bar{B})''_0$ obtained in this way are discussed in section VI.4.

In the same way, $^{P}Q_{K}(10_0^1) - {}^{P}Q_{K}(0)$ versus $(K-1)^2$ gives ν'_{10} and $(A-\bar{B})'_{10} - (A-\bar{B})'_{0}$. The results are discussed in VIII.11.

It is interesting to note that whereas the 10_0^1 bands of HCCCHO and DCCCHO are of almost pure type B, the parallel component being very weak or absent, that of HCCCDO has type A and B components of roughly equal intensity. This can be checked by the combination relations $^{R}Q_{K} - {}^{Q}Q_{K+1} = {}^{Q}Q_{K} - {}^{P}Q_{K+1} = \Delta_1^K F''(0,K)$ and $^{R}Q_{K} - {}^{Q}Q_{K} = {}^{Q}Q_{K+1} - {}^{P}Q_{K+1} = \Delta_1^K F'(0,K)$.

The value of the overtone $2\nu'_{10}$ is crucial in deciding whether the excited state is planar; its assignment is discussed in section VIII.12 .

VIII.10. $\underline{\nu}_{11}$.

In HCCCHO a medium-weak type C band is found at 0+128.9 , 44 cm^{-1} above 12_1^1. The lower-state K-type combination differences of this band are equal to those of 12_1^1 and so are characteristic of the Coriolis-coupled ν''_{12} level. The possibility of an accidental equality of such distinctive combination differences for two different levels is remote, so we may presume that there is an excited state $^{v}A''$ level at 390 cm^{-1}, and this can only be interpreted as a fundamental - in fact the remaining a'' fundamental ν'_{11} ; so the 0+128.9 is to be assigned as $11_0^1 12_1^0$.

The 44 cm^{-1} difference reappears between two strongly degraded type C bands at 0-303.6 and 0-347.4. These bands also have identical lower-state combination differences,

characteristic of a strongly Coriolis-coupled level; and the sense of the Coriolis contribution shows that the level involved must be the upper of the Coriolis-coupled pair. If we take ν'_{11} and ν'_{12} as the upper states of these bands, we obtain for the common lower state a $^{V}A''$ level at 693.5 cm^{-1}, which must be the fundamental ν''_{11}. The a'' fundamental ν''_{11} is therefore the upper of the ν''_{7}, ν''_{11} pair observed in the infra-red spectrum, contrary to our original assignment (1960,8). It is possible to calculate the positions of the sub-bands observed in the infra-red from the ultraviolet bands by means of the equation

$$^{R}Q_{K}(\nu''_{11},IR) = {}^{Q}Q_{K}(12^{1}_{0}) + {}^{P}Q_{K+1}(11^{1}_{0}12^{0}_{1}) - {}^{P}Q_{K+1}(12^{1}_{1}) - {}^{P}Q_{K+1}(11^{1}_{1}).$$

The results are :

K	$^{R}Q_{K}(\nu''_{11},IR)$		
	obs.	calc.	obs.-calc.
2	(708.0)	707.1	(0.9)
3	713.0	714.0	-1.0
4	720.5	721.0	-0.5
5	728.0	728.1	-0.1
6	735.5	735.8	-0.3
7	742.7	743.2	-0.5

Thus, apart from a systematic discrepancy of about 0.5 cm^{-1}, possibly due to inadequate calibration in the infra-red, the unusual structure of this band is satisfactorily predicted.

From the combination $^{Q}Q_{K}(11^{1}_{0}) = {}^{Q}Q_{K}(12^{1}_{0}) + {}^{P}Q_{K+1}(11^{1}_{0}12^{0}_{1}) - {}^{P}Q_{K+1}(12^{1}_{1})$, it is possible to calculate the parallel component of the 11^{1}_{0} band. Weak features were observed in the

positions of the expected sub-bands, but the presence of this band cannot be definitely claimed.

We have seen that for HCCCHO we observe, in addition to the normal sequences 11_1^1 and 12_1^1, the cross sequences $11_0^1 12_1^0$ and $11_1^0 12_0^1$; in each case the normal sequence is the more intense of the bands with the same lower level (same Boltzmann factor). The normal sequences are observed for the other two isotopes, and 11_1^1 of DCCCHO shows the expected large isotope shift; but the occurrence of the cross sequences must be fortuitous for HCCCHO, since for the other isotopes only $11_0^1 12_1^0$ of DCCCHO was observed, very weakly. This may be due to the interaction between the ν'_{11} and ν'_{12} motions, which will be greatest for HCCCHO, where the difference in frequencies is smallest.

VIII.11. ν_8 and ν_7.

A type C band of medium intensity at 0+507.0 cannot be explained on the basis of the fundamentals so far identified, and so presumably represents a new fundamental; it lies 614 cm^{-1} above another type C band, which is fairly temperature-sensitive, at 0-106.7 , and this interval is almost equal to $\nu''_8 = 615$ cm^{-1} observed in the infra-red. The bands may therefore be assigned as 8_0^1 and 8_1^1 respectively. The band 8_1^0 was not observed, but it may be obscured by triplet bands in the same region. Similar results hold for HCCCDO, with small changes in the frequencies ; but the position is more complic-

ated in DCCCHO, which is discussed below.

The sub-bands of the 8_0^1 band are rather hazy, but it is possible to get values of ν_8' and $(A-\bar{B})_8'-(A-\bar{B})_0'$ from them. The results for ν_8' and ν_{10}' (see VIII.9) are shown in Table 22. The HCCCDO values correspond to a fairly typical example of Coriolis coupling and the second-order perturbation of III.8 is applied to them, giving quite a large value for $|\zeta^a_{8,10}'|$. In the same treatment the HCCCHO results are less satisfactory, since we are left with a rather large value of $(\overline{A-\bar{B}})_{8,10}' - (A-\bar{B})_0'$.

Table 22. Coriolis Coupling of ν_8' and ν_{10}'.

	HCCCHO	HCCCDO	
ν_8'	506.9	499.9	cm^{-1}
$(A-\bar{B})_8' - (A-\bar{B})_0'$	+0.086	+0.049	cm^{-1}
ν_{10}'	462.1	411.6	cm^{-1}
$(A-\bar{B})_{10}' - (A-\bar{B})_0'$	-0.043	-0.048	cm^{-1}
$\lvert\zeta^a_{8,10}'\rvert$	0.45	0.69_5	

In contrast to the other two isotopes, DCCCHO shows the 8_1^0 band at 0-610.0 . By comparison with the other isotopes, one would expect the 8_0^1 band very close to 0+500. However, two type C bands are found at 0+486.4 and 0+529.0 , roughly symmetrical about the expected position, and approximately equal in intensity ; and similarly two bands of about equal intensity are found at 0-80.6 and 0-123.5 near where the sequence 8_1^1 is expected. It therefore appears that there are

two levels of $^{V}A'$ symmetry near 500 cm^{-1}, one of which must be ν'_8. No summation of the known fundamentals gives a level in this region, so that we must interpret the other level as a fundamental also. The only possibility remaining after the assignments to be given later is the ethynyl C≡Ĉ-D bend, ν'_7. We therefore choose (the numbering of the modes is arbitrary) ν'_8=486 cm^{-1} and ν'_7=529 cm^{-1}; and the assignments of the bands at 0+529, 0+486, 0-81 and 0-124 are then 7^1_0, 8^1_0, $7^1_0 8^0_1$ and 8^1_1 respectively.

The precise value of ν'_7 cannot be obtained definitely from the infra-red spectrum, since we must first number the sub-bands there. However in DCCCHO a weak band is observed at 0+21 and similar bands are found 21 cm^{-1} above other strong bands; interpreting this as 7^1_1 gives $\nu''_7 = 7^1_0 - 7^1_1 = 507.7$ cm^{-1}; and one possible numbering of the infra-red sub-bands gives $\nu''_7 = 507.9$ cm^{-1}. We should also expect the other cross sequence $7^1_0 8^0_1$, which is then calculated to be centred at 26170.5 cm^{-1}; a line is observed very near this frequency, but it is at the position and of about the intensity expected for $^{R}Q_2(0)$ of HCCCHO, present as an impurity in our sample of DCCCHO.

No trace of these ν_7 bands - suitably shifted - is found in HCCCHO and HCCCDO. But, although the occurrence of 7^1_0 and $7^1_0 8^0_1$ may be a consequence of the accidental near-degeneracy of ν'_7 and ν'_8, the presence of the sequence 7^1_1 should not be accidental, since its intensity is determined almost purely

just by the Boltzmann factor. However the results for DCCCHO suggest that in the absence of the ν'_7, ν'_8 interaction, the value of ν'_7 would be almost the same in both electronic states. The 7^1_1 bands of HCCCHO and HCCCDO therefore probably lie in the intense region at the centre of the O band, and its Boltzmann factor of 0.05 prevents its identification. We tentatively put $\nu'_7 = \nu''_7$, the latter value being obtained by interpreting the infra-red spectra by analogy with that of DCCCHO.

VIII.12. ν_6, ν_5 and $2\nu_{10}$.

Most of the bands to low frequencies of 0+900 can be explained on the basis of the fundamentals so far identified, although some of the assignments are, of course, quite tentative. In the region between 0+900 and 4^1_0 at 0+1300 occur several strong bands, some of which are 1300 cm^{-1} up from corresponding bands below the O band and so can be explained as hot bands related to 4^1_0. The remaining strong bands in this region are discussed here.

A close pair of strong type C bands are observed at 0+956.7 and 0+943.9 with an intensity ratio of about 3:2 respectively. Interpreting this as a Fermi resonance in which all the intensity is due to one of the unperturbed levels, we obtain as the unperturbed frequency of that level 951.6 cm^{-1}, the other unperturbed frequency being 949.0 cm^{-1}; the perturbation matrix element (27, p. 282) is $|W| = 6.3$ cm^{-1}. A similar

pair of bands is observed for DCCCHO at 0+947.5 and 0+932.2 , with an intensity ratio of 2:5 respectively ; similar arguments give the intensity-bearing unperturbed frequency at 936.6 cm^{-1} and the other at 943.1 cm^{-1}, with $|W| = 6.9\ cm^{-1}$. The similarity of these results suggests that the frequencies should have comparable assignments for the two isotopes. The corresponding frequencies are therefore as follows :

	HCCCHO	DCCCHO
"strong"	951.6	936.6
"weak"	949.0	943.1
Harmonic $2\nu'_{10}$	924.2	918.0

Now the only A′ summations of the other fundamentals of HCCCHO expected in the range 900 to 1000 cm^{-1} are $2\nu'_{10}$ (924), $\nu'_9+2\nu'_{11}$ (969), $\nu'_9+\nu'_{11}+\nu'_{12}$ (925) and $5\nu'_9$ (946), the harmonic values in cm^{-1} being given in parentheses. Of these, all except $2\nu'_{10}$ are ruled from further consideration by the isotope shifts in passing to DCCCHO. Thus whether $2\nu'_{10}$ is to be identified with the "strong" or the "weak" component, it has a significant positive anharmonicity of 20 to 30 cm^{-1}; if $2\nu'_{10}$ is the strong component, this would be definite Franck-Condon evidence foe non-planarity of the excited state. This issue may be settled by a comparison with HCCCDO. In this isotope the harmonic value of $2\nu'_{10}$ is 823 cm^{-1}, so that 10^0_0 may be expected at about 0+840 . In fact only very weak bands are found in this region, the nearest band of intensity comparable to the above pair being at 0+942. We may therefore assign

the unperturbed $2\nu'_{10}$ as the weak component, which lies 24.8 and 25.1 cm^{-1} above the harmonic value in HCCCHO and DCCCHO respectively; this assignment also gives the more consistent anharmonicities. A few weak bands occur in the 0+840 region of HCCCDO, and it is not possible to identify 10β definitely; however, we tentatively assign it to the otherwise unexplained band at 0+834.8 .

We are left with the strong component above, which must represent a new a′ fundamental. Its assignment is discussed later in this section.

A further strong type C band is found at 0+1120.0 in HCCCHO. The only binary or ternary combination whose harmonic value is near this frequency is $\nu'_9+2\nu'_{10}$ (harmonic 1113 cm^{-1}); but the large anharmonicity found for ν'_{10} rules this out. This frequency is therefore an additional a′ fundamental. The corresponding band of DCCCHO is doubled, the two components being of roughly equal intensity at 0+1119.8 and 0+1112.8 ; the perturbing level in this Fermi resonance can readily be ascribed to the addition of ν'_9 = 183.6 cm^{-1} to the 0+932.2 band discussed above. The unperturbed fundamental may be roughly estimated as 1115 cm^{-1}.

The only likely possibilities for these two fundamentals are ν'_5 (formyl C-Ĉ-H bend) and ν'_6 (C-C single-bond stretch). The larger isotope effect in DCCCHO on the lower of the frequencies suggests that we assign ν'_6 = 951.6 (corrected) and ν'_5 = 1120.0 cm^{-1} in HCCCHO.

So far the strong band of HCCCDO in this region has only been mentioned in passing. In fact, instead of the two bands 5_0^1 and 6_0^1, only one strong one is observed, at 0+941.9 , the other bands in this region being much weaker. Now if, as a rough estimate, we attribute to each of ν_5' and ν_6' the same fractional shift in passing from HCCCHO to HCCCDO as was found in the ground state, we calculate $\nu_6'(\mathrm{HCCCDO}) \approx 952 \times 877 / 944 = 884\ \mathrm{cm}^{-1}$ and $\nu_5'(\mathrm{HCCCDO}) \approx 1120 \times 1080 / 1389 = 871\ \mathrm{cm}^{-1}$. These frequencies are so close together that the fundamentals will interact strongly and so be thrown apart in frequency. The upper one can then become $942\ \mathrm{cm}^{-1}$, in which case the lower will be about $810\ \mathrm{cm}^{-1}$.

Whether we call $941.9\ \mathrm{cm}^{-1}$ of HCCCDO ν_5' or ν_6' is purely arbitrary on the basis of our method of numbering; because of the similarity in frequencies for the three isotopes, we shall call it ν_6'. The possible assignment of ν_5' for this isotope is discussed in VIII.17.

The large change in the intensity distribution between 5_0^1 and 6_0^1, as between HCCCHO and HCCCDO, may have a Franck-Condon explanation. We may suppose that the intensities of 5_0^1 and 6_0^1 in HCCCHO are due to changes in the C_2-C_3 length and in the $C_2\hat{C}_3H_2$ angle upon excitation. When these modes become strongly coupled together in HCCCDO, the two normal coordinates will each have roughly equal contributions from both internal coordinates, the latter being compounded together in sum and difference fashion. Thus one of the

resulting modes will be able to combine a Franck-Condon-favoured change in both internal coordinates, whereas the other must combine a favoured change in one internal coordinate with a disfavoured change in the other; in other words, the latter mode cannot distort the excited state into a configuration which more nearly corresponds to the equilibrium one of the ground state, because as it improves the match in one coordinate it worsens the match in the other coordinate (see I.2). Accordingly only one of the coupled modes can achieve intensity from the Franck-Condon effect.

It is worth noting in this context that both of the hot bands 5^0_1 and 6^0_1 are observed for HCCCDO; the band 6^0_1 is found for HCCCHO and DCCCHO, but 5^0_1 is not observed, probably on account of its forbidding Boltzmann factor. The weakness of 5^1_0 in HCCCDO is therefore probably due to some fortuitous type of forbiddenness as suggested above.

VIII.13. Fermi Resonance of ν'_4.

The Fermi resonance affecting ν'_4 of HCCCHO and DCCCHO can now be easily explained. For HCCCHO the perturbing level was calculated to be at 1308.0 cm^{-1} (see VIII.5); the harmonic value of $\nu'_5+\nu'_9$ is 1308.9 cm^{-1}. For DCCCHO, the ν'_5 level is already doubled by Fermi resonance; addition of ν'_9 to each of the observed components gives calculated levels at 1303.4 and 1296.4 cm^{-1} which nicely flank the position estimated for the fundamental, namely 1298.6 cm^{-1} (see VIII.5), thus explaining

the observed triple structure.

Most of the bands to high frequencies of 4_0^1 in HCCCHO and DCCCHO are perturbed by the Fermi resonance in ν_4', making detailed analysis difficult. However, there is evidence for two further fundamentals in this region.

VIII.14. ν_3.

In HCCCHO a medium-strong type C band is observed at 0+1945.5 , which is single and so does not appear to involve the Fermi-resonating fundamentals ν_4' or ν_6'. The only A′ binary or ternary combinations expected at this frequency are $\nu_4'+\nu_7' = 1950$ and $\nu_5'+\nu_9'+\nu_7' = 1960$ cm^{-1}, i.e. the two Fermi components of $\nu_4'+\nu_7'$. But if $4_0^1 7_0^1$ is present in the spectrum, we should also expect 7_0^1 itself in the previous octave of the ν_4' progression, with intensity comparable to the 0+1945.5 band. No such band is found, so we must assign 1945.5 cm^{-1} as a new fundamental.

In HCCCDO a close doublet of type C bands is observed at 0+1945.8 and 0+1949.7 . This pair lies one quantum of ν_4' to high frequencies of the single band $8_0^1 9_0^1$; the expected position of $4_0^1 8_0^1 9_0^1$, obtained by adding ν_9' to the observed position of $4_0^1 8_0^1$, is 0+1951 . The only other A′ binary or ternary combination expected here is $\nu_6'+2\nu_8' = 1942$ cm^{-1}(harmonic). But if $\nu_4'+\nu_8'+\nu_9'$ resonates with $\nu_6'+2\nu_8'$, we should expect $\nu_4'+\nu_9'$ to resonate with $\nu_6'+\nu_8'$; which is not observed. In any case the present doublet is more intense than is expected on either of

the above assignments. We therefore assign the extra band to a fundamental whose unperturbed value will be about 1947 cm^{-1}

In DCCCHO a single band of medium intensity is found at 0+1850.9 . This is near the position expected for 6_0^2, since $2\nu'_6$ = 1873 (harmonic). However 6_0^2 is much weaker than this in HCCCHO, so we assign the present band also to the new fundamental.

Of the three remaining fundamentals, the only one which is likely to have this frequency is the C≡C stretch, ν'_3. The observed isotope effects support this assignment.

VIII.15. ν_2.

In the HCCCHO spectrum there is a fairly strong single type C band at 0+2952.5 , which has no analogue in the previous octave of the main progression, the only band in the corresponding position being the type A one $4_0^1 12_0^1$. The only A' binary, ternary or quaternary combinations expected in this region are $\nu'_3+\nu'_9+\nu'_{10}+\nu'_{12}$ = 2943 (harmonic) and $\nu'_4+\nu'_6+2\nu'_{12}$ = 2947 (harmonic). Since these would be derived from parent bands $10_0^1 12_0^1$ and 12_0^2 which are themselves weak, they may be ruled out on intensity grounds; so this frequency represents a further fundamental.

A similar band at 0+2953.1 in DCCCHO is assigned to the same fundamental, rather than to the combinations $\nu'_3+\nu'_5$ = 2968 (harmonic) or $\nu'_4+\nu'_5+\nu'_7$ = 2945 (harmonic), which would be expected to be weaker.

In HCCCDO two strong bands are found at 0+2189.8 and 0+2221.0 , one of which is obviously to be assigned as $4_0^1 6_0^1$, since the band 6_0^1 is of similar intensity. The harmonic value of $\nu_4'+\nu_6'$ is 2209.9 cm^{-1}, and, allowing for some anharmonicity, the unperturbed position of the other band will be about 0+2204 . No other A' binary or ternary summation is expected here, so we assign this frequency to the same fundamental.

The large effect of formyl deuteration on this fundamental identifies it as the formyl C-H stretch, ν_2'.

There is an abrupt change in the appearance of the ^PQ_K branches of the band 0+2189.8 of HCCCDO at K=13 (see Fig. 11). Up to $^PQ_{12}$ they are sharp and apparently normal, while from $^PQ_{14}$ onwards they appear diffuse; some rather complex structure, which need not necessarily belong to this band, is found in the position expected for $^PQ_{13}$. It was previously thought (6) that this was due to a predissociation in the K-structure, the predissociation limit on this basis being 28595 ± 17 cm^{-1}. However, plates taken at higher vapour pressure have revealed that discrete J-structure is present in $^PP_{14}$ and $^PP_{15}$, so that the change in appearance is probably due mainly to a sudden change in the degradation of the J-structure; in addition some of the sub-bands are displaced from their expected positions. It seems definite therefore that there is an irregular perturbation affecting the rotational levels. This being so, the predissocittion would have to be an accidental one (27, p.415),

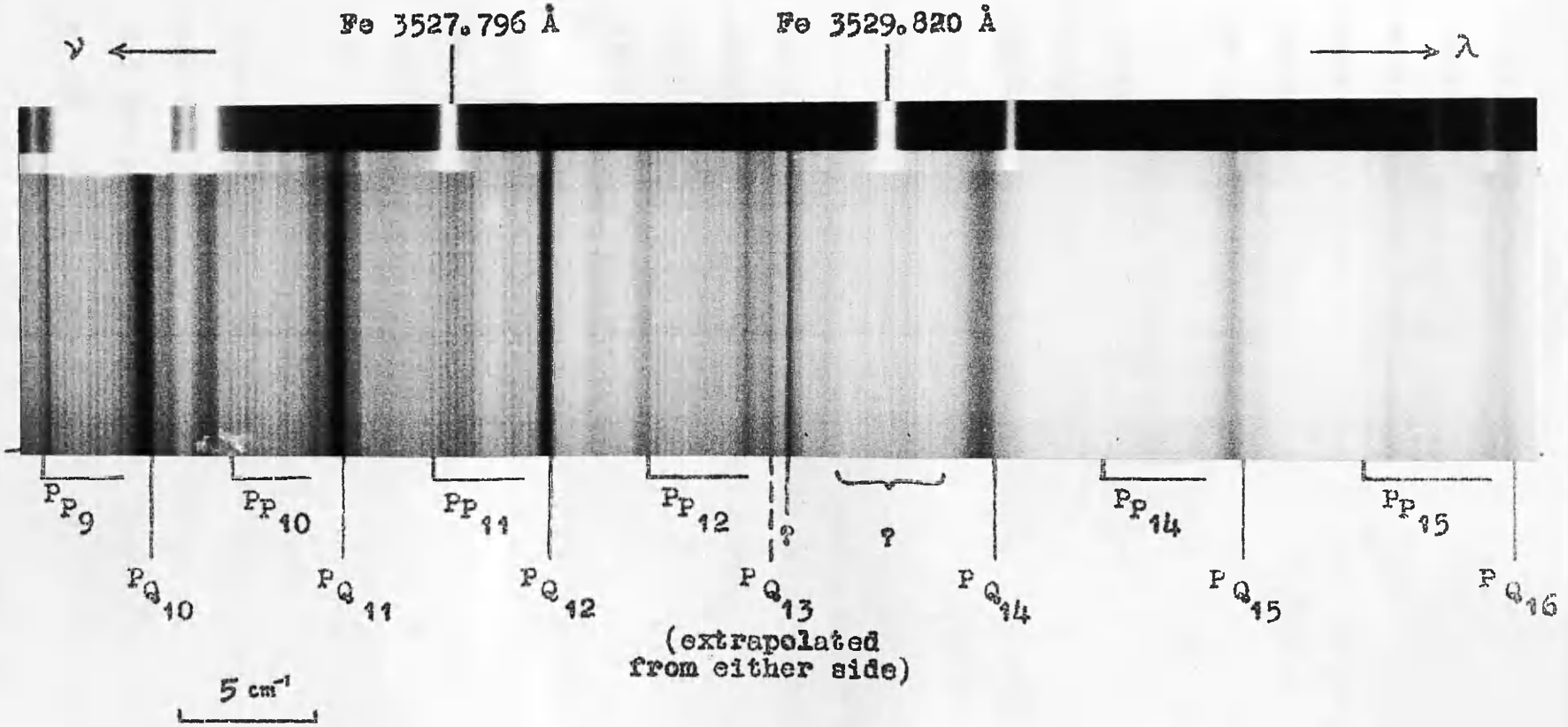

Fig. 11. Sub-band structure of the band of HCCCDO at 28395.8 cm^{-1} (0 + 2189.8), showing the abrupt change in appearance of the ^{P}Q branches at $^{P}Q_{13}$.

involving a perturbation by a predissociated state; and it would have to be specific to $K'=12$. In fact, in view of the lack of definite evidence for the diffuseness of individual lines, it is doubtful if the predissociation explanation can be upheld.

An alternative possibility is that there is a $\Delta K = 1$ perturbation (28,p.413) between the rotational levels of the Fermi-resonating vibrations; the centre of the perturbation corresponds closely to the point at which the K levels of the 2189.8 level catch up on the (K-1) levels of the 2221.0 level. This possibility has not been explored very fully yet.

Less striking anomalies are observed in the sub-bands of the 0+2221.0 band, but for the moment these do not serve to distinguish the above possibilities.

VIII.16. ν_1.

No definite evidence of the presence of bands due to the ethynyl C-H stretching fundamental ν_1 in any of the spectra has yet been obtained.

VIII.17. ν'_5 of HCCCDO.

We have so far obtained values for all the excited-state fundamentals except ν'_1 of all three isotopes and ν'_5 of HCCCDO. The value of ν'_7 for HCCCHO and HCCCDO is a hypothetical one, but all that matters for the present purpose is that it should be nearly the same for both isotopes. In the same way, ν'_1

should be nearly the same for both (cf. the ground-state values). With this assumption, we can calculate the value of ν'_5 of HCCCDO by two independent methods.

(i) The isotope shift of the 0 band (VIII.4) is due to changes in the zero-point energy between the electronic states. The purely electronic term value $T_e = \nu_{00} + \frac{1}{2}\sum_i(\nu''_i - \nu'_i)$ should be the same for all isotopes. This is only true for HCCCHO and HCCCDO if ν'_5(HCCCDO) = 804 cm^{-1}.

(ii) The Teller-Redlich product rule (28, p.231) can be applied to the a′ fundamentals of HCCCHO and HCCCDO. Strictly speaking we require the rotational constant C′ for both isotopes in order to calculate the theoretical (harmonic) value of the product ratio; but, since the harmonic value depends only on the ratio of the C's, we shall not be committing too serious an error in using the ground-state harmonic value. Solving, we obtain ν'_5(HCCCDO) = 825 cm^{-1}.

The agreement between these estimates is good enough to suggest that the other fundamentals are correctly identified.

On the basis of these results, the most likely candidates for 5^1_0 among the unassigned bands in this region of HCCCDO are 0+802.2 and 0+824.1 ; since the latter is appreciably more intense, we assign it to the fundamental.

The large amount of information available from the spectra concerning the overtone and combination levels of the excited state has not so far been examined systematically.

CHAPTER IX.

DISCUSSION OF THE ANALYSIS OF THE 3820 Å SYSTEM.

IX. 1. Excited-State Fundamentals.

The values proposed for the fundamental frequencies of the excited state are collected in Table 23 ; wherever possible they are origin-origin separations derived from the analysis of the K-structure and have been corrected for Fermi resonance.

The consistency of the a″ assignments may be tested by means of the product rule (28, p. 231). Lacking the excited-state B values, we use ground-state B values and excited-state A values in the harmonic calculation; since only the ratio of the B's is required, the error introduced should not be serious. The results are also shown in Table 23; the agreement is reasonably good, although it is unusual that the observed product ratio should be greater than the harmonic one, as it is in both cases.

IX. 2. Planarity of Excited State.

Since the rotational analysis of the origin band is not sufficiently far advanced to enable us to derive a reliable value of the inertial defect in the excited state, our discussion of the planarity or non-planarity of the excited

Table 23. Excited-State Fundamentals (in cm^{-1}).

		HCCCHO	DCCCHO	HCCCDO
	ν_1	-	-	-
	ν_2	2952.5 a	2953.1 a	2204 d
	ν_3	1945.8 a	1850.9 a	1947 d
	ν_4	1304.0 d	1298.6 d	1267.6 a
a'	ν_5	1119.5 a	1115 d	824.1 e
	ν_6	951.6 d	936.6 d	942.3 a
	ν_7	650 e	529.3 b	650 e
	ν_8	506.9 b	486.5 b	499.9 b
	ν_9	189.4 a	183.6 a	187.4 a
	ν_{10}	462.1 a	459.0 a	411.3 a
a''	ν_{11}	389.7 a	291 c	375 c
	ν_{12}	345.9 a	346.9 a	321.8 a

a - from origins; b - from centres; c - from centres, using infra-red frequencies; d - corrected for Fermi resonance; e - unobserved or doubtful.

Product Rule for a'' Fundamentals.

	$\frac{HCCCHO}{DCCCHO}$	$\frac{HCCCHO}{HCCCDO}$
Observed	1.344	1.255
Harmonic	1.331	1.242

(see p. 155)

state must be confined to the vibrational evidence.

There being apparently no departure from $\underline{C}_s$ vibronic selection rules, the possible Franck-Condon progressions in out-of-plane vibrations should proceed in double quanta (see II.3). The bands which are tentatively assigned in Tables 14, 15 and 16 to the first overtones and binary combinations of the a″ fundamentals are all weak, with the exception of 10_0^2 of HCCCHO and DCCCHO which are intensified by Fermi resonance. The possibility that the intensity of this Fermi pair is due to 10_0^2 rather than the fundamental is ruled out by comparison with HCCCDO where 10_0^2 is weak. Thus there is no Franck-Condon evidence to suggest that the excited state is non-planar.

However, as was seen in VIII.12 , the second quantum of ν'_{10} is about 25 cm^{-1} larger than the first. This mode is analogous to the one which has a double minimum in excited formaldehyde, and the anharmonicity observed in excited propynal is in the same sense, but not nearly as large, as that found for formaldehyde (II.2).

To test what this anharmonicity might imply in terms of a central potential energy barrier in the ν'_{10} coordinate, the potential function described in III.5 was fitted to the two observed quanta. Since there are three independent parameters ν,α and β required to specify this potential, one of them (β) was given several arbitrary values and the first-order perturbation elements given in III.5 were solved for the other two. The second-order perturbation corrections due to the off-diag-

onal elements were calculated and found to be negligible.

The results of three such calculations are shown in Table 24 and Fig. 12.

Table 24. Potential Function for ν'_{10} Coordinate.

$\nu'_{10} = 462.1$ cm^{-1} ; $2\nu'_{10} = 949.0$ cm^{-1}.

β	α	ν (cm^{-1})	$V_{max}-V_{min}$ (cm^{-1})	q_{min}	$3\nu'_{10}$ (calc.)
1	0.1911	495.6	0	0	1440.6
8	0.1326	480.9	11.12	0.3067	1424.3
24	0.1907	479.6	59.33	0.3037	1421.3

This potential does not necessarily have a central maximum to fit the two observed quanta. For higher values of β than those quoted, the potentials have increasingly sharp central maxima which appear physically unlikely, so that a probable upper limit to the potential barrier is about 100 cm^{-1}. A critical test for the existence of a barrier seems to be the size of the third quantum of ν'_{10} : if this is smaller than the second one, the presence of a barrier appears to follow. Unfortunately the $3\nu'_{10}$ level has not yet been observed.

For both of the calculated functions which have central maxima, the two minima are at $q = \pm 0.30$; with $\nu = 480$ cm^{-1}, this corresponds to $Q = \pm 0.080$ amu$^{\frac{1}{2}}$ Å. Assuming an effective vibrating mass of 1 amu, this implies a displacement of 0.08 Å out of plane or an angle of about 4° between the C-H bond and

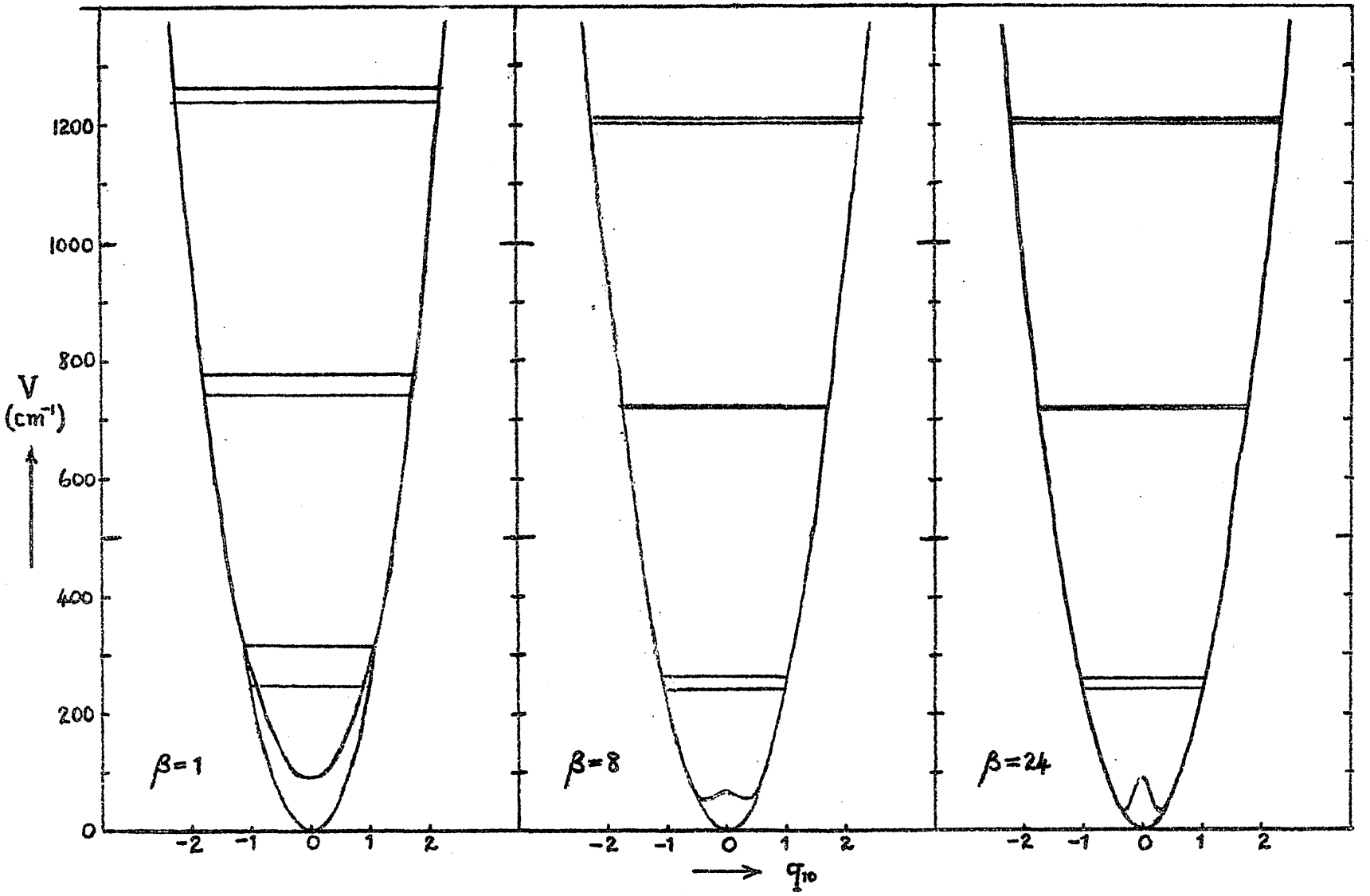

Fig. 12. Possible potential functions for the ν_{10} mode of excited propynal. The anharmonic well and energy levels are shown in black, the harmonic part and its energy levels in blue.

the CCO plane. Thus the potential function is probably rather flat for about 4° on either side of the planar configuration, possibly with a central maximum.

In summary, the evidence relating to the precise planarity of the excited state of propynal is not quite definite. But any potential barrier at the planar configuration is unlikely to be more than a third of the zero-point energy in the ν'_{10} mode, so that the excited state is to all intents and purposes planar.

IX.3. Structure of the Excited State.

In view of the activity of all of the a′ fundamentals except ν_7 and possibly ν_4, it follows from the Franck-Condon principle that extensive geometry changes are occurring in the molecular plane. However, since the two-quantum changes in all these modes except ν_4 are fairly weak, most of these changes will be relatively small.

Estimates of the changes in bond lengths resulting from the excitation could be made using Clark's rule or Badger's rule (27, p.457; 22), preferably with force constants. Since the required normal coordinate analysis has not been carried out, we shall assume that each normal coordinate involves a change in only one internal coordinate, and use the observed stretching frequencies to obtain a preliminary idea of the changes taking place.

Clark's rule was used in the form $\frac{r'}{r''} = (\frac{\nu''}{\nu'})^{\frac{1}{3}}$; and Badger's in the form $\frac{r'-d}{r''-d} = (\frac{\nu''}{\nu'})^{\frac{2}{3}}$, where d = 0.680 Å for CO and CC bonds and d = 0.340 Å for CH bonds. The ground-state bond lengths were taken from Costain and Morton's paper (see IV). The results are quoted in Table 25.

Table 25. Bond Lengths of Excited Propynal (in Å).

Bond	r''	r'(Clark)			r'(Badger)			r' (mean)
		I	II	III	I	II	III	
$C_3{=}O$	1.215	1.327	1.328	1.334	1.318	1.319	1.325	1.325
$C_1{\equiv}C_2$	1.209	1.241	1.236	1.240	1.238	1.233	1.237	1.238
$C_2{-}C_3$	1.445	1.441	1.443	-	1.441	1.443	-	1.442
$C_3{-}H_2$	1.106	1.094	1.094	1.092	1.090	1.090	1.087	1.091

I ≡ HCCCHO ; II ≡ DCCCHO ; III ≡ HCCCDO .

Apart from the C-C single bond, where the HCCCDO molecule is ignored because of the interaction between ν_5' and ν_6', the results are consistent for the three isotopes, suggesting that this treatment may have some validity.

Using Craig's equations (14) for the relative intensities in a Franck-Condon progression, Howe and Goldstein obtained from their solution spectra an estimate of 0.10 Å for the increase in the C=O length, in good agreement with the above.

The lengths of the C=O and formyl C-H bonds in excited propynal are found to be similar to those in excited formaldehyde (II.2). The triple bond apparently lengthens markedly.

When the full set of rotational constants for the three isotopes is available, they will provide additional information regarding the structure, although not sufficient in themselves to determine it completely. The various methods will have to be used in conjunction in order to obtain the detailed structure. As yet it it is difficult to say anything about the changes in bond angles.

IX.4. Allowed and Forbidden Components.

Since the origin of the band system is a type C band, the excited-state electronic wave-function must have A'' symmetry, as is required by the $\pi^* \leftarrow n$ assignment. All the stronger bands are of type C and are therefore Herzberg-Teller allowed. An approximate integration of the low-resolution spectrum gave $f \approx 5 \times 10^{-4}$ for the oscillator strength of the whole transition.

In addition to the allowed bands there are bands of medium intensity which are polarised in the molecular plane, and so are forbidden by the Herzberg-Teller selection rules. The theory of I.2 shows that such bands derive their intensity by vibronic coupling, through unsymmetrical vibrations, with other electronic transitions which must be polarised in the molecular plane. However, if all the forbidden bands borrow their intensity from the same electronic transition, it follows that their transition moments will all be parallel to the transition moment of that electronic transition, and so they should all give bands consisting of type A and type B components with the same intensity

ratio. In fact the forbidden component of propynal has bands which are of almost pure type A and almost pure type B. Thus we are forced to conclude that the forbidden component borrows intensity from two (or more) other electronic transitions. It does not necessarily follow that these transitions are polarised along the a- and b-axes, since the observed bands could correspond to a fortuitous mixture of the two transitions, with transition moment formed by vector summation.

The 10_0^1 band is of almost pure type B in HCCCHO and DCCCHO, whereas in HCCCDO it has a type A component of comparable intensity. Now with either isotopic substitution, the orientation of the principal axes of inertia of the ground state relative to molecule-fixed axes changes by less than 1^o, using Costain and Morton's structure (see IV); and the same will probably be true of the excited state. It follows that the above change represents a fairly large change of direction of the transition moment relative to molecule-fixed axes. Since a single electronic transition would give a unique direction of transition moment relative to these axes, we have to conclude that ν_{10} can mix in at least two other electronic states ; the relative borrowing-power for these states depends upon whether the C-H or the C-D out-of-plane vibration is operating. In contrast, the 12_0^1 band is of pure type A in all three isotopes, no perpendicular component being observed.

The two lowest strong ${}^eA' \leftarrow {}^eA'$ transitions expected for propynal are the $\pi^* \leftarrow \pi$, tentatively assigned to the 2140 Å

system (VII.5), and the $\sigma^* \leftarrow n$, which probably lies beyond 2000 Å, and these are probably the ones which induce the forbidden components of the 3820 Å system.

In the formaldehyde $\pi^* \leftarrow n$ system the intensity lies mainly in a forbidden component polarised along the b-axis; this must be borrowed by the $\nu_4(b_2)$ vibration from a $^eB_1 \leftarrow {}^eA_1$ transition (see II.2). The upper state of the $\sigma^* \leftarrow n$ transition has $^eB_1$ symmetry, and it was sugg-ested by Pople and Sidman (52) that this state donates the intensity to the $\pi^* \leftarrow n$ system. The $\pi^* \leftarrow \pi$ transition is of type $^eA_1 \leftarrow {}^eA_1$ and there are no fundamentals of symmetry a_2 to couple this with the $\pi^* \leftarrow n$ transition; thus there is no Herzberg-Teller forbidden component of type A bands borrowed from the $\pi^* \leftarrow \pi$ transition (the weak parallel bands observed play the rôle of a Herzberg-Teller allowed component).

The glyoxal $\pi^* \leftarrow n$ ($^eA_u \leftarrow {}^eA_g$) system is also observed to have a strong forbidden component, borrowed from a $^eB_u \leftarrow {}^eA_g$ transition (4, 37). In this case $^eB_u \leftarrow {}^eA_g$ transitions of both $\pi^* \leftarrow \pi$ and $\sigma^* \leftarrow n$ types are possible; only the unique b_g fundamental can perform the mixing. In view of the propynal results, it would be interesting to compare the relative intensities of the type A and type B components of the hybrid bands in $(CHO)_2$ and $(CDO)_2$.

IX.5. Electronic Structure of the Excited State.

If the effects of the electronic excitation are measured by the percentage changes in the various fundamental frequencies,

the three fundamentals most seriously affected are the out-of-plane (a″) bending ones. Both a″ C-H bending frequencies drop by about 50%, while the a″ skeletal bend rises by 33%. The most drastic change in the in-plane vibrations is the drop of 23% in the carbonyl stretch.

The changes produced in the vibrations of the formyl group closely parallel those found for the formaldehyde π^*-n transition, which is good vibrational evidence for the analogy between the two transitions. Table 26 compares the changes in the appropriate frequencies of the two molecules. The value quoted for the wagging vibration of excited formaldehyde is an estimate of its effective value for a planar molecule obtained by taking the mean of the second and third quanta (403 and 421 cm^{-1}), since the theory of III.5 shows that these should lie respectively above and below the harmonic value; in the absence of more detailed information the first quantum is used for propynal.

Table 26. Fundamental Frequencies of Formaldehyde and Propynal. The frequencies are in cm^{-1}.

	HCHO			HCCCHO		
	ground	excited	change	ground	excited	change
CO stretch	1744	1182	-32%	1698	1303	-23%
CHO wag	1164	412	-65%	981	462	-53%
CH rock	1503	1322	-12%	1389	1120	-19%
CH stretch	2780	2875	+3.4%	2858	2953	+3.3%

However, the changes in the acetylenic frequencies show that the electronic transition cannot be regarded as localised in the carbonyl group. The single bond seems to be almost unaffected, but the triple bond is definitely weakened. The out-of-plane C≡Ĉ-C bending frequency now has a fairly typical value for a linearly hybridised carbon atom, as in substituted acetylenes and in allenes, while the in-plane frequency remains unusually low. The large drop in ν_{11}, similar to that of ν_{10}, suggests that the two end carbon atoms are affected similarly.

If the formaldehyde excited state can be represented by

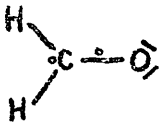

(see II.2), then the observations for propynal suggest that its excited state can be represented by

with roughly equal weights of the two structures. Since the two structures have equal numbers of bonding electrons, a first-order resonance with approximately equal contributions seems reasonable. This delocalisation will also partly relieve the strain which forces formaldehyde out of plane, in agreement with the near-planarity of excited propynal.

REFERENCES.

1. R.A.B.Bannard, A.T.Morse and L.C.Leitch, Can. J. Chem., 1953, 31, 351.

1a. L.J.Bellamy, Infra-red Spectra of Complex Molecules, Methuen, London, 1958.

2. M.Born and R.Oppenheimer, Ann. Physik, 1927, 84, 457.

3. D.R.J.Boyd and H.C.Longuet-Higgins, Proc. Roy. Soc., 1952, A 213, 55.

4. J.C.D.Brand, Trans. Faraday Soc., 1954, 50, 431.

5. J.C.D.Brand, J. Chem. Soc., 1956, 858.

6. J.C.D.Brand, J.H.Callomon and J.K.G.Watson, Can. J. Phys., 1961, 39, 1508.

7. J.C.D.Brand, G.Eglinton and J.F.Morman, J. Chem. Soc., 1960, 2526.

8. J.C.D.Brand and J.K.G.Watson, Trans. Faraday Soc., 1960, 56, 1582.

9. S.F.Chan, J.Zinn, J.Fernandez and W.D.Gwinn, J. Chem. Phys., 1960, 33, 295, 1643; 1961, 34, 1319.

10. E.U.Condon, Phys. Rev., 1926, 28, 1182; 1928, 32, 858.

11. C.C.Costain, J. Chem. Phys., 1958, 29, 864.

12. C.C.Costain and J.M.Dowling, J. Chem. Phys., 1960, 32, 158.

13. C.C.Costain and J.R.Morton, J. Chem. Phys., 1959, 31, 389.

14. D.P.Craig, J. Chem. Soc., 1950, 2146.

15. D.P.Craig, J.M.Hollas, M.F.Redies and S.C.Wait Jr, Phil.

Trans. Roy. Soc., 1961, A 253, 543, 569.

16. A.Danti, W.J.Lafferty and R.C.Lord, J. Chem. Phys., 1960, 33, 294.

17. J.M.Dowling, J. Mol. Spec., 1961, 6, 550.

18. A.R.Downie, M.C.Magoon, T.Purcell and B.Crawford Jr., J. Opt. Soc. Amer., 1953, 43, 941.

19. B.Edlen, Vacuum Corrections, Lund, 1951.

20. J.C.Evans, J. Chem. Phys., 1954, 22, 1228.

20a. J.C.Evans and H.J.Bernstein, Can. J. Chem., 1956, 34, 1083.

21. J.Franck, Trans. Faraday Soc., 1925, 21, 536.

22. F.M.Garforth, C.K.Ingold, H.G.Poole et al., J. Chem. Soc., 1948, 406 et seq.

23. S.L.Gerhard and D.M.Dennison, Phys. Rev., 1933, 43, 197.

24. L.E.Giddings Jr. and K.K.Innes, J. Mol. Spec., 1961, 6, 528; 1962, 8, 328.

25. S.Golden, J. Chem. Phys., 1948, 16, 78.

25a. R.J.Grisenthwaite and H.W.Thompson, Trans. Faraday Soc., 1954, 50, 212.

26. G.R.Harrison (editor), Massachusetts Institute of Technology Wavelength Tables, Wiley, New York, 1939.

27. G.Herzberg, Spectra of Diatomic Molecules, Van Nostrand, New York, 1950 (second edition).

28. G.Herzberg, Infrared and Raman Spectra of Polyatomic Molecules, Van Nostrand, Princeton, 1945.

29. G.Herzberg and E.Teller, Z. physik. Chem., 1933, B 21, 410.

30. J.A.Howe and J.H.Goldstein, J. Chem. Phys., 1955, 23, 1223.

31. J.A.Howe and J.H.Goldstein, J. Amer. Chem. Soc., 1958, 80, 4846.

32. C.K.Ingold and G.W.King, J. Chem. Soc., 1953, 2702 et seq.

33. K.K.Innes, J. Chem. Phys., 1954, 22, 863.

34. K.K.Innes and L.E.Giddings Jr., J. Mol. Spec., 1961, 7, 435.

35. International Union of Pure and Applied Chemistry, Tables of Wavenumbers for the Calibration of Infrared Spectrometers, Butterworths, London, 1961.

36. H.A.Jahn, Phys. Rev., 1939, 56, 680.

37. G.W.King, J. Chem. Soc., 1957, 5054.

38. G.W.King, J. Sci. Instr., 1958, 35, 11.

39. G.W.King and D.Moule, Spectrochim. Acta, 1961, 17, 286.

40. G.W.King, R.M.Hainer and P.C.Cross, J. Chem. Phys., 1943, 11, 27.

41. N.J.Leonard (editor), Organic Syntheses, 1956, 36, 66.

42. S.F.Mason, Quart. Revs., 1961, 15, 287.

43. H.L.McMurray, J. Chem. Phys., 1941, 9, 231, 241.

44. J.H.Meal and S.R.Polo, J. Chem. Phys., 1956, 24, 1119, 1126.

45. R.S.Mulliken, J. Chem. Phys., 1935, 3, 739.

46. R.S.Mulliken, Phys. Rev., 1941, 59, 873; 60, 506.

47. R.S.Mulliken, J. Chem. Phys., 1955, 23, 1997.

48. National Bureau of Standards, Tables Relating to Mathieu Functions, Columbia University Press, 1951.

49. H.H.Nielsen, Revs. Mod. Phys., 1951, 23, 90.

50. R.A.Nyquist and W.J.Potts, Spectrochim. Acta, 1960, 16, 419.

51. J.Overend and B.Crawford Jr., J. Chem. Phys., 1958, 29, 1002.

52. J.A.Pople and J.W.Sidman, J. Chem. Phys., 1957, 27, 1270.

53. S.R.Polo, Can. J. Phys., 1957, 35, 880.

54. V.R.Rao and I.A.Rao, Indian J. Phys., 1954, 28, 491.

55. G.W.Robinson and V.E.DiGiorgio, Can. J. Chem., 1958, 36, 31.

56. I.G.Ross, Trans. Faraday Soc., 1952, 48, 973.

57. N.Sheppard and D.M.Simpson, Quart. Revs., 1952, 6, 1.

58. J.W.Sidman, Chem. Revs., 1958, 58, 689.

59. H.Sponer, G.Nordheim, A.L.Sklar and E.Teller, J. Chem. Phys., 1939, 7, 207.

60. R.F.Stratton and A.H.Nielsen, J. Mol. Spec., 1960, 4, 373.

61. J.D.Swalen and J.A.Ibers, J. Chem. Phys., 1962, 36, 1914.

62. E.Teller, Handb. und Jahrb. der Chem. Phys., 1934, 9, II, 43.

63. E.Teller and L.Tisza, Z. Physik, 1932, 73, 791.

64. C.H.Townes and A.L.Schawlow, Microwave Spectroscopy, McGraw-Hill, New York, 1955.

65. A.D.Walsh, J. Chem. Soc., 1953, 2306.

66. F.Wille and L.Saffer, Ann. Chem., 1950, 568, 34.

67. J.K.Wilmshurst, J. Mol. Spec., 1957, 1, 201.

68. E.B.Wilson Jr., J.C.Decius and P.C.Cross, Molecular Vibrations, McGraw-Hill, New York, 1955.